

## STATUS OF THESIS

Title of thesis	Development of a Non-ionic Surfactant Derived from High Oleate Ester for Potential EOR Application
-----------------	--

I SUSAN LEE YUN CHING

hereby allow my thesis to be placed at the Information Resource Center (IRC) of Universiti Teknologi PETRONAS (UTP) with the following conditions:

1. The thesis becomes the property of UTP
2. The IRC of UTP may make copies of the thesis for academic purposes only.
3. This thesis is classified as

☒ Confidential

☐ Non-confidential

If this thesis is confidential, please state the reason:

Filing for patent on the EOR formulation blend.  
\_\_\_\_\_  
\_\_\_\_\_

The contents of the thesis will remain confidential for 5 years.

Remarks on disclosure:

\_\_\_\_\_  
\_\_\_\_\_  
\_\_\_\_\_

Endorsed by

\_\_\_\_\_  
Signature of Author

\_\_\_\_\_  
Signature of Supervisor

Permanent address: \_\_\_\_\_

Name of Supervisor

30, Jalan Bukit Mewah 62

Assoc. Prof. Dr. Isa M. Tan

Taman Bukit Mewah

43000 Kajang, Selangor, Malaysia

Date : \_\_\_\_\_

Date : \_\_\_\_\_

UNIVERSITI TEKNOLOGI PETRONAS

DEVELOPMENT OF A NON-IONIC SURFACTANT DERIVED FROM HIGH

OLEATE ESTER FOR POTENTIAL EOR APPLICATION

by

SUSAN LEE YUN CHING

The undersigned certify that they have read, and recommend to the Postgraduate Studies Programme for acceptance this thesis for the fulfillment of the requirements for the degree stated.

Signature: \_\_\_\_\_

Main Supervisor: Assoc. Prof. Dr. Isa. M. Tan \_\_\_\_\_

Signature: \_\_\_\_\_

Co-Supervisor: \_\_\_\_\_

Signature: \_\_\_\_\_

Head of Department: Assoc. Prof. Dr. Azmi Bustam \_\_\_\_\_

Date: \_\_\_\_\_

DEVELOPMENT OF A NONIONIC SURFACTANT DERIVED FROM HIGH  
OLEATE ESTER FOR POTENTIAL EOR APPLICATION

by

SUSAN LEE YUN CHING

A Thesis

Submitted to the Postgraduate Studies Programme  
as a Requirement for the Degree of

MASTER OF SCIENCE

CHEMICAL ENGINEERING

UNIVERSITI TEKNOLOGI PETRONAS

BANDAR SERI ISKANDAR,

PERAK

DECEMBER 2013

## DECLARATION OF THESIS

Title of thesis

Development of a Non-ionic Surfactant Derived from High Oleate Ester  
for Potential EOR Application

I SUSAN LEE YUN CHING

hereby declare that the thesis is based on my original work except for quotations and citations which have been duly acknowledged. I also declare that it has not been previously or concurrently submitted for any other degree at UTP or other institutions.

Witnessed by

\_\_\_\_\_  
Signature of Author

\_\_\_\_\_  
Signature of Supervisor

Permanent address: \_\_\_\_\_

30, Jalan Bukit Mewah 62

Taman Bukit Mewah

43000 Kajang, Selangor, Malaysia.

Name of Supervisor

Assoc. Prof. Dr. Isa M. Tan

Date : \_\_\_\_\_

Date : \_\_\_\_\_

## DEDICATION

To my husband and my parents.

## ACKNOWLEDGEMENTS

I would like to express my sincere thanks to those who have helped me in my journey of completing this master's program. I would like to thank my supervisor, Assoc. Prof. Dr. Isa M Tan for his continuous guidance, patience and support throughout the entire process. It had been a most pleasant experience working with him. I would also like to thank my colleagues – Mr. Muhammad Mushtaq, Mr. Saeed Majidaie, Mr. Muhammad Sagir and Dr. Ivy Chai for their help, advice and support.

Special thanks to PETRONAS Research Sdn, Bhd. for the opportunity given to enroll in this program. It was indeed, an opportunity that had taught me much.

I would also like to take this opportunity to thank my family for their moral support: to my husband, for being my faithful cheerleader and pillar throughout the ups and downs of this program; to my parents, for their love and support in my pursuit of this master's degree. Without them, it would have been a difficult journey.

Last but not least, I thank my God for the grace given to complete this thesis. Without Him, this would not have been possible.

2 Corinthians 12:9a – “And He has said to me, My grace is sufficient for you, for My power is perfected in weakness.....”

## ABSTRACT

Natural oil as an alternative raw material to petroleum fractions for various applications have been given much attention due to the fluctuation of global oil price and increasing environmental issues. Although surfactants derived from natural oil have been produced and used in various industries, natural oil derived surfactants have never been applied in EOR applications. This research looked into the possibility of applying natural oil derived surfactant in EOR applications. In this research, a nonionic surfactant has been synthesized successfully using natural oil having high oleate ester content with a simple two-step reaction: epoxidation followed by alkoxylation. While optimization study for epoxidation is quite established, optimization study for alkoxylation using PEG-ME has never been established. Optimization studies were done for both epoxidation and alkoxylation. High yield of product was obtained in both steps: 94.49% in epoxidation and 86.6% in alkoxylation. The synthesized surfactant was successfully developed to possess properties suitable for a Malaysian oilfield's condition. The conditions that were addressed were the surfactant's ability to tolerate harsh conditions of high temperature and high salinity (more than 100°C and 35000 ppm respectively); and to generate stable foam in the presence of oil to make it a suitable candidate for gas mobility control. These were achieved by blending the synthesized surfactant with two additives – an anionic surfactant as a cloud point booster (sodium dodecyl sulfate) and an amphoteric surfactant as a foam booster (lauryl hydroxysultaine) with a 4:3:3 ratio to form a new formulation. The new formulation of blended surfactants was found to be stable at 100°C, compatible with high salinity of 35 000 ppm and produced foams that are stable in the presence of oil with an increase of 116.22% of its original half-life.

## ABSTRAK

Banyak perhatian telah diberikan kepada minyak semulajadi sebagai bahan mentah alternatif kepada pecahan petroleum untuk pelbagai aplikasi. Ini disebabkan oleh harga minyak sedunia yang tidak stabil serta isu-isu alam sekitar yang semakin banyak. Walaupun surfaktan yang dihasilkan daripada minyak semulajadi telah dihasilkan dan digunakan dalam pelbagai industri, surfaktan yang dihasilkan daripada minyak semulajadi tidak pernah digunakan dalam aplikasi EOR. Penyelidikan ini menyelidik kemungkinan menggunakan surfaktan yang dihasilkan daripada minyak semulajadi dalam aplikasi EOR. Dalam penyelidikan ini, satu surfaktan tidak-ionik telah berjaya disintesiskan dengan menggunakan minyak semulajadi yang mempunyai kandungan oleat ester yang tinggi melalui dua reaksi yang mudah: epoksidasi dan alkoksilasi. Walaupun kajian optimasi pernah dikaji untuk reaksi epoksidasi, kajian optimasi tidak pernah dilaksanakan untuk reaksi alkoksilasi yang melibatkan PEG-ME. Melalui kajian optimasi untuk kedua-dua reaksi, hasil produk yang diperolehi adalah tinggi: 94.49% untuk epoksidasi dan 86.6% untuk alkoksilasi. Surfaktan yang disintesiskan telah berjaya dimajukan untuk mempunyai ciri-ciri yang sesuai untuk keadaan satu medan minyak di Malaysia. Surfaktan yang disintesis dimajukan untuk mempunyai ketahanan terhadap keadaan suhu tinggi dan saliniti tinggi (melebihi 100°C dan 35000 ppm masing-masing); dan menghasilkan busa yang stabil dalam kehadiran minyak untuk menjadikannya satu calon yang sesuai untuk kawalan pergerakan gas. Ini telah dicapai dengan mengadunkan surfaktan yang disintesis dengan dua aditif – satu surfaktan anionic sebagai penggalak takat kabur (natrium dodesil sulfat) dan satu surfaktan amfoterik sebagai penggalak busa (lauril hidroksi-sultain) dengan nisbah 4:3:3 untuk menghasilkan satu formulasi yang baru. Formulasi adunan surfaktan baru itu didapati stabil pada 100°C dalam tahap saliniti sebanyak 35000 ppm dan menghasilkan busa yang stabil dalam kehadiran minyak dengan peningkatan sebanyak 116.22% daripada separuh hayat asal.



In compliance with the terms of the Copyright Act 1987 and the IP Policy of the university, the copyright of this thesis has been reassigned by the author to the legal entity of the university,

Institute of Technology PETRONAS Sdn Bhd.

Due acknowledgement shall always be made of the use of any material contained in, or derived from, this thesis.

© Susan Lee Yun Ching, 2013

Institute of Technology PETRONAS Sdn Bhd

All rights reserved.

## TABLE OF CONTENT

ABSTRACT .....	vii
ABSTRAK .....	viii
LIST OF FIGURES .....	xiii
LIST OF TABLES .....	xvi
CHAPTER 1 INTRODUCTION .....	1
1.1 Problem statement .....	3
1.2 Objectives .....	4
1.3 Scope of study.....	4
1.4 Organization of thesis .....	4
CHAPTER 2 BACKGROUND AND LITERATURE REVIEW .....	7
2.1 Enhanced Oil Recovery .....	7
2.1.1 Oil trap mechanism .....	8
2.1.2 EOR methods .....	10
2.1.2.1 Chemical .....	10
2.1.2.2 Gas .....	11
2.2 Surfactant.....	13
2.2.1 Types of surfactant .....	15
2.2.1.1 Cationic surfactant .....	15
2.2.1.2 Anionic surfactant.....	16
2.2.1.3 Amphoteric surfactant.....	16
2.2.1.4 Nonionic surfactant.....	17
2.2.2 Foam.....	19
2.2.3 Surfactants in EOR.....	21
2.2.3.1 Surfactants as mobility control agent.....	22
2.3 Synthesis of surfactant.....	23
2.3.1 Natural oils as raw material.....	23
2.3.2 Epoxidation .....	24
2.3.3 Attachment of ethylene oxide (EO) chain.....	26
2.4 Formulation of foaming agents for EOR applications.....	27
2.4.1 Foam stability .....	28

2.4.2 Elevation of cloud point .....	30
2.5 Summary .....	31
CHAPTER 3 METHODOLOGY .....	33
3.1 Overview .....	33
3.2 Materials used .....	34
3.3 Synthesis of surfactant .....	35
3.3.1 Epoxidation .....	35
3.3.1.1 Experimental design .....	36
3.3.1.2 Experimental procedure .....	37
3.3.2 Attachment of PEG-ME .....	37
3.3.2.1 Experimental design .....	37
3.3.2.2 Experimental procedure .....	38
3.4 Characterization .....	39
3.4.1 GC-MS (ASTM D 6584-00) .....	39
3.4.2 NMR .....	39
3.4.3 FT-IR .....	39
3.4.4 Oxirane oxygen value (AOCS Cd 9-57) .....	39
3.4.5 Critical Micelle Concentration (CMC) .....	41
3.4.6 Cloud point (ASTM D2024-09) .....	41
3.4.7 Nonionic titration .....	41
3.4.7.1 Preparation of titrant .....	43
3.4.7.2 Preparation of sample .....	43
3.5 Formulation .....	44
3.5.1 Screening test .....	44
3.5.2 Foam stability .....	47
CHAPTER 4 RESULTS AND DISCUSSION .....	49
4.1 Overview .....	49
4.2 Synthesis of surfactant .....	49
4.2.1 Epoxidation .....	49
4.2.1.1 Optimization study .....	50
4.2.2 Attachment of PEG-ME .....	65
4.2.2.1 Optimization study .....	66

4.2.2.2 Cloud point study .....	70
4.3 Characterization.....	72
4.3.1 HOE.....	72
4.3.2 Epoxides .....	75
4.3.3 ENS-750 .....	79
4.3.3.1 Critical Micelle Concentration.....	83
4.4 Formulation.....	84
4.4.1 Addition of ionic surfactants as cloud point boosters (CPB) .....	84
4.4.1.1 Without electrolyte.....	84
4.4.1.2 With electrolyte.....	85
4.4.2 Addition of foam booster .....	90
4.4.2.1 Screening test .....	90
4.4.2.2 Foam stability.....	92
CHAPTER 5 CONCLUSION.....	99
5.1 Recommended future work/direction .....	100
5.2 Journal Publications and Conferences .....	100
REFERENCES .....	103
APPENDIX A ADDITIONAL ANALYTICAL SPECTRA.....	111
APPENDIX B PUBLISHED PAPERS AND CONFERENCES .....	115

## LIST OF FIGURES

Figure 2.1: Oil trapping by (a) snap-off mechanism and (b) bypass .....	8
Figure 2.2: Number and classification of EOR projects for the US from 1971-2010 .	11
Figure 2.3: Some important indicators of micelle formation: abrupt changes in solution conductivity, a discontinuity in the surface tension-concentration curve; a sudden change in solution turbidity .....	14
Figure 2.4: Formation of (a) micelle and (b) reverse micelle .....	14
Figure 2.5: Some examples of cationic surfactants .....	15
Figure 2.6: Some examples of anionic surfactants .....	16
Figure 2.7: Some examples of amphoteric surfactants .....	17
Figure 2.8: Some examples of nonionic surfactants .....	18
Figure 2.9: A foam system with details on a foam lamella .....	19
Figure 2.10: a) Foam structure during the process of foam generation and liquid drainage. b) Plateau border with $P_A > P_B$ , causing liquid to flow into the borders.....	21
Figure 2.11: (a) In-situ generation of peroxy formic acid (b) Epoxidation of oleic acid methyl ester (c) Ring opening of epoxide.....	26
Figure 2.12: Alkoxylation reaction – the attachment of EO chain .....	27
Figure 2.13: Oil destabilizing foam mechanism .....	29
Figure 3.1: Flow chart depicting the screening test procedure .....	46
Figure 4.1: Effect of varying $H_2O_2/C=C$ and $HCOOH/C=C$ mole ratios on epoxidation yield (%).....	54
Figure 4.2: The effect of varying $H_2O_2/C=C$ mole ratio and reaction temperature on epoxidation yield (%).....	56
Figure 4.3: The effect of varying $HCOOH/C=C$ mole ratio and reaction temperature on epoxidation yield (%).....	57
Figure 4.4: The effect of varying reaction temperature and time on epoxidation yield (%).....	58
Figure 4.5: The effect of varying $HCOOH/C=C$ mole ratio and reaction time on epoxidation yield (%).....	60

Figure 4.6: The effect of varying $\text{H}_2\text{O}_2/\text{C}=\text{C}$ mole ratio and reaction time on epoxidation yield (%).....	61
Figure 4.7: Comparison between predicted and actual epoxidation yield (%) .....	64
Figure 4.8: The effect of varying the reaction temperature on yield at reaction time = 30 mins and 60 mins. ....	67
Figure 4.9: The effect of varying the reaction time on yield at reaction temperature = 40°C and 60°C.....	68
Figure 4.10: The effect of varying the catalyst amount on yield at reaction temperature = 40°C and 60°C.....	69
Figure 4.11: The effect of salinity on the cloud point of ENS-750 .....	71
Figure 4.12: $^1\text{H}$ NMR spectrum for HOE explained in respect to methyl linoleate ....	74
Figure 4.13: FT-IR spectrum for HOE .....	74
Figure 4.14: FT-IR spectrum of epoxide derived from HOE .....	76
Figure 4.15: $^1\text{H}$ NMR spectrum for epoxides synthesized explained in respect to: 1) diepoxy derived from methyl linoleate and 2) monoepoxy derived from methyl oleate .....	77
Figure 4.16: Comparison of $^1\text{H}$ NMR spectra of HOE and epoxides.....	78
Figure 4.17: FT-IR spectrum of ENS-750 .....	81
Figure 4.18: $^1\text{H}$ NMR spectrum of ENS-750.....	81
Figure 4.19: Comparison of $^{13}\text{C}$ NMR spectra of epoxide and ENS-750 with (molecule from top to bottom): monoepoxy, diepoxy and ENS-750 .....	82
Figure 4.20: Molecular structure of ENS-750 .....	83
Figure 4.21: Conductivity measurements of ENS-750 surfactant solutions.....	83
Figure 4.22: Cloud point of AOS/ENS-750 mixtures in the presence of NaCl.....	87
Figure 4.23: Cloud point of CTABr/ENS-750 mixtures in the presence of NaCl.....	88
Figure 4.24: Cloud point of SDS/ENS-750 mixtures in the presence of NaCl.....	88
Figure 4.25: Cloud point of MES/ENS-750 mixtures in the presence of NaCl.....	89
Figure 4.26: Cloud point of DBS/ENS-750 mixtures in the presence of NaCl .....	89
Figure 4.27: A graphical illustration of a dynamic foam stability test .....	93
Figure 4.28: Foam relative height for 1.0 wt% surfactant formulations in the absence of diesel.....	95

Figure 4.29: Foam relative height for 1.0 wt% surfactant formulations in the presence of diesel .....	96
Figure 4.30: Comparison of foam relative height of 1.0 wt% of AOS:ENS:LHS formulation with and without the presence of diesel .....	97
Figure 4.31: Comparison of foam relative height of 1.0 wt% of SDS:ENS:LHS formulation with and without the presence of diesel .....	97
Figure 4.32: Comparison of foam relative height of 1.0 wt% of MES:ENS:LHS formulation with and without the presence of diesel .....	98
Appendix 0.1: GC-MS spectrum of HOE used. ....	113

## LIST OF TABLES

Table 2.1: Commercially available surfactants tested for EOR application .....	24
Table 3.1: Composition of 1L of synthetic seawater .....	34
Table 3.2: Range and levels of reaction parameters using CCRD.....	36
Table 3.3: Anionic surfactants and foam boosters used for formulation .....	44
Table 4.1: Full factorial CCRD matrix of four variables in coded and natural units along with the observed and predicted responses (% epoxidation yield) .....	52
Table 4.2: ANOVA for the fitted quadratic polynomial model.....	63
Table 4.3: Comparison of epoxidation yield (%) for three studies.....	65
Table 4.4: Composition of HOE .....	73
Table 4.5: Comparison of FT-IR spectra of HOE and epoxides synthesized.....	75
Table 4.6: <sup>1</sup> H NMR peak table for HOE and epoxides synthesized from HOE .....	78
Table 4.7: Comparison of FT-IR spectrum for epoxides and ENS-750 .....	80
Table 4.8: <sup>1</sup> H NMR peak table for epoxides synthesized from HOE and ENS-750 ...	82
Table 4.9: The gradient of plotted lines for Figures 4.22 – 4.26 .....	85
Table 4.10: Results obtained for screening test .....	92







## CHAPTER 1

### INTRODUCTION

It is a well-known fact that about 60% of oil in place (OIP) remains uncovered in oil reservoirs after the primary and secondary oil recovery. In Malaysia as of 2003, the oil reserves and OIP amount to 3.5 billion stock tank barrels (BSTB) and 24.9 BSTB respectively, with the cumulative oil production at 4.9 BSTB. This brings to an average oil recovery factor of 34% [1]. The existing oilfields are entering the mature stage – the declining reservoir pressure and the increasing water and gas production point to the fact that the time when secondary oil recovery would no longer produce oil is approaching fast.

With considerable amount of oil left in the reservoir, the interest of implementing EOR techniques to the current existing fields is increasing in recent years. A screening of the Malaysian oilfields in the early 2000's found that most oilfields are suitable for CO<sub>2</sub> water-alternating-gas (WAG) method. This is due to the abundant source of seawater as well as CO<sub>2</sub>, as the produced gas in most oilfields has a high content of CO<sub>2</sub> [1].

However, one known problem with WAG processes is that the difference in densities between the gas phase – in this case the CO<sub>2</sub> gas, and water causes these two phases to separate the moment they are injected. And since gas travels at a much faster rate than water, water will be inefficient to control the mobility of gas and hence there will be early gas breakthrough, bringing about a poor recovery of oil. Recognizing this, PETRONAS has been showing interest in combining the conventional WAG with chemical EOR, termed as 'hybrid EOR' or FAWAG (foam-assisted WAG) for EOR applications in Malaysia [2], with the intent of reducing the mobility of gas and hence, increasing the oil production.

In FAWAG, foam is generated in situ by injecting a suitable surfactant in the gas phase. The foam functions to increase the apparent viscosity of the gas phase, hence lowering its mobility. FAWAG has been practiced in at least one oilfield in other parts of the world, and has been implemented successfully in Snorre Field, North Sea. FAWAG has produced an attractive 25-40 million USD at the then-oil prices for every 1 million USD cost of treatment [3].

Although the profit brought in by FAWAG is lucrative, issues such as the cost of chemicals for FAWAG, namely, surfactants as well as the market oil price play an important role in determining the execution of FAWAG. As will be discussed in Chapter 2, the cost of chemicals used in chemical EOR is high and the execution of a chemical EOR plan in oilfields depends largely on the market oil price. Studies on chemical EOR are only conducted as the oil price increases, because at low oil price, the profit brought in will be unnoticeable. Hence, ways should be looked into to lower the cost of surfactants. As it is, studies on the use of surfactants in EOR focus on minimizing the concentration of chemicals used.

One way to lower the cost of surfactants used in chemical EOR is to produce surfactants derived from natural resources. The surfactants used in EOR currently are all derived from petrochemical stocks. Petrochemical feedstocks are generally more expensive as they depend firstly on the market oil price and secondly on the availability. Since petrochemical feedstocks are non-renewable resources, its availability will only decrease and hence increase the cost of surfactants produced.

The primary benefits in substituting the petrochemical feedstock with natural oil resources are best summarized into three points. Firstly, they are renewable resources. Natural oils are renewable because they are derived from a continuous ecological cycle. They are constantly produced in nature and thus, they are available for commercial use with little risk of shortage. This is particularly so for inedible natural oils such as *Jatropha* oil.

Secondly, they are a cheaper starting material. The natural oils are easier to obtain as compared to petrochemical feedstocks, since they are renewable resources. When combined with cheap, simple procedures to produce surfactants, the natural oil-

derived surfactants projects an attractive substitute to lower the cost of chemicals used for EOR treatments.

Besides these, natural oils are known to produce less environmental impact, compared to petrochemical feedstocks. Natural oils are biodegradable, and are able to degrade into their natural, smaller components. The combination of cheap raw materials and processes leading to effective surfactants with little or no environmental harm makes natural oil-derived surfactants very desirable.

The starting material used for the synthesis of natural oil derived surfactants in this study would be the fatty acid methyl esters derived from natural oil. These derivatives are normally derived from the transglycerides of oil by treating with methanol.

### **1.1 Problem statement**

Many surfactants have been produced commercially for EOR applications. However, none of these surfactants were produced from natural oil resources. Besides using non-renewable resources as the raw material, commercial surfactants produced are a mixture of unknown additives, which could result in chromatographic separation in a complex environment such as the oil reservoirs. However, additives are inevitable as there are many issues to combat, e.g. high temperature, high salinity, and adsorption of material on reservoir rocks. Hence, in this research, we would develop our own surfactant formulation with the below target:

- Synthesizing surfactant using natural oil as a renewable resource
- Tolerant surfactant towards high temperature and high TDS
- Development of synthesized surfactants to improve foam stability

## **1.2 Objectives**

The objectives of this study are as follows:

- To synthesize and optimize the yield of nonionic surfactants from safflower oil derivatives (fatty acid methyl esters) through epoxidation and alkoxylation
- To characterize surfactants synthesized using analytical methods such as GC-MS, NMR and FT-IR
- To study the cloud point behavior of the synthesized surfactant in saline and high temperature conditions
- To formulate a surfactant blend using the surfactants synthesized and commercially available ionic surfactants to produce a surfactant formulation that can foam in the presence of oil and compatible with harsh conditions (100°C and 35000 ppm total dissolved solids)

## **1.3 Scope of study**

This research work is confined to the synthesis of surfactant, characterization and the early developments of the synthesized surfactant. The raw material for the synthesis of surfactants is confined to resources from natural oils. The scope of development is limited to the compatibility of synthesized surfactants to conditions of the reservoirs in Malaysia, particularly the Dulang oilfield. This translates to limiting studies to the condition of 100°C and in solutions with total dissolved solids (TDS) of 35000 ppm.

## **1.4 Organization of thesis**

Chapter 1 provides a brief introduction to the development of surfactant blends from natural oil resources that caters to the EOR interest in Malaysian oilfields. Chapter 2 gives a background and detailed literature review on the topic of this thesis.

It includes the development of chemical and gas EOR as reported by previous studies, as well as the synthesis of surfactants from natural oil resources. Chapter 3 describes the methodology adopted throughout the entire study, which includes: synthesis of surfactant, characterization of surfactants synthesized, and the formulation of a surfactant blend using the synthesized surfactant. Chapter 4 discusses the results obtained from the experiments conducted in the synthesis, characterization and formulation of surfactant blend. Chapter 5 concludes the findings and recommendations for future work is also presented in this chapter.





## CHAPTER 2

### BACKGROUND AND LITERATURE REVIEW

In this chapter, a background and a detailed literature review will be presented on the topics related to the research work conducted. Section 2.1 provides a detailed background and review for Enhanced Oil Recovery (EOR), particularly on the chemical and gas EOR methods. Section 2.2 and 2.3 present a background for surfactants, which play an important role in EOR and a detailed literature review on the synthesis of surfactants using natural oil as its raw material respectively. Finally in Section 2.4, a literature review is provided on the formulation of foaming agents which are composed of surfactants for EOR applications, combating issues such as foam stability against oil and elevation of cloud point of nonionic surfactants.

#### **2.1 Enhanced Oil Recovery**

It is estimated about 60% of Original Oil in Place (OOIP) remain unrecovered in reservoirs after primary and secondary recovery. The remaining oil exists as immobile oil droplets trapped in porous media due to high capillary forces caused by the high oil/water interfacial tension (IFT). As the discovery rate of giant fields have been declining for the last four decades [4], much study and work have been focused on developing mature oilfields, i.e. fields which are beyond primary and secondary recovery.

Tertiary recovery or better known as Enhanced Oil Recovery (EOR) is defined as the process of oil recovery enhancement method using sophisticated technique that alters the original properties of oil, rock and fluids of the mature oil field reservoirs.

### 2.1.1 Oil trap mechanism

Secondary recovery method is accomplished mainly through water injection into the reservoir to maintain the pressure of the reservoir. However, after a certain point, water injection is no longer useful to recover more oil. This is due to the oil being trapped in the reservoir rock's porous media by capillary action. There are two mechanisms for capillary trapping of oil: snap-off and bypass [5].

Snap-off occurs in pores having a high pore body to pore throat ratio. In this mechanism, the wetting phase (in this case, water) would form a collar around the non-wetting phase (oil), which would eventually cause the non-wetting phase to break off at the narrow throat. What results from the break off is immobilized oil droplet being trapped in the pore. Bypass mechanism on the other hand, occurs due to the competition of flow through the pores. Two forces that are taken into account in oil trapping in this mechanism are viscous force and capillary force. Viscous forces make the fluid flow faster in larger pores while capillary forces draw the displacing fluid (water) into the smaller pores. Thus, at low water injection rate with low water viscosity, water would be drawn preferentially into smaller pores and displaces oil in the smaller pores, hence bypassing the larger pores.

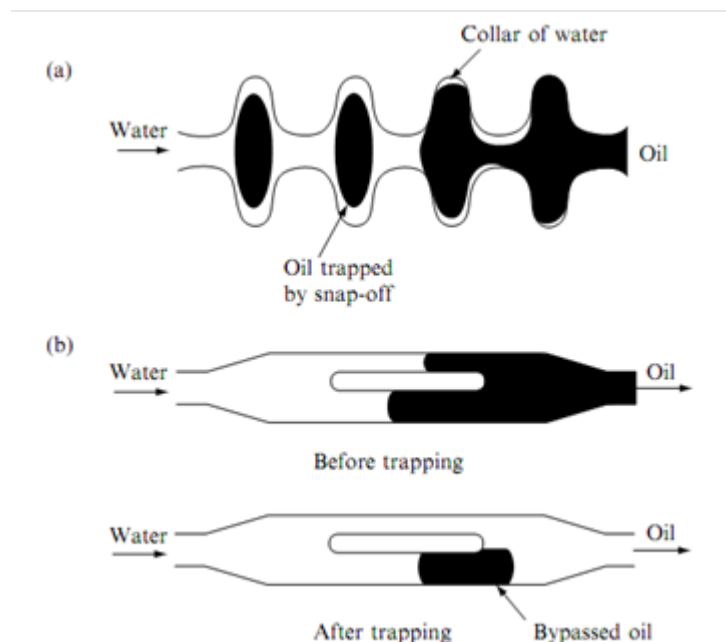


Figure 2.1: Oil trapping by (a) snap-off mechanism and (b) bypass [5]

The amount of oil trapped in a reservoir is dependent on the ratio between viscous forces and capillary forces. This relationship between viscous and capillary forces is expressed in a dimensionless number known as capillary number,  $N_c$ :

$$N_c = \frac{\mu v}{\gamma_{ow}}$$

where  $\mu$  = viscosity of displacing fluid,

$v$  = velocity of displacing fluid, and

$\gamma_{ow}$  = interfacial tension between oil and water

Normally, the residual oil saturation becomes constant below a certain capillary number value,  $N_c$ , typically in the range of  $10^{-4} - 10^{-5}$ . The  $N_c$  value of water flood on the other hand is  $10^{-7}$ , which is even lower than that of residual oil saturation, thus making water ineffective in sweeping oil out of reservoir. Above a certain range of  $N_c$  known as the critical  $N_c$ , the residual oil saturation after flooding decreases almost linearly with  $\log N_c$ .

Thus, in order to achieve good oil recovery, the  $N_c$  value must be high. This can be achieved by increasing the viscous forces i.e. by increasing the viscosity and velocity of the displacement fluid or decreasing the interfacial tension (IFT) between oil and displacing fluid, or combining both. Increasing the  $N_c$  value by increasing viscous force is not favorable, as this requires very high-pressure condition, which can cause reservoir rock fracture. The other parameter, the capillary force reduction, which is governed by the IFT between oil and water, becomes an important approach adopted to increase  $N_c$ . This can be achieved through surfactant flooding or gas flooding.

### **2.1.2 EOR methods**

The techniques used in EOR are classified into four methods: chemical, thermal, gas and microbial. Techniques used can be from a single method or a combination of any two or more. In this research, only two methods will be discussed: chemical and gas.

#### *2.1.2.1 Chemical*

Chemical EOR is a method whereby chemicals are added into injected water to reduce the IFT between water and oil, and to alter mobility. Chemicals used are polymer, surfactant and alkali. A single chemical or a combination of two or all three chemicals can be used.

Due to the high cost of chemicals, chemical EOR is not a method of choice as compared to other methods to further increase the recovery of oil. This is evident in the statistics compiled by Alvarado and Manrique [6] (see Figure 2.2). Except for the 1980's, the use of chemicals to enhance the recovery of oil comes after thermal and gas methods. To date, the chemical most used in chemical EOR is polymer. Polymer flooding became the most important technique used in the 1980's [7] due to economic interests. Surfactants cost much more than polymer and a high concentration of surfactant was usually required for a proper surfactant flooding. However, as surfactant technology advances (i.e. lower concentrations of surfactants needed) and lower cost of chemicals, more parties are showing interest to chemical EOR and numerous laboratory studies and screening can be found on re-evaluating the potential of chemical EOR [6, 8].

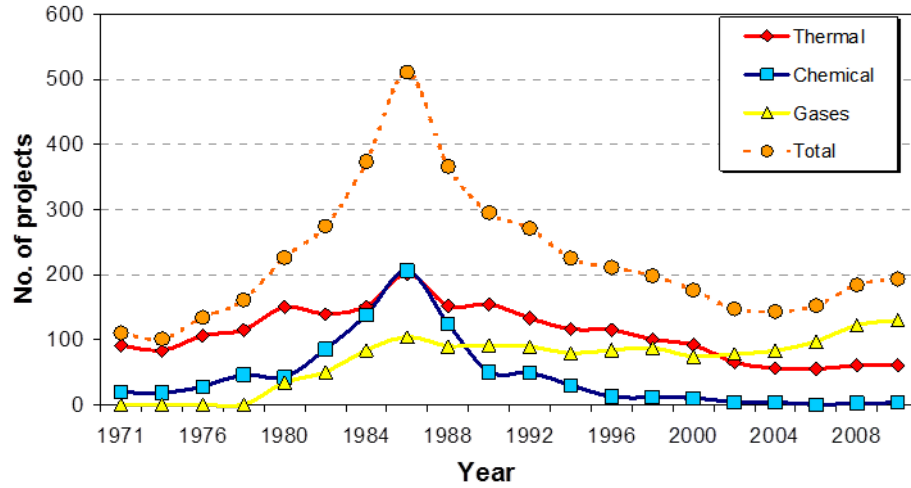


Figure 2.2: Number and classification of EOR projects for the US from 1971-2010 [6]

#### 2.1.2.2 Gas

EOR by gas injection is by far the most common kind of EOR method. The gases used that have been reported are air, nitrogen ( $N_2$ ), carbon dioxide ( $CO_2$ ) and hydrocarbon gas (produced gas). Of all these  $CO_2$  remains the most commonly used gas in gas EOR [6]. In this method, gas is usually injected alternately with water to aid mobility.

Water-alternating-gas (WAG) is an EOR technique first applied in North Pembina field in Alberta, Canada in 1957 [9]. As the name suggests, gas and water are injected alternately into the reservoir in repeated cycles in this technique. Injected gas acts as ‘replacement units’ to displace oil droplets and occupies part of the pore spaces, thereby mobilizing the oil. Water is injected to control the mobility of gas injected, as well as displacing some of the remaining oil and gas [10]. Another view is that the recovery of oil obtained from WAG is attributed to contact of unswept zones i.e. attic or cellar portion of the reservoir brought about by the segregation of gas towards the top or accumulation of the denser water to the bottom of the formation[11]. Thus, WAG injection is thought to be able to improve oil recovery by combining better

mobility control and contacting unswept zones for an improved microscopic displacement.

To be successful in lowering the residual oil saturation in reservoir, the mobility ratio between displacing fluid (gas) and displaced fluid (oil) is thought to be ‘favorable’ when it is less than 1. The mobility ratio is defined as follows:

$$M = \frac{(k/\mu)_{displacing}}{(k/\mu)_{displaced}}$$

where  $k$  = effective or relative permeability and  $\mu$  = viscosity.

An extensive review was done by Christensen et al. [11] on WAG field experience. Christensen compiled from available literature a total of 60 field trials implementing WAG from 1957-1986. From the results obtained for these fields, it was observed that most field applications result in around or less than 5% of increment in recovery with very few exceptional cases reaching 20%.

This moderate recovery rate is thought to be attributed to an early gas breakthrough which is a result of poor mobility control of gas. This in turn limited oil production. To this, the idea of using foam to enhance WAG process was first initiated in the 1990’s. Foam-assisted water-alternating-gas (FAWAG) is a technique employing the combination of two methods: gas and chemical. In this technique, surfactants, in the form of foam are applied during WAG for increased gas mobility control. With the application of foam, the apparent viscosity of injected gas increases, leading to a decrease in gas mobility. The only FAWAG field application found in the literature is in Snorre Field, North Sea. It is also the biggest foam application in the oil industry [12]. After many years of active research and two-year planning, foam injection was started in the Central Fault Block, Snorre Field in 1998 [13-15]. Few more literatures on Snorre field followed after this foam injection and a conclusion is drawn. It is found that foam was successful to delay the breakthrough time of gas injected, and the Gas-Oil-Ratio (GOR) is considerably lowered compared to gas injection cycles prior to foam treatment [3, 12]. A laboratory study conducted recently by Andrianov et. al showed that with foam, the recovery of oil can be increased by as

much as 10% above what is achieved by a gas injection [16]. With this successful application, FAWAG has the potential of increasing oil recovery beyond what is capable of a WAG process alone.

## **2.2 Surfactant**

Surfactants, also known as ‘surface active agents’, are organic compounds with at least one lyophilic (solvent-loving) group and at least one lyophobic (solvent-fearing) group in the molecule [17]. When the solvent used is water, surfactant can be defined as organic compounds with at least one hydrophilic (water-loving) group and at least one hydrophobic (water-fearing) group. As the name suggests, surfactants are compounds that are active at the surfaces. Surfactants have the tendency to adsorb at the surfaces and the interfaces of two dissimilar fluids. Due to its amphiphilic nature, surfactants possess the ability to solubilize both in water and oil (non-polar). The hydrophilic part (polar head) of the surfactants solubilize in water while the hydrophobic part (non-polar tail) solubilize in oil. When there are two immiscible phases i.e. oil and water present in a system, surfactants adsorb at the interface between water and oil and lower the interfacial tension between these two immiscible phases, making it possible for one (called the dispersed phase) to exist in another (the continuous phase). Due to this special characteristic of surfactants, much research have been conducted to explore the application of surfactants in soaps, detergents, pharmaceutical, cosmetics, agriculture, food processing, petroleum industry and many more [18].

When surfactant molecules are introduced into a water and oil system, the surfactants tend to remain and adsorb on the oil-water interface. If the concentration of surfactant is increased continually in the system, the surfactant molecules start assembling into organized structures called micelles. The minimum concentration required to commence a micelle formation is called Critical Micelle Concentration (CMC). It is one of the very important properties of surfactants. Many of the solution properties of the surfactants changed after the CMC. As seen in the Figure 2.3, conductivity of the surfactant solution decreased linearly and this trend changes after

its CMC is achieved. Surface tension also decreased and after the CMC is achieved, it becomes constant. Turbidity increases with increasing surfactant concentration and a sharp increase of turbidity is detected after achieving the CMC.

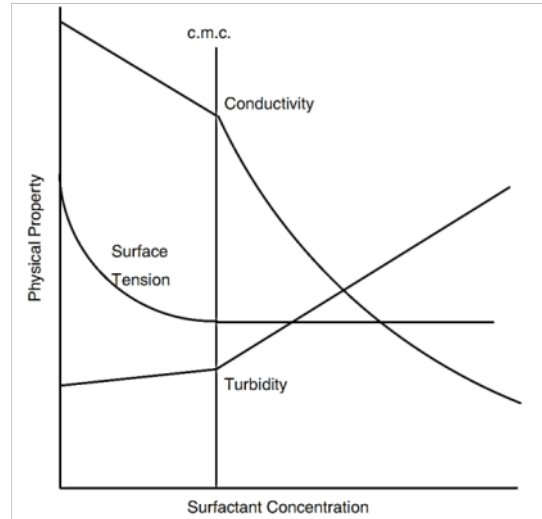


Figure 2.3: Some important indicators of micelle formation: abrupt changes in solution conductivity, a discontinuity in the surface tension-concentration curve; a sudden change in solution turbidity [19]

Micelles are dynamic structures that form and break in the speed of microseconds [20]. When the continuous phase is water, surfactants encapsulate the oil droplet in the micelle by forming a core with their non-polar tails while their polar heads remain in the water, making an outer shell. Conversely, when the continuous phase is oil, the micelles formed by the polar heads make an inner core around the polar water droplet and non-polar tails form the outer shell in the oil. These micelles are called reverse micelles (Figure 2.4).

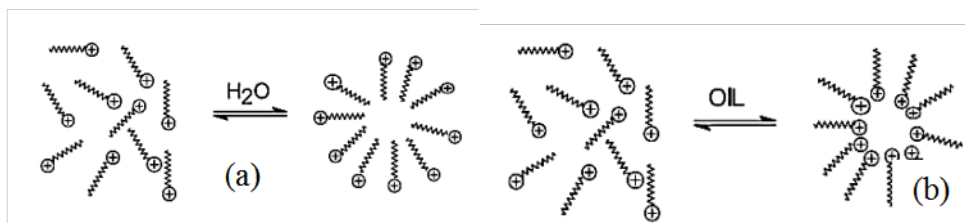


Figure 2.4: Formation of (a) micelle and (b) reverse micelle [20]



### 2.2.1 Types of surfactant

Depending on the charge of the hydrophilic polar head of the surfactant when in contact with water, surfactants can be classified into four classes:

#### 2.2.1.1 Cationic surfactant

Cationic surfactants are surfactants with a positively charged hydrophilic head when dissolved in water. Cationic surfactants that are hydrolytically stable exhibit more aquatic toxicity than any other class of surfactants [5], rendering these surfactants unappealing for offshore applications due to environmental issues. Cationic surfactant is also not a suitable candidate to be considered for EOR applications in sandstone reservoirs. Due to the negatively charged rocks, cationic surfactants would be electrostatically attracted and adsorb preferentially on silica rocks. To overcome the excessive adsorption, more surfactant is used to increase its effectiveness. This causes the process to become uneconomical. Examples of cationic surfactants are:

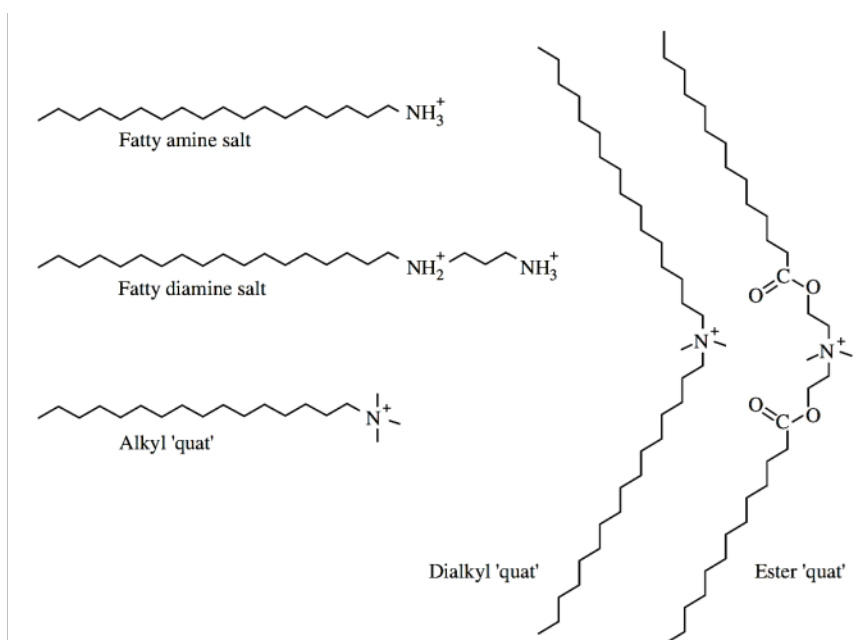


Figure 2.5: Some examples of cationic surfactants [5]

### 2.2.1.2 Anionic surfactant

Anionic surfactants are the largest surfactant class produced among other classes. Anionic surfactants are surfactants with negatively charged polar head groups in aqueous solution. Examples of polar head for anionic surfactants are carboxylates, phosphates, sulfates and sulfonates. Anionic surfactants are generally sensitive toward hard water [5]. Some of the more popular anionic surfactants that have been used for EOR applications are internal olefin sulfonate (IOS) [21, 22] and alpha-olefin sulfonate (AOS) [13].

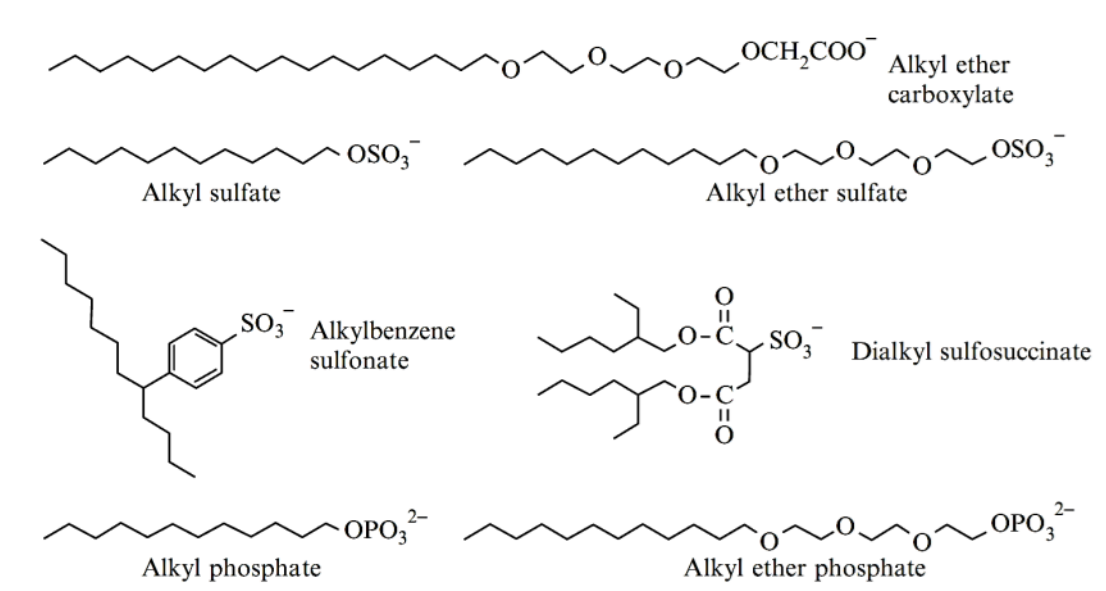


Figure 2.6: Some examples of anionic surfactants [5]

### 2.2.1.3 Amphoteric surfactant

Amphoteric surfactants contain two charged groups of different polarities. Depending on the pH of the aqueous solution, amphoteric surfactants could be either positively or negatively charged. The source of positive charge is always ammonium while the common source for negative charge is carboxylate [5]. At low pH, amphoteric surfactants are positively charged while at higher pH, they are negatively charged. Due to the high cost of production, amphoteric surfactants are not the surfactant of choice in the industry.

There are two groups of amphoteric surfactants manufactured and used commercially: real amphoterics and betaines [23]. Betaines are zwitterionics – they do not exhibit ionic properties with regards to changes in solution's pH. This is due the fully quaternized nitrogen structure in betaines. Amphoteric surfactants are mostly employed in personal care products due to their mildness.

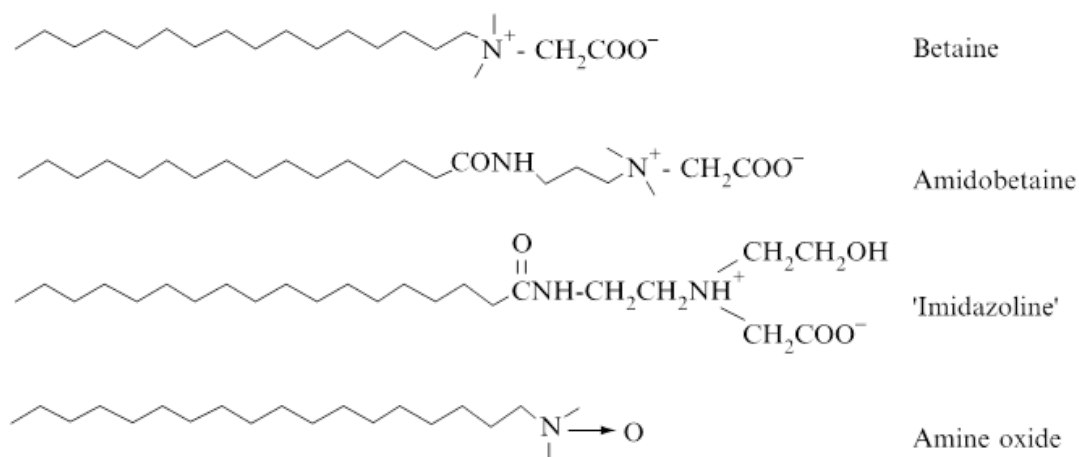


Figure 2.7: Some examples of amphoteric surfactants [5]

#### 2.2.1.4 Nonionic surfactant

Nonionic surfactants are the second largest surfactant group produced in the industry with about 45% of total surfactant production [18]. Nonionic surfactants are surfactants that do not produce any polar charge in aqueous solutions. The polar head of nonionic surfactants are composed of organic groups containing oxygen atom (O). The most common polar head for nonionic surfactants is varying chain lengths of ethylene oxides (EO). The solubility of nonionic surfactants in water depends on the O-H bonding between the surfactant and water. One advantage of nonionic surfactants is that nonionic surfactants are more tolerant toward hard water [24] as compared to ionic surfactants. This would be an important quality to be possessed by surfactant formulations formulated for use with seawater that has high  $\text{Ca}^{2+}$  and  $\text{Mg}^{2+}$  contents.

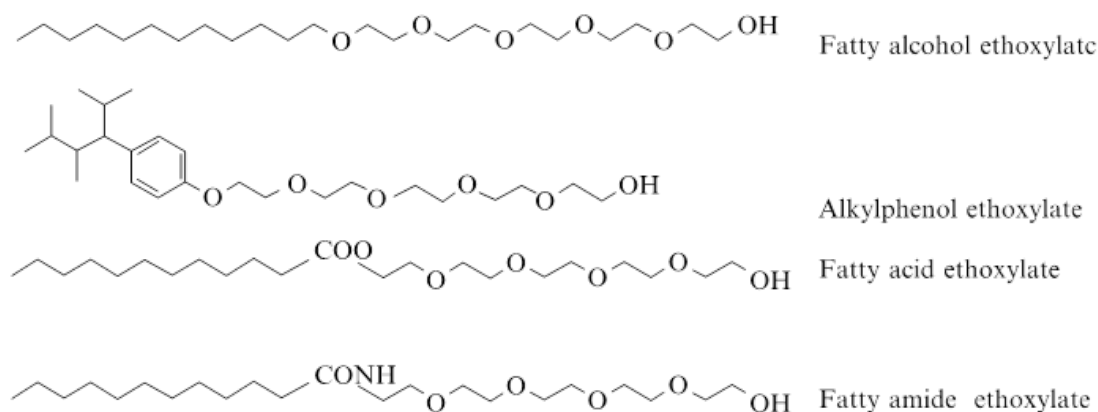


Figure 2.8: Some examples of nonionic surfactants [5]

One unique characteristic of nonionic surfactant is that nonionic surfactant exhibits clouding behavior when the nonionic surfactant solution is heated up to a certain temperature. The temperature at which the nonionic surfactant solution shows turbidity is called the cloud point (CP). Below this temperature, the nonionic surfactant solution exists in a single phase. Above this temperature, nonionic surfactants lose sufficient water solubility and aggregates together to form a cloudy dispersion, creating two phases [25]. This phase separation is reversible. On cooling the solution to a temperature below its CP, the two phases merge to form a clear solution again. The clouding behavior is believed to be attributed to the sudden dehydration of the EO chain at the CP. Dehydration of the EO chain is thought to be induced by the conformational change of the EO chain associated with temperature rise [26]. As the temperature of the solution increases, the micelle weight of nonionic surfactant is believed to increase (due to the aggregation of surfactants) [27] and becomes much larger with increases in temperature until the nonionic surfactants separate out of water. When nonionics separate out of water, these surfactants lose their function. As such, it is important to determine the CP of nonionic surfactant used as suspension, emulsions, foams and ointments containing nonionic surfactants become unstable when heated in the vicinity of the cloud point [25].

### 2.2.2 Foam

Foam is formed when gas (the dispersed phase) is dispersed in a liquid; usually water (the continuous phase). Foam is the system formed when pockets of gas are trapped in a liquid. In order for foam to be generated, there needs to be a mechanical work in order to introduce gas into the liquid. However, due to the high surface tension between gas and liquid, gas bubbles formed in liquid via mechanical work quickly travel to the surface of the liquid to be joined to the gas phase. The surface tension between gas and liquid needs to be reduced in order for foam to be generated. This is accomplished by introducing surfactants into the system. Surfactants in a solution are adsorbed on the surface of the solution and lower the surface tension between gas and water. When gas is introduced into the surfactant solution, foam is generated.

Foams have a distinct structure. Plateau's laws describe the structure possessed by stable foam. For a foam system to be stable, bubbles are arranged in order to possess minimal surface area as well as for equal distribution of surface tension forces along the liquid films of the bubbles [28, 29]. The bubbles in a foam system arrange themselves into polyhedral in such a way where three bubbles films (lamellae) always come together at an angle of  $120^\circ$ . The point where these three bubbles meet is the Plateau border. In three dimensions, four bubbles meet at a point at the tetrahedral angle ( $\sim 109^\circ$ ).

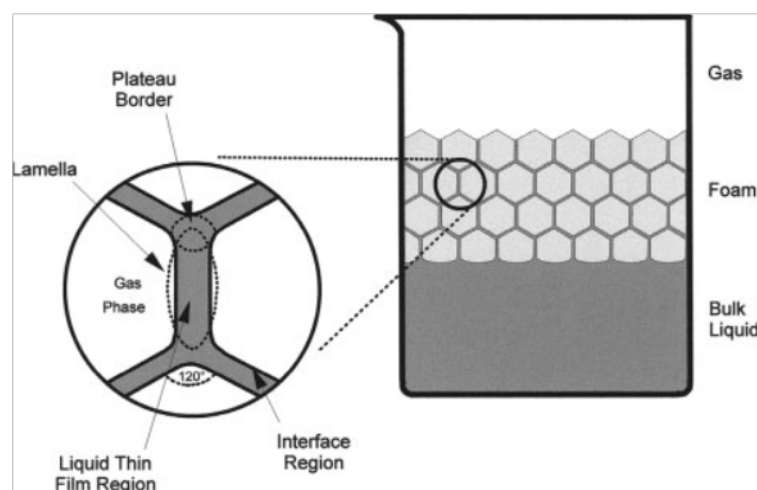


Figure 2.9: A foam system with details on a foam lamella [28]

Figure 2.10 shows the foam structure during foam generation and drainage. When foam is freshly generated, the foam consists of spherical bubbles separated by thick films. This is called wet foam or *kugelschaum*. As the foam ages the liquid within the foam films drain out due to gravity. The structure of the foam would gradually change and adapt to the more stable polyhedral structure with relatively planar films separating the bubbles. This is called the dry foam or *polyederschaum*. By now the drainage of the liquid is no longer caused by gravity but capillary forces, depicted in the Young-Laplace equation:

$$\Delta p = \frac{2\gamma}{r}$$

where  $\gamma$  is the surface tension and  $r$  is the curvature radius.

Due to the curvature ( $r$ ) of the interface of water/air at the Plateau border, the pressure at the border region is lower ( $P_B$ ). Since the interface is flat along the thin film, a higher pressure resides here ( $P_A$ ). This pressure difference forces the liquid to flow towards the Plateau borders causing thinning of the films. These thin foam films rupture easily as they are more susceptible to external disturbances such as vibration, shock and temperature change [30]. The rupture of the foam films causes foam to collapse.

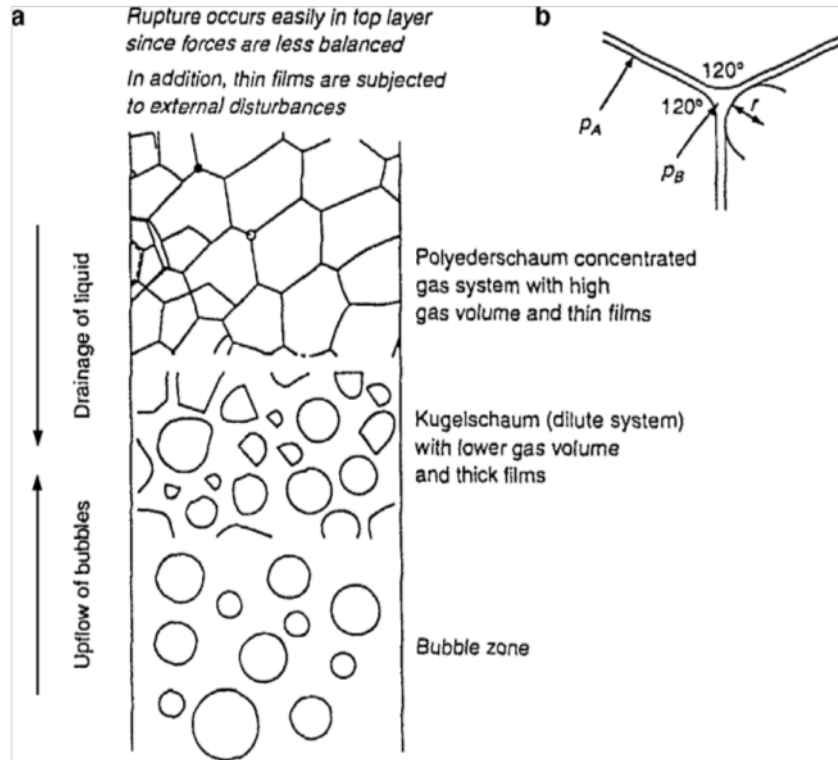


Figure 2.10: a) Foam structure during the process of foam generation and liquid drainage. b) Plateau border with  $P_A > P_B$ , causing liquid to flow into the borders [30]

### 2.2.3 Surfactants in EOR

The idea of using surfactants to enhance the recovery of oil dates back to as early as 1927 [31]. The use of low concentrations of detergent (surfactant) to reduce the interfacial tension (IFT) between water and oil is found in patents from the late 1920's and early 1930's [32]. Over the years, extensive studies have been conducted for the use of surfactants in reducing IFT between oil and water. The areas of study covered are surfactant adsorption on rock, wettability alteration, microemulsion formation, structure of surfactant and use of co-surfactants such as alkali. Hirasaki et. al [8] compiled a review on the advances in surfactant EOR and it is found that the technology of surfactant flooding in EOR has advanced to overcome causes which result in many past failures as well as reducing the amount of surfactant needed.

Unlike surfactants for IFT reduction, the application of surfactants in foam for mobility control was first introduced more than fifty years later in 1980 by Lawson

and Reisberg [33]. Since then, laboratory experiments have been conducted to better understand the mechanism of foam mobility control. Field tests have been conducted [34, 35] but only one known field application, Snorre Field, has been reported in the literature [12].

Foam increases the apparent viscosity of gas, hence lowering the mobility of gas, resulting in a slower gas breakthrough [12]. As such, studies were conducted to evaluate foam as a potential substitute for polymer in alkaline-surfactant-polymer (ASP) flooding [8, 36]. Li et al. [36] reported that ASP process experiments using 1-D sandpacks having the polymer drive replaced by a foam drive, which is generated in situ by surfactant alternated with gas injected, is equally efficient. This is particularly useful for reservoirs with high temperatures, as polymer tends to degrade prematurely at high temperature and thus loses its function as a water viscosifier [37].

#### *2.2.3.1 Surfactants as mobility control agent*

In the literature, foam related studies for EOR applications have been conducted using commercially available surfactants. The surfactants used are ionic surfactants, with only one study conducted on nonionic surfactants. In Lawson and Reisberg's study (the first study on foam as mobility control agent), petroleum sulfonate, an anionic surfactant was used [33]. In the 1990's, the most famous study is perhaps the study conducted on evaluating foam potential for Snorre field in North Sea. The surfactant used was alpha-olefin sulfonate (AOS), another anionic [13]. Other types of anionic surfactants found in the literature are sodium dodecyl sulfate (SDS), internal olefin sulfonate (IOS), diphenyletherdisulfonate, ammonium propoxylate sulfate, alcohol ethoxysulfate and alcohol ethoxysulfonate, with more recent studies focusing on AOS, IOS and SDS [16, 36, 38-41].

Kuehne et. al [42] evaluated 5 different surfactants: 3 anionic and 2 nonionic surfactants. The anionic surfactants are AOS, alcohol ethoxysulfate and alcohol ethoxysulfonate while the nonionics are alkyl phenol ethoxylate and ethoxy alcohol. It was found that surfactants containing alcohol group are weak foamers. There are also



studies on amphoteric surfactants (betaine-based) on boosting the tolerance of foam towards crude oil [16, 38]. These studies will be discussed in Section 2.4.1.

In the literature, the surfactants reported for foam studies are derived from petrochemical feedstocks. None of the reported surfactants used were derived from natural oils.

## **2.3 Synthesis of surfactant**

### **2.3.1 Natural oils as raw material**

Surfactants are produced globally from two raw materials: petrochemical feedstocks and renewable resources (natural oils). Due to the increasing costs for petrochemical feedstocks [43, 44], natural oils as potential substitute for petrochemical feedstocks are becoming more attractive. Besides cost factor, environmental factor contributes to the gradual increase in interest toward developing surfactants from natural oils. Factors such as low toxicity, good biocompatibility and rapid biodegradation are the main reasons for increasing industrial interests toward natural oils [45]. Besides these factors, switching raw material from non-renewable to renewable resources was one of the strategies proposed to lower the CO<sub>2</sub> emission from industrial processes [46].

Natural oils are triglycerides of fatty acids. The fatty acids found in natural oils range from 10 – 30 carbon chain length. The composition of fatty acids varies according to types of oil. The major fatty acids found in natural oils are fatty acids with carbon chain length 16 and 18. A comparison between surfactants that have been tested for EOR applications (Table 2.1) and fatty acids from natural oils shows that the carbon chain lengths for major fatty acids are compatible to that of hydrophobic tail of commercially available surfactants. This gives a strong support to venture into the possibilities of using surfactants derived from natural oils as a substitute for commercially available surfactants produced traditionally from petroleum feedstocks.

Most reactions involving fatty acids are those occurring at the carboxylic head. Literature found from the 1980's suggests that only around 10% of reactions involving natural oils are on transforming the alkyl chains, mainly the double bonds present on the alkyl chains [47]. To this, Biermann et. al [48] compiled a review on the various types of chemical reactions reported for alkyl chains of fatty acids. In recent years, more studies have been conducted to utilize the double bonds found in the alkyl chains of natural oils, especially on biodiesel studies [49-51]. With regards to surfactant studies, only one report has been found on the synthesis of nonionic surfactant by utilizing double bonds in fatty acids [52]. This report will be discussed further in Section 2.3.3.

Table 2.1: Commercially available surfactants tested for EOR application [53]

Descriptive Name	Abbreviated Chemical Formula*
C <sub>11-13</sub> Alkyl Benzene Sulfonate (ABS)	$bC_{11-13}(C_6H_5)-SO_3^-$
C <sub>16</sub> <i>o</i> -Xylene Sulfonate	$C_{16}-(C_8H_{12})-SO_3^-$ where $C_8H_{12}$ = <i>o</i> -xylene
Secondary Alkane Sulfonate (SAS)	$R-CH(SO_3^-)-R'$ where $R + R' = C_{14}-C_{17}$
C <sub>14</sub> AOS	$bC_{11}-CH(OH)-CH_2-CH_2-SO_3^-$ ( $\approx 75\%$ ) $bC_{11}-CH=CH-CH_2-SO_3^-$ ( $\approx 25\%$ )
C <sub>16-18</sub> AOS	$bC_{13-15}-CH(OH)-CH_2-CH_2-SO_3^-$ ( $\approx 75\%$ ) $bC_{13-15}-CH=CH-CH_2-SO_3^-$ ( $\approx 25\%$ )
C <sub>20-24</sub> AOS	$bC_{17-21}-CH(OH)-CH_2-CH_2-SO_3^-$ ( $\approx 75\%$ ) $bC_{17-21}-CH=CH-CH_2-SO_3^-$ ( $\approx 25\%$ )
C <sub>15-18</sub> IOS	$R-CH(OH)-CH_2-CH(SO_3^-)-R'$ ( $\approx 75\%$ ) $R-CH=CH-CH(SO_3^-)-R'$ ( $\approx 25\%$ ), where $R+R' = C_{12-15}$
C <sub>16-17</sub> Alcohol 3-Propoxy Sulfate (C <sub>16-17</sub> -(PO) <sub>3</sub> -SO <sub>4</sub> )	$bC_{16-17}-O-[CH_2(CH_3)CH-O]_3-SO_3^-$
C <sub>16-17</sub> Alcohol 5-Propoxy Sulfate (C <sub>16-17</sub> -(PO) <sub>5</sub> -SO <sub>4</sub> )	$bC_{16-17}-O-[CH_2(CH_3)CH-O]_5-SO_3^-$
C <sub>16-18</sub> Alcohol 5.7-Propoxy Sulfate (C <sub>16-18</sub> -(PO) <sub>5.7</sub> -SO <sub>4</sub> )	$C_{16-18}-O-[CH_2(CH_3)CH-O]_{5.7}-SO_3^-$
C <sub>16-17</sub> Alcohol 7-Propoxy Sulfate (C <sub>16-17</sub> -(PO) <sub>7</sub> -SO <sub>4</sub> )	$bC_{16-17}-O-[CH_2(CH_3)CH-O]_7-SO_3^-$

\* b = Branching in the carbon chain.

## 2.3.2 Epoxidation

Epoxidation is a reaction whereby a double bond is transformed into an epoxide (oxirane) group. Epoxides have been applied in detergents, polymers, resins, and lubricants and as plasticizers and additives for polyvinyl chloride; and more recently, as intermediates in chemical reactions [54-57]. With such vast applications, there have been extensive studies conducted on epoxidation.

Traditionally, an organic acid such as formic acid or acetic acid is used with hydrogen peroxide to generate peroxyacids as oxygen carriers [58]. Since then, there have been studies on epoxidation using enzymatic peroxygenase [59, 60] and heterogeneous catalysts [61, 62] to enhance the yield of epoxides. These experiments, however, require long reaction time [61] and do not produce yield higher than 60% [61, 62]. Also, the costs for these heterogeneous catalysts are extremely expensive hence making them unsuitable for larger scale production.

Figure 2.11 shows the mechanism of an epoxidation reaction using formic acid to generate peroxyacid. Oxirane formed possesses high strain energy due to the three-membered oxirane group. As such, epoxides possess high reactivity and the oxirane ring formed can easily undergo ring-opening reaction during reaction, which is highly undesirable. To better understand the kinetics involved, the ring opening reaction has been studied extensively and there are reports on the kinetics of ring opening [55, 63]. From the literature, it seems that reaction temperature plays a significant role in epoxidation. Campanella et. al [54] found that reaction temperature has a significant impact to epoxidation yield. Increase in the reaction temperature is significantly detrimental for achieving high yields. Gan et. al did a kinetic study on ring opening reaction of epoxides [55]. The ring opening reaction is associated with the presence of hydrogen peroxide and formic acid at elevated reaction temperature. Goud et. al [64] used toluene as an organic solvent during epoxidation at elevated temperature and found that the inert solvent helped to stabilize the epoxidation reaction and minimize the ring opening reaction. However, it has been demonstrated by kinetic studies that although the rate of ring opening can be reduced in the presence of toluene, the conversion efficiency is compromised [65].

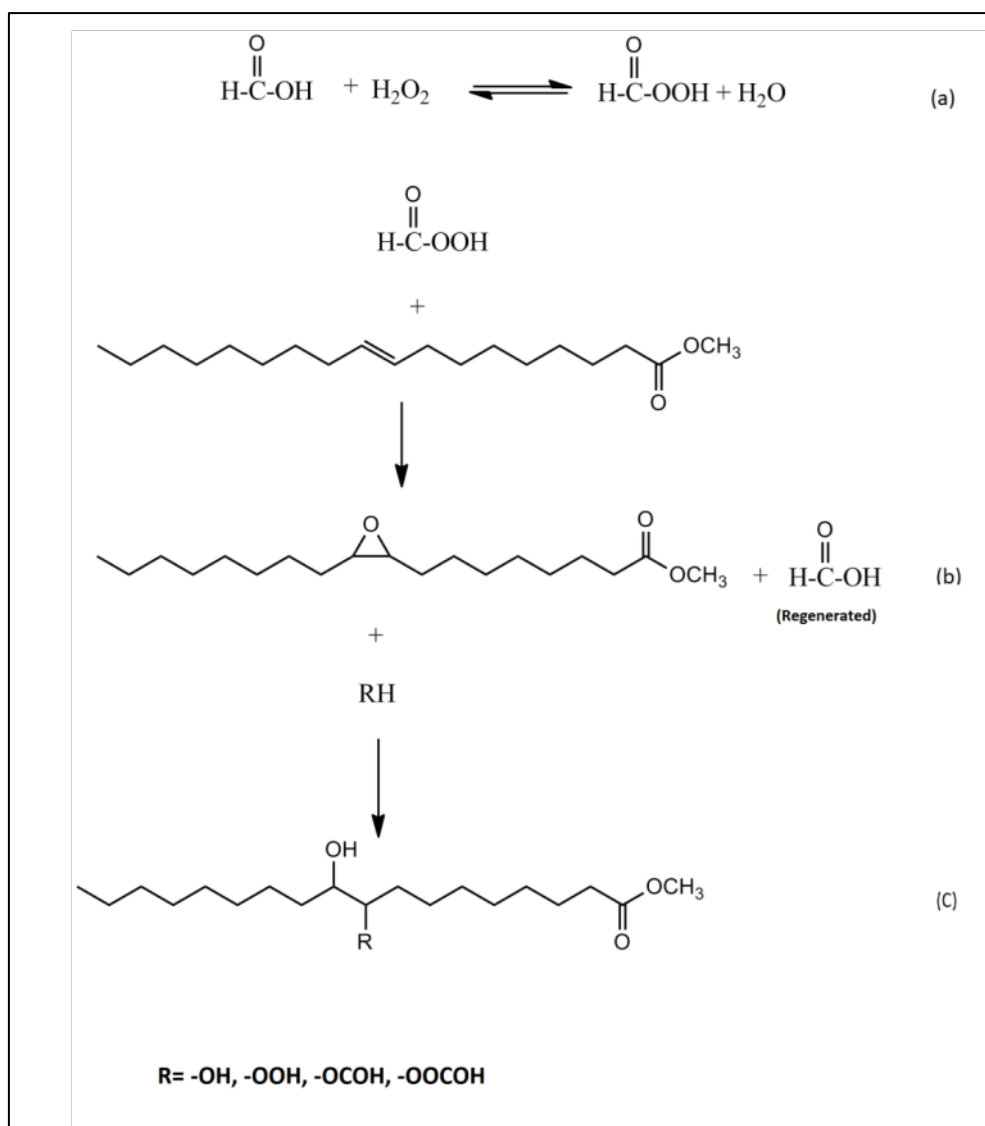


Figure 2.11: (a) In-situ generation of peroxy formic acid (b) Epoxidation of oleic acid methyl ester (c) Ring opening of epoxide [54, 55]

### 2.3.3 Attachment of ethylene oxide (EO) chain

Attachment of EO chains to fatty acids as side chain attachment has not been widely studied. Only one study, reported by Hedman et. al [52] describes the attachment of EO chain with various lengths onto the fatty acids hydrocarbon chains. The source of EO used in this study was polyethylene glycol (PEG) methyl ether. Fatty acids were converted to fatty acid methyl esters (FAMES) to protect the

carboxylic group of the fatty acids. Three PEGs were used – PEG 350 (corresponding roughly to 7 units of EO), PEG 550 (11 units of EO) and PEG 750 (16 units of EO). The yield reported for this attachment was 98%.

The catalyst used for the attachment was boron trifluoride ( $\text{BF}_3$ ).  $\text{BF}_3$  is a widely used catalyst especially in organic synthesis reactions due to its Lewis acid property. It is used widely in esterification reactions [66]. However, due to its reactivity, there are a lot of side reactions due to the use of  $\text{BF}_3$  as a catalyst in organic syntheses [66]. Hence, there needs to be an optimum amount of  $\text{BF}_3$  used in order to obtain high yield with minimum occurring side reactions.

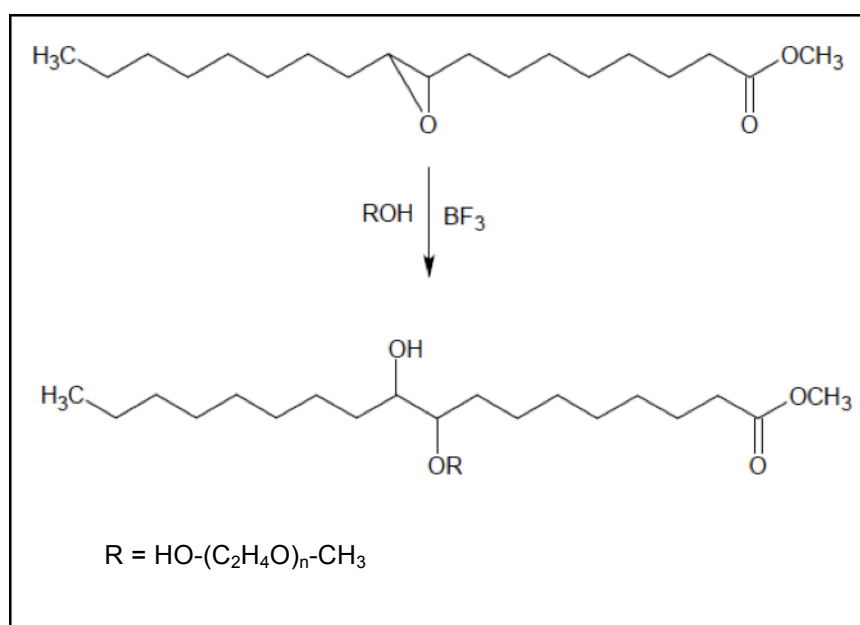


Figure 2.12: Alkoxylation reaction – the attachment of EO chain

## 2.4 Formulation of foaming agents for EOR applications

Commercial surfactants are mixtures of multiple species [8] for the purpose of combating different issues encountered during the application of the commercial surfactants. As the composition of mixtures is not revealed, questions are raised as to whether the commercial surfactant solutions undergo chromatographic separation, i.e.

preferential adsorption on pore surfaces or preferential partitioning into the oil phase of some species, can cause interfacial tension (IFT) variations with possible adverse effects on oil recovery [8]. However, a mixture is inevitable as the matrix of oil reservoir is very complicated and would need more than one chemical compound to perform satisfactorily.

#### 2.4.1 Foam stability

One of the major concerns with foam is the stability of the foam generated. It is well known that oil, particularly light crude oils, destabilize foam. The mechanisms of foam stability against oil have been studied [28, 67, 68]. Garrett [67] used three coefficients to explain the mechanisms of oil destabilizing foam: the entering coefficient  $E$ , the spreading coefficient  $S$ , and the bridging coefficient,  $B$ . These coefficients are defined as follows:

$$E = \gamma_{AW} + \gamma_{OW} - \gamma_{AO}$$

$$S = \gamma_{AW} - \gamma_{OW} - \gamma_{AO}$$

$$B = \gamma_{AW}^2 + \gamma_{OW}^2 - \gamma_{AO}^2$$

where,  $\gamma_{AW}$ ,  $\gamma_{OW}$ , and  $\gamma_{AO}$  stand for air/water, oil/water, and air/oil surface or interfacial tensions. When the entering coefficient,  $E$ , is positive, a drop of oil is predicted to be drawn up into the lamellar region between two bubbles. The entry of oil droplet into the lamellar region and thus breaching the water/air interface causes the film to lose its foam stabilizing capability and thin to the rupture point. When the bridging coefficient,  $B$ , is positive, the oil droplet bridges the lamellar region between the two adjacent bubbles. When the spreading coefficient,  $S$ , is positive, the oil droplet in the lamella region is predicted to spread as a lens over a foam. The spreading of an oil droplet over a foam lamella causes the foam lamella to rupture.

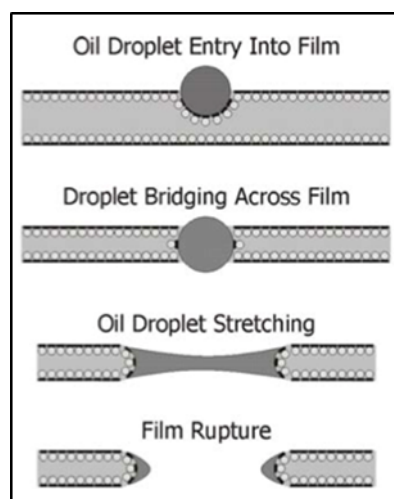


Figure 2.13: Oil destabilizing foam mechanism [69]

Foam boosters can be used to combat the problem of foam instability against oil. These foam boosters are usually betaines (amphoteric surfactants). While the above mechanism explains the stability of foam, it cannot explain the role of betaine in enhancing the foam stability against oil. Basheva et. al conducted a study to determine the role of betaine as foam booster in the presence of silicon oil [70]. In this study, they found that there is no correlation between coefficients E, S, and B, and foam stability when betaine is present. Instead, they found that the barrier to drop entry is much higher in the presence of betaine. The critical capillary pressure for the oil drop entry into the air/water interface was found to increase strongly with the relative concentration of the betaine. This finding shows that the main role of betaine as a foam booster in the studied systems is to increase the barrier to drop entry, which leads to suppressed activity of the silicone oil as an antifoam.

Two recent, notable studies were conducted for formulations combining surfactants with good foaming ability and surfactants with high tolerance toward oil to produce foams with high stability in the presence of oil. Li et. al [38] reported a blend of anionic surfactants (ammonium propoxy sulfate and IOS) with lauryl betaine as a good foaming agent even in the presence of oil. In this formulation, betaine constituted as much as two thirds of the entire blend. Andrianov et. al [16] did a study on the effect of carbon chain length in the oil molecule on foam stability and found

that foam stability increases with increasing carbon chain length. The two surfactants used as foaming agent were AOS and SDS, and the two surfactants used for high oil tolerance were FluoroChemical (fluorinated surfactant – nonionic) and fluoroalkyl betaine (amphoteric). The experiments conducted included AOS and SDS used singly as well as a combination of a foaming agent and high oil tolerance surfactant. The AOS-FluoroChemical blend was found to be the best. However, the recipes of the blends used were not provided in this study.

#### **2.4.2 Elevation of cloud point**

As discussed in Section 2.2.1.4, a unique characteristic of nonionic surfactants is that nonionic surfactants exhibit clouding behavior. The cloud point (CP) – the temperature at which clouding occurs can be elevated or suppressed through the addition of chemicals. For high temperature conditions such as for reservoir applications, addition of chemicals to elevate the CP of nonionic surfactants becomes essential to ensure that these surfactants are able to perform at high temperature conditions.

Early studies have determined that ionic surfactants (cationic and anionic) elevate the CP of nonionic surfactants [71]. More recent studies explore the capability of other chemicals to elevate the CP such as salts, nonionic surfactants, alcohols, hydrotropes, long chain fatty acids and phospholipids [25, 72-74].

Na et. al [74] conducted an extensive study on possible cloud point boosters (CPB) and classified them into two groups: nonionic and ionic cloud point boosters. Nonionic group CPB consists of chemicals with no net charge, namely water-soluble alcohols, polyethylene and polypropylene glycols (PEG and PPG). Ionic group consists of chemicals with amphiphilic nature – meaning the chemicals each have an apolar group and an ionic group. The chemicals considered as ionic CPBs in this study were ionic surfactants (anionic and cationic), long chain fatty acids and charged phospholipids. It was concluded that the ionic CPBs were effective in boosting CP at millimolar concentrations whereas nonionic CPBs require molar concentrations to elevate CP. This indicates that the nonionic CPBs are weak boosters and they interact



weakly with nonionic surfactants. On the other hand, the ability of long chain fatty acids and charged phospholipids to elevate CP confirmed the perception that a CPB needs two key structural features: a hydrophobic group to allow association with the nonionic surfactant and a net negative charge to impart electrostatic repulsion to the surfactant molecules hence preventing the nonionic surfactant to coalesce.

## **2.5 Summary**

In this chapter, the subject is approached by first discussing FAWAG, an EOR method, as a viable method to increase the oil recovery beyond the capability of WAG. The focus was then redirected to surfactants – the chemical responsible for FAWAG. The surfactants used by far for EOR applications have all been derived from the petroleum feedstock, having none derived from natural oil. This leaves a huge area for exploration on the possibility of replacing petroleum feedstock with natural oil for economic as well as environmental benefits. The specific area brought to attention is the utility of the double bonds present in natural oils against the commonly used carboxylic group in synthesizing surfactants for the producing of a natural oil derived surfactant for EOR applications.



## CHAPTER 3

### METHODOLOGY

In this chapter, the complete methodology used throughout the entire research work is presented. In Section 3.1, the summary of the research work is presented, followed by the materials used in this study in Section 3.2. Sections 3.3 and 3.4 discuss the methodology used in the synthesis of the surfactant and all the characterizations done for the synthesized surfactant respectively. Finally in Section 3.5, the methodology used for the formulation of the synthesized surfactant with two other additives is discussed

#### **3.1 Overview**

The study is divided into two sections: synthesis and characterization of nonionic surfactant, and formulation of a foaming agent using synthesized nonionic surfactant with two other additives.

Nonionic surfactant with polyoxyethylene (EO) as the polar head was synthesized from natural resources. The raw material used was fatty acid methyl esters (FAMES) derived from a plant oil – safflower oil with high oleate ester content.

A formulation of foaming agent was produced from the synthesized nonionic surfactant. Additives such as ionic surfactants and amphoteric surfactants were blended with the synthesized nonionic surfactant to produce the foaming agent. Ionic surfactants were added to increase the cloud point of nonionic surfactants while amphoteric surfactants act as “foam boosters” to increase the stability of foam generated against oil. The formulation was tested in terms of its foam stability.

### 3.2 Materials used

FAMES derived from safflower oil with high oleate ester content were used for the synthesis of surfactants. The FAMES used were donated by Solutions Engineering Sdn. Bhd.. As the FAMES donated had a high percentage of oleate ester, the FAMES will be referred to as HOE (high oleate ester) for the rest of this study. The composition of HOE donated is as shown in Table 4.4 (see Section 4.3.1).

All chemicals used for the synthesis of surfactants were as follows. Hydrogen peroxide (30% solution) - Analytical Reagent (AR) grade, ethyl acetate – ACS grade and polyethylene glycol methyl ether (PEG-ME, Mw. 350, 550 and 750) were obtained from Fisher Scientific. Boron trifluoride - diethyl etherate complex (50%  $\text{BF}_3$ ), formic acid (ACS grade, assay 98%) and sodium bicarbonate were obtained from Merck. Hexanes, anhydrous sodium sulfate, and sodium chloride used were ACS grade and obtained from J.T Baker. The chemicals were all utilized as received without further purification.

Chemicals used for formulating 1L of synthetic seawater to mimic the composition of seawater of an oilfield in Malaysia were as in Table 3.1. All chemicals used are AR and ACS grade and were purchased from Merck and Fisher. The chemicals were used as received without any purification.

Table 3.1: Composition of 1L of synthetic seawater

Chemical	Formula	Weight (mg)	Concentration (ppm)
Calcium chloride	$\text{CaCl}_2 \cdot 2\text{H}_2\text{O}$	1075.1706	1075.1706
Magnesium chloride	$\text{MgCl}_2 \cdot 6\text{H}_2\text{O}$	10174.8811	10174.8811
Potassium chloride	KCl	618.9113	618.9113
Barium chloride	$\text{BaCl}_2 \cdot 2\text{H}_2\text{O}$	0.00178	0.00178
Strontium chloride	$\text{SrCl}_2 \cdot 6\text{H}_2\text{O}$	12.9549	12.9549
Sodium bicarbonate	$\text{NaHCO}_3$	224.4296	224.4296
Sodium carbonate	$\text{Na}_2\text{CO}_3$	3844.3820	3844.3820
Sodium chloride	NaCl	23600.8565	23600.8565

The chemicals used as additives for formulations of surfactant solutions were commercially available surfactants and foam boosters. Cetyltrimethylammonium bromide (CTABr), sodium dodecyl sulfate (SDS) and sodium dodecylbenzene sulfonate (DBS) were obtained from Sigma-Aldrich with purity >98%. Alpha-olefin sulfonate C14-16 (AOS) was obtained from Ronas Chemicals Industry Company (purity 92%). Methyl ester sulfonate C16-18 (MES) with purity 87.72% was an in-house surfactant. Kao Corporation provided commercially available foam boosters – BETADET SHR and BETADET HR-60K. Lauryl hydroxysultaine was provided by Guangzhou Flower's Song Fine Chemical Co. Ltd. (35% active). All these chemicals were utilized as received without further purification.

### **3.3 Synthesis of surfactant**

The synthesis work of nonionic surfactant was focused on the double bonds present in the raw material, rather than the usual carboxylic group. The purpose was to explore the possibility of using nonionic surfactants with its hydrophilic head as a side chain to its hydrocarbon tail, as a surfactant fit for reservoir applications. This was accomplished in two steps: epoxidation and oxirane ring opening via attachment of PEG-ME. The raw material used for the synthesis of surfactant was HOE fatty acid methyl esters. HOE was used as a starting material due to its high content of unsaturation (see Table 4.4) to maximize the yield of end product, as saturated FAMES would remain inert for the rest of the synthetic work.

#### **3.3.1 Epoxidation**

Epoxidation of HOE was conducted using peroxy formic acid generated in situ by the reaction of hydrogen peroxide and formic acid. The epoxidation reaction is sensitive to several reaction parameters, including reactant concentration, reaction temperature and time. The effects of these parameters on epoxidation yield and the optimization of reaction conditions for maximum yield were investigated. The optimization experiment was designed using response surface methodology (RSM) techniques.

### 3.3.1.1 Experimental design

Four variables: hydrogen peroxide/C=C bond molar ratio (hydrogen peroxide amount in mol), formic acid/C=C bond molar ratio (formic acid amount in mol), reaction temperature and reaction time were selected as the reaction variables and the epoxidation yield was designated as the response factor. Design Expert software version 8.0.7.1 from Stat-Ease Inc. Minneapolis, USA was used to design the experiments and to analyze the statistical data obtained.

Full factorial central composite rotatable design (CCRD) for four independent variables at five levels proposed 30 runs of experiment by using relation  $2^k + 2k + 6$ , where  $k$  is the number of independent variables. The ranges of designed reaction variables for 1 mol of C=C were as follows: hydrogen peroxide (0.5 – 4 moles), formic acid (0.20 – 2.0 moles), reaction temperature (25°C – 85°C) and reaction time (30 – 360 minutes). Experiment design contained eight axial points, sixteen factorial points and six center points. The parameters for the 30 runs are depicted in Table 4.1 (see Section 4.2.1.1). Centre points are the replications of trials for the estimation of the experimental error.

Table 3.2: Range and levels of reaction parameters using CCRD

Variables	Coded variable level				
	Lowest	Low	Centre	High	Highest
	-2	-1	0	1	2
Hydrogen peroxide/C=C mole ratio	0.500	1.375	2.250	3.125	4.000
Formic acid/C=C mole ratio	0.200	0.650	1.100	1.550	2.000
Reaction temperature (°C)	25	40	55	70	85
Reaction time (min)	30.0	112.5	195.0	277.5	360.0

### *3.3.1.2 Experimental procedure*

In a round bottom flask equipped with magnetic bar, HOE and formic acid (HCOOH) were added and stirred at room temperature at the speed of 1500 rpm for 5 minutes. Hydrogen peroxide (H<sub>2</sub>O<sub>2</sub>) was introduced into the flask dropwise in the space of 30 minutes at room temperature with continuous stirring. Temperature was raised slowly to required temperature and maintained at required temperature for required time with continuous stirring. The mixture was then poured into a separating funnel and the aqueous layer was immediately drained out. The remaining organic layer was washed with saturated sodium bicarbonate solution to remove HCOOH, followed by distilled water and finally with saturated sodium chloride solution to remove sodium bicarbonate. The remaining product was diluted in hexanes and dried over anhydrous sodium sulfate. Hexanes were removed by vacuum distillation. Product obtained was characterized to determine the conversion of HOE to epoxides using NMR, GC-MS, FT-IR and oxirane oxygen value titration.

### **3.3.2 Attachment of PEG-ME**

Attachment of PEG-ME with molecular weight 750 onto epoxides synthesized from HOE was according to Hedman et al. [52] with some modifications. The attachment of PEG-ME was aided by BF<sub>3</sub> as catalyst. As there is no previous work done to understand the reaction of attachment of PEG-ME, three reaction parameters – reaction time, reaction temperature and amount of catalyst used were identified as variables for optimization study to better understand the reaction.

#### *3.3.2.1 Experimental design*

Three variables: reaction temperature, reaction time and amount of catalyst used were selected as the reaction variables and the nonionic surfactant yield was designated as the response factor. The ranges of selected reaction variables used in optimization study were as follows: BF<sub>3</sub> (0.25 – 2.50 wt% on PEG-ME), reaction

temperature (30°C – 70°C) and reaction time (0 – 120 minutes). All experiments were conducted at a fixed stirring speed of 1500 rpm.

### *3.3.2.2 Experimental procedure*

In a 100-mL round bottom flask equipped with magnetic bar, 0.07 mol PEG-ME was added and stirring speed was kept constant at 1500 rpm. PEG-ME was gradually heated to required temperature. Required amount of BF<sub>3</sub> (in diethyl ether complex) was injected into the PEG-ME beneath the surface to avoid loss of BF<sub>3</sub> fumes to surroundings. Mixture was stirred for a few seconds to allow mixing of BF<sub>3</sub> with PEG-ME before the addition of epoxides. The amount of epoxides that was added was calculated such that 1 mol of available oxirane oxygen corresponds with 1.05 mol of PEG-ME. For the case of epoxides with conversion yield of 92.9%, 0.072 mol epoxides were added dropwise in the space of 30 minutes into the mixture at required temperature with continuous stirring. After the addition of epoxides, mixture was stirred for required reaction time at required temperature. After reaction was completed, sodium bicarbonate was added in excess to the mixture to remove remaining catalyst with continuous stirring for 20 minutes. An inert solvent, ethyl acetate was also added into the mixture to dilute it during the removal of BF<sub>3</sub>. Excessive sodium bicarbonate was removed by gravity filtration. Remaining filtrate consisted of nonionic surfactant and unreacted PEG-ME. Separation of product from unreacted PEG-ME was achieved through thorough washing with saturated sodium chloride solution in a separating funnel. Remaining organic layer was dried over anhydrous sodium sulfate. Ethyl acetate was removed by vacuum distillation. Product obtained was characterized to determine the attachment of PEG-ME and yield of nonionic surfactant using NMR, GC-MS, FT-IR and nonionic surfactant titration. Oxirane oxygen value was determined for product to determine the amount of oxirane oxygen still present, if any, in product.



### **3.4 Characterization**

#### **3.4.1 GC-MS (ASTM D 6584-00)**

A number of data can be obtained from characterization using GC-MS. For this synthesizing work, GC-MS is used to determine the profile and purity of FAMES and epoxides synthesized. The conditions used are as follows:

An Agilent 7890A GC system coupled with Agilent 5975C inert XL EI/CI MSD with Triple-Axis Detector. The capillary column used was BP5, 30 m x 250  $\mu\text{m}$  x 0.25  $\mu\text{m}$ . The oven temperature program was according to Wilson et. al[75] as follows: 3 min at 100°C, then 25°C/min to 170°C, then 2°C/min to 230°C, then 20°C/min to 250°C and maintained at 250°C for 10 minutes. Helium was used as carrier gas with a flow rate of 0.5mL/min.

#### **3.4.2 NMR**

$^1\text{H}$  NMR and  $^{13}\text{C}$  NMR analyses were done on BrukerUltrashield 400 at 400 MHz using  $\text{CDCl}_3$  and acetone as solvent.

#### **3.4.3 FT-IR**

FT- IR on Perkin Elmer Spectrum One FT-IR spectrometer equipped with ZnSe 45° HATR assembly. An average of 30 scans was used with spectral resolution of  $4\text{cm}^{-1}$  in the range of 4000 to  $600\text{cm}^{-1}$ .

#### **3.4.4 Oxirane oxygen value (AOCS Cd 9-57)**

Oxirane oxygen value was determined according to the standard method AOCS Cd 9-57. This method determines the oxirane oxygen content, which is the oxygen contained in an oxirane ring. This method was used to determine the conversion yield of FAMES to epoxides.

Sample within 0.3-0.5 g was accurately weighed into a 50-mL flask. Sample was dissolved in 10 mL acetic acid glacial and titrated against 0.1N HBr solution in acetic acid with crystal violet solution (in acetic acid) as indicator. As HBr is volatile in acetic acid solution and tends to vaporize and evaporate from solution, titration was done in a closed system to minimize loss of HBr into surroundings and minimize error of titration. The tip of burette containing HBr solution was fitted to the flask-containing sample using a rubber stopper. The tip of burette was lowered until the titrant would discharge just above the surface of sample solution. Solution was stirred using a magnetic bar on a stirrer plate. The sample was titrated to a blue-green end point that persisted for 30 seconds. The oxirane oxygen value was calculated with the following formula:

$$\text{Oxirane oxygen, \%} = \frac{\text{mL HBr} \times N \times 1.60}{\text{weight of sample, g}}$$

where N is the normality of HBr solution. Epoxidation yield (%) was calculated based on the following expression:

$$\text{Epoxidation Yield, \%} = \frac{O_{\text{exp}}}{O_{\text{theo}}} \times 100\%$$

where  $O_{\text{exp}}$  and  $O_{\text{theo}}$  are the experimental and theoretical oxirane oxygen (%) respectively. The theoretical oxirane oxygen value was calculated to be 5.272% by using the following expression:

$$O_{\text{theo}} = \left[ \frac{1.0295 \times 16}{M_{w_{\text{oil}}} + (1.0295 \times 16)} \right] \times 100\%$$

where  $M_{w_{\text{oil}}}$  is the molecular weight of HOE used, and the value 1.0295 indicates the number of mole of available site for epoxidation (C=C bonds) in 1 mole of HOE. The molecular weight of HOE was calculated based on the composition of HOE as analyzed by GC-MS.

### **3.4.5 Critical Micelle Concentration (CMC)**

The CMC of the surfactant synthesised was determined by the conductivity method. Surfactant solutions in various concentrations were prepared and the conductivity of the surfactant solutions was measured. The CMC of the surfactant synthesised was determined by a plot of the conductivity measured against the surfactant concentration. All conductivity measurements were performed at 23°C. The surfactant solutions were prepared in ultra-pure water in different concentrations and were left standing for 3 hours to attain the laboratory temperature of 23°C. A Trans Instrument bench top conductometer model BC3020 was used to measure the conductivity of the solutions. The electrode was washed with ultra-pure water after each measurement and rinsed with a portion of the sample solution tested twice before conducting the measurement.

### **3.4.6 Cloud point (ASTM D2024-09)**

The cloud points (CP) of surfactant solutions prepared was determined according to standard method ASTM D2024-09 with some modifications. The range of temperature for CP measurement was 25°C-95°C. All surfactant solutions were prepared at 2.0 wt% surfactant concentration. Five milliliter of a surfactant solution was placed in a sealed 10-mL test tube. The test tube was placed in a water bath and was gently heated with the heating rate of 0.8°C/min. The first appearance of turbidity in the surfactant solution was taken as the CP.

### **3.4.7 Nonionic titration**

Nonionic surfactant content in synthesized surfactant was determined through potentiometric titrations [76]. Nonionic surfactants are converted into pseudo-cationic compound with the assistance of barium ions,  $\text{Ba}^{2+}$ . The pseudo-cationic compound, when titrated against sodium tetraphenylborate (NaTPB) produces precipitates that are insoluble in water. A sharp increase in the concentration of tetraphenylborate ion is detected as the titration reaches its equivalence point.

Nonionic surfactant content titrations were conducted with Metrohm Titrando 888 using an NIO electrode, which is an indicator electrode, developed by Metrohm [77]. The titrant used, NaTPB 0.01M, was prepared in the laboratory. Samples were titrated against NaTPB 0.01M and the nonionic surfactant content was calculated using the following formula:

$$\text{Nonionic surfactant content, \%} = \frac{V \times f}{10 \times E}$$

where     V       = consumption of NaTPB solution in mL  
               f       = calibration factor in mg/mL  
               E       = sample weight in g

Nonionic surfactants with polyethoxylates as the polar head are non-uniform substances and the precipitation with NaTPB is not strictly stoichiometric. Hence, a calibration factor has to be determined first before proceeding with nonionic titration of surfactant studied. The determination of the calibration factor f was based on PEG-ME 750 as a standard surfactant. This polymer was chosen as the standard surfactant because it is the raw material for the synthesis of nonionic surfactant. The calibration factor f was calculated from the nonionic titration of PEG-ME 750 with the following equation:

$$f = \frac{E \times 1000}{V}$$

The yield of conversion of epoxide to nonionic surfactant (surfactant yield, %) was calculated based on the following expression:

$$\text{Surfactant Yield, \%} = \frac{N_{\text{exp}}}{N_{\text{theo}}} \times 100\%$$

where  $N_{\text{exp}}$  and  $N_{\text{theo}}$  are the experimental and theoretical nonionic surfactant content (%) respectively. The theoretical nonionic surfactant content was calculated to be 69.396% by using the following expression:

$$N_{theo} = \left[ \frac{\frac{Yield_{epoxide}}{100} \times 1.0295 \times 750}{Mw_{epoxide} + \left( \frac{Yield_{epoxide}}{100} \times 1.0295 \times 750 \right)} \right] \times 100\%$$

where  $Mw_{epoxide}$  is the molecular weight of synthesized epoxide, and the values 1.0295 and 750 indicate the number of mole of available C=C bonds in 1 mole of HOE and molecular weight of PEG-ME 750 respectively. The molecular weight of epoxide was calculated based on the epoxidation yield obtained from oxirane oxygen value titration.

#### 3.4.7.1 Preparation of titrant

In a 1 L volumetric flask, 10 g of polyvinyl alcohol were dissolved in 300 mL of distilled water with heating to approximately 80°C and left to cool to room temperature. In a separate beaker, 3.4223 g of NaTPB were dissolved in 300 mL distilled water. The NaTPB solution was rinsed into the volumetric flask containing polyvinyl alcohol. Ten milliliter buffer solution pH 10.0 was added and the volumetric flask was filled up to the mark.

The buffer solution used for preparation of titrant was also prepared in the laboratory. In a 100 mL volumetric flask, 1.24 g of boric acid ( $H_3BO_3$ ) was dissolved in distilled water. Ten milliliter of NaOH 1 M was added into the solution and the volumetric flask was filled up to the mark.

#### 3.4.7.2 Preparation of sample

An auxillary solution,  $BaCl_2$  with concentration approximately 0.1 M was needed to convert the nonionic surfactants to pseudo-cationic compound. To prepare the auxillary solution, 21 g of  $BaCl_2$  was dissolved in distilled water in a 1 L volumetric flask. One milliliter of concentrated HCl was added and the volumetric flask was filled up to mark with distilled water.

To prepare a sample for titration, the sample within the weight range 25 – 50 mg was accurately weighed into a beaker. Ten milliliter of prepared BaCl<sub>2</sub> solution was added and beaker was filled up to approximately 100 mL with distilled water. Sample solution was stirred to completely solubilize the sample to be tested in distilled water. Sample was then titrated against 0.01M NaTPB.

### 3.5 Formulation

The nonionic surfactant synthesized was blended with two additives: an ionic surfactant and a foam booster. A total of 3 best performing anionic surfactants in CP study (refer to Section 4.4.1.2) and 3 foam boosters were used in a screening test to determine the surfactant formulation that is tolerant toward high temperature and high salinity. Table 3.3 shows the anionic surfactants and foam boosters used in the screening test.

Table 3.3: Anionic surfactants and foam boosters used for formulation

Foaming agent (main)	Anionic surfactant	Foam booster
ENS-750	AOS	Betadet HR-60K (HR)
	SDS	Betadet SHR (SHR)
	MES	Lauryl hydroxysultaine (LHS)

#### 3.5.1 Screening test

Formulations with various ratio of ENS-750, anionic surfactants and foam boosters were prepared for a screening test to determine the formulations that could withstand high temperature and high salinity. Formulations were tested for their compatibility with synthetic sea water with high total dissolved solids content (TDS, approximately 35 000 ppm) at high temperature (100°C) for 15 days.

The flowchart presented in Figure 3.1 shows the screening test process conducted. Solutions of synthesized ENS-750, anionic surfactants and foam boosters were prepared in 2.0 wt% concentration in synthetic seawater. These solutions were mixed in different proportions to form a 5 ml surfactant system with a total 2.0 wt% concentration. Formulations formed were placed in sealed 10-mL test tubes. The test tubes were shaken to ensure solutions in the test tubes were homogeneous. The test tubes were then placed in an oven at 100°C for 24 hours. After 24 hours, the test tubes were taken out individually and shaken immediately. Any cloudiness or precipitation observed was recorded. The observation was done as soon as the test tubes were taken out of the oven to ensure little change in the temperature of the test tubes. Test tubes with clear formulations were placed in the oven at 100°C for 15 days for compatibility test. At the end of 15 days, test tubes were observed for visible precipitation and cloudiness.

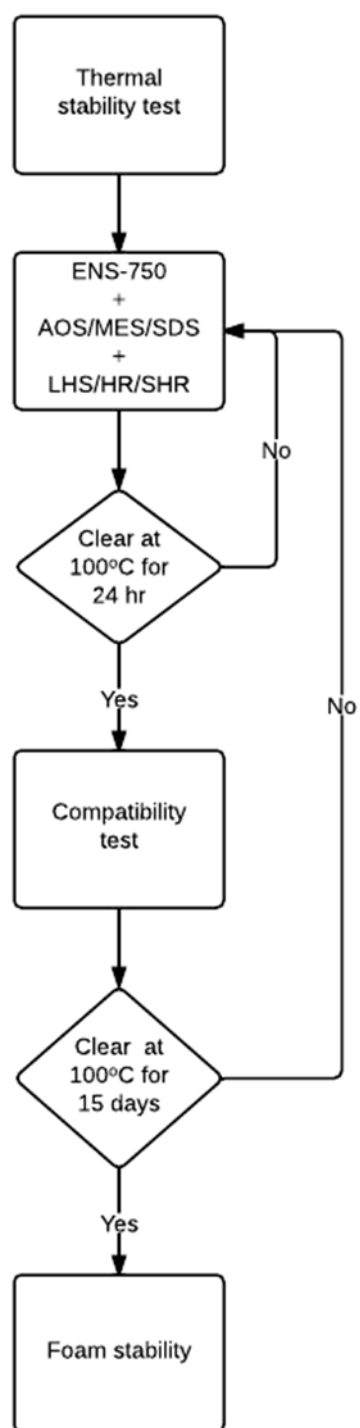


Figure 3.1: Flow chart depicting the screening test procedure



### 3.5.2 Foam stability

Formulations that could withstand high temperature and high salinity were selected to conduct foam stability test in the presence of CO<sub>2</sub>, with and without the presence of oil (diesel) at room conditions.

Foam stability was measured by the time it takes for generated foam height to decrease to half its initial height. This point is called the half-life. For foam stability test, 1.0 wt% concentration of selected formulations from Section 3.5.1 were used. The gas used to generate foam was pure CO<sub>2</sub>, and the test was conducted with and without diesel. Diesel was used to represent oil in the study of the effect of oil to destabilize foam and was obtained from a local petrol station.

A 1-L graduated measuring cylinder was used for the experiment. One hundred milliliter of 1.0 wt% surfactant formulation solution was poured into the measuring cylinder. A gas dispersion tube to dispense the CO<sub>2</sub> gas was placed below the surface of surfactant solution. CO<sub>2</sub> gas was flowed at 65 psifor 1 minute. The initial foam height was measured, followed by foam height at t = 30 seconds, 1 minute, 1.5 minute and 5 minutes. The time taken for foam height to decrease to half of its initial height was recorded as half-life. For experiments involving diesel, 5 mL of diesel was added into the 100 mL surfactant formulation in the measuring cylinder and shaken gently to mix the solution with the diesel before the introduction of CO<sub>2</sub> gas into the system.



## CHAPTER 4

### RESULTS AND DISCUSSION

#### 4.1 Overview

This chapter will discuss the results obtained in this study in three major categories: the synthesis of surfactant in Section 4.2, the characterization of the synthesized surfactant in Section 4.3 and the formulation of surfactant recipe using the synthesized surfactant in Section 4.4.

#### 4.2 Synthesis of surfactant

The starting material used for the synthesis work was FAMES with high oleate ester content (HOE). The composition of HOE was confirmed using GC-MS and is given in Table 4.4 (see Section 4.3.1).

##### 4.2.1 Epoxidation

The epoxidation reaction has been commonly used to introduce molecules of different functional groups into unsaturated hydrocarbons, particularly in the biodiesel industry [49-51, 78, 79]. Epoxides are highly labile and hence different functional groups could easily be introduced into hydrocarbons. This lability is due to the high ring strain possessed by the oxirane ring. Due to this nature, optimization and kinetics studies have been conducted extensively in order to minimize the production of by-products during the epoxidation reaction (refer to Figure 2.11).

#### 4.2.1.1 Optimization study

In the optimization study of epoxidation, the effect of and relation between four reaction variables: hydrogen peroxide (H<sub>2</sub>O<sub>2</sub>) concentration, formic acid (HCOOH) concentration, reaction temperature and reaction time were studied. Experimental design for a set of 30 experiments is presented in Table 4.1, together with observed and predicted results. The data obtained was used to fit an empirical quadratic model. Multiple regression analysis of the experimental data produced a second-degree polynomial equation (in terms of coded factors) for the yield of epoxidation as shown below:

$$\begin{aligned} y = & +72.00 + 11.66X_1 - 2.14X_2 + 9.48X_3 + 8.50X_4 \\ & - 0.82X_1X_2 + 4.48X_1X_3 + 1.52X_1X_4 + 1.64X_2X_3 - 2.04X_2X_4 \\ & + 1.39X_3X_4 - 5.03X_1^2 - 4.59X_2^2 - 4.82X_3^2 - 4.87X_4^2 \end{aligned}$$

where y is the response factor (epoxidation yield %), and X<sub>1</sub>, X<sub>2</sub>, X<sub>3</sub> and X<sub>4</sub> are the coded values of the following variables: hydrogen peroxide concentration, formic acid concentration, reaction temperature and reaction time. The terms X<sub>1</sub>X<sub>2</sub>, X<sub>1</sub>X<sub>3</sub>, X<sub>1</sub>X<sub>4</sub>, X<sub>2</sub>X<sub>3</sub>, X<sub>2</sub>X<sub>4</sub>, X<sub>3</sub>X<sub>4</sub> are the first order interaction terms for each paired combination showing interaction among the pre-defined variables.

Interactions and effects of different variables can be noted by viewing the polynomial model as shown in the above equation. The positive coefficients of X<sub>1</sub> (hydrogen peroxide), X<sub>3</sub> (temperature) and X<sub>4</sub> (time) and for interaction terms, X<sub>1</sub>X<sub>3</sub> (hydrogen peroxide × reaction temperature), X<sub>1</sub>X<sub>4</sub> (hydrogen peroxide × time), X<sub>2</sub>X<sub>3</sub> (formic acid × reaction temperature), and X<sub>3</sub>X<sub>4</sub> (reaction temperature × time) indicate a linear effect of increasing yield of epoxidation, while the negative coefficient of X<sub>2</sub> (formic acid), interaction terms, X<sub>1</sub>X<sub>2</sub> (hydrogen peroxide × formic acid), X<sub>2</sub>X<sub>4</sub> (formic acid × time), and the quadratic terms X<sub>1</sub><sup>2</sup>, X<sub>2</sub><sup>2</sup>, X<sub>3</sub><sup>2</sup> and X<sub>4</sub><sup>2</sup> have negative effect and decrease the epoxidation yield.

Besides the polynomial equation, 2-D contour plots were also generated to assess the relationship between the independent variables for the optimization of the reaction conditions. These contour plots are graphical representations of the regression

equation. Six contour plots were generated according to the paired combinations  $X_1X_2$ ,  $X_1X_3$ ,  $X_1X_4$ ,  $X_2X_3$ ,  $X_2X_4$ ,  $X_3X_4$ . The contour lines represent the effect of two variables on the response factor (epoxidation yield, %) by using an infinite number of combinations of the two variables while keeping the other two variables constant. The surface encircled by the smallest ellipse represents the maximum response [80]. The 2-D contour plots predicted from the model are presented in Figures 4.1 – 4.6.

Table 4.1: Full factorial CCRD matrix of four variables in coded and natural units along with the observed and predicted responses (% epoxidation yield)

Exp. No.	Point type	Coded level of variables				Actual level of variables				Epoxidation yield (%)		
		X <sub>1</sub>	X <sub>2</sub>	X <sub>3</sub>	X <sub>4</sub>	X <sub>1</sub>	X <sub>2</sub>	X <sub>3</sub>	X <sub>4</sub>	Predict ed value	Actual value	Resid ual
1	Factorial	-1	-1	-1	-1	1.375	0.65	40	113	31.34	30.45	-0.89
2	Factorial	1	-1	-1	-1	3.125	0.65	40	113	44.32	45.22	0.90
3	Factorial	-1	1	-1	-1	1.375	1.55	40	113	29.51	30.43	0.92
4	Factorial	1	1	-1	-1	3.125	1.55	40	113	39.19	37.22	-1.97
5	Factorial	-1	-1	1	-1	1.375	0.65	70	113	35.28	35.38	0.10
6	Factorial	1	-1	1	-1	3.125	0.65	70	113	66.18	65.69	-0.49
7	Factorial	-1	1	1	-1	1.375	1.55	70	113	40.01	37.29	-2.72
8	Factorial	1	1	1	-1	1.375	1.55	40	278	36.61	35.14	-1.47
9	Factorial	-1	-1	-1	1	3.125	1.55	40	278	52.37	50.45	-1.92
10	Factorial	1	-1	-1	1	1.375	0.65	70	278	56.10	56.11	0.01
11	Factorial	-1	1	-1	1	3.125	0.65	70	278	93.07	90.34	-2.73
12	Factorial	1	1	-1	1	1.375	1.55	70	278	52.66	49.94	-2.72
13	Factorial	-1	-1	1	1	3.125	1.55	70	278	86.34	85.27	-1.07
14	Factorial	1	-1	1	1	0.5	1.1	55	195	28.56	30.22	1.66
15	Factorial	-1	1	1	1	4	1.1	55	195	75.22	77.34	2.12
16	Factorial	1	1	1	1	2.25	0.2	55	195	57.90	57.34	-0.56
17	Axial	-2	0	0	0	2.25	2	55	195	49.33	53.67	4.34
18	Axial	2	0	0	0	1.375	0.65	40	113	31.34	30.45	-0.89
19	Axial	0	-2	0	0	3.125	0.65	40	113	44.32	45.22	0.90
20	Axial	0	2	0	0	1.375	1.55	40	113	29.51	30.43	0.92
21	Axial	0	0	-2	0	2.25	1.1	25	195	33.76	33.87	0.11
22	Axial	0	0	2	0	2.25	1.1	85	195	71.66	75.33	3.67
23	Axial	0	0	0	-2	2.25	1.1	55	30	35.50	36.44	0.94
24	Axial	0	0	0	2	2.25	1.1	55	360	69.50	72.34	2.84
25	Center	0	0	0	0	2.25	1.1	55	195	72.00	73.31	1.32
26	Center	0	0	0	0	2.25	1.1	55	195	72.00	71.76	-0.24
27	Center	0	0	0	0	2.25	1.1	55	195	72.00	69.03	-2.97
28	Center	0	0	0	0	2.25	1.1	55	195	72.00	70.87	-1.13
29	Center	0	0	0	0	2.25	1.1	55	195	72.00	74.95	2.96
30	Center	0	0	0	0	2.25	1.1	55	195	72.00	72.05	0.05

#### 4.2.1.1.1 Effect of reactants' concentrations

In order to generate peroxy formic acid (the oxygen carrier responsible for the generation of the oxirane ring), hydrogen peroxide and formic acid are needed. Since peroxy formic acid is the product of both hydrogen peroxide and formic acid, these two reactants should play equally significant roles. However, this was not the case observed. Of all the variables, hydrogen peroxide concentration ( $\text{H}_2\text{O}_2/\text{C}=\text{C}$  mole

ratio) is the most significant first order reaction term. While the role of hydrogen peroxide is directly associated with formic acid, the latter is not as significant as the former is. In fact, the concentration of formic acid plays the least significant role among all four variables. This is mainly due to the regenerating ability of the formic acid. Formic acid can be regenerated from peroxy formic acid after its oxygen atom has been utilized [65]. Therefore, the effect of the concentration of formic acid is relatively less pronounced than that of hydrogen peroxide.

This is portrayed in the 2-D contour plot generated by the model showing the interaction between hydrogen peroxide and formic acid concentrations. Figure 4.1 shows the effect of hydrogen peroxide and formic acid concentrations on epoxidation yield. The effect of varying hydrogen peroxide concentration is more significant as compared to that of formic acid. This supports the vital role played by hydrogen peroxide in generating peroxy formic acid for oxirane generation. Therefore, an almost linear effect in increasing yield can be observed by increasing hydrogen peroxide amount while increase in formic acid amount is comparatively less important. However, there needs to be an optimum concentration of formic acid. It can be observed that at both low and high concentrations of formic acid, the epoxidation yield is low. Insufficient peroxy formic acid is generated at low concentrations of formic acid while high concentrations of formic acid promote a ring-opening reaction. Optimum conditions can be determined as 3.32 moles of hydrogen peroxide/C=C mole ratio and 0.90 moles of formic acid/C=C mole ratio while the reaction temperature and time are fixed at 70°C and 264 minutes respectively.

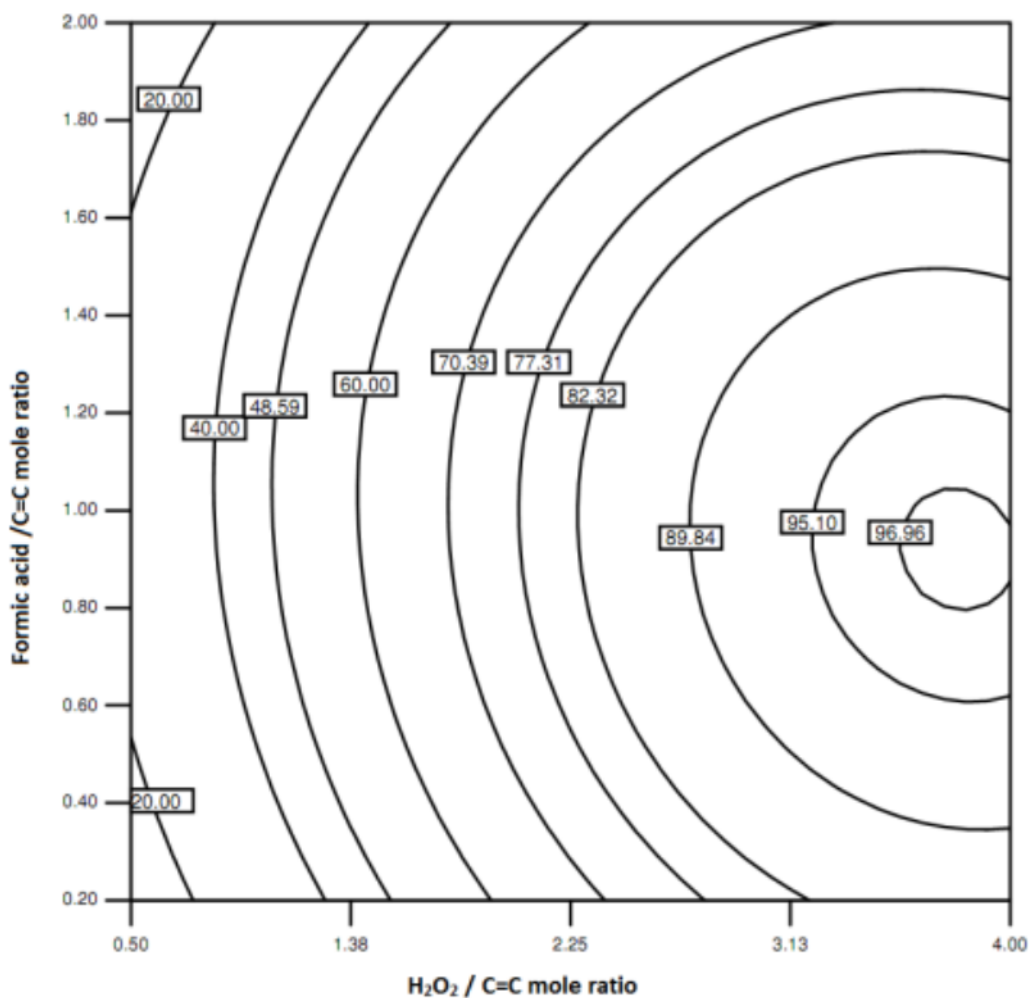


Figure 4.1: Effect of varying  $\text{H}_2\text{O}_2/\text{C}=\text{C}$  and  $\text{HCOOH}/\text{C}=\text{C}$  mole ratios on epoxidation yield (%)

#### 4.2.1.1.2 Effect of reaction temperature

The reaction temperature is the second most significant reaction parameter. The role of reaction temperature in this reaction is manifold: it is important in the generation of peroxy acid [57], the epoxidation of the double bond [56] and in the cleavage of oxirane ring (ring-opening reaction) [81]. At low temperatures, the overall epoxidation reaction is very slow. A long reaction time is required and at high temperature, yield becomes low when the opening of oxirane ring intensifies. Therefore, more attention should be paid to the control of reaction temperature for good epoxidation yields.



The relationship between reaction temperature and the other 3 variables are shown in Figures 4.2 – 4.4. Figure 4.2 shows the relationship between the concentration of hydrogen peroxide/C=C mole ratio and reaction temperature. It can be observed that the effect of hydrogen peroxide concentration is linear over a wide range but the effect of temperature is marginally negative at higher values. From the plot, it is observed that a high concentration of hydrogen peroxide is required for temperature to play a significant role in epoxidation yield. A slight increase in temperature at high concentrations of hydrogen peroxide can increase the yield significantly. Optimum conditions can be assessed at hydrogen peroxide/C=C mole ratio of 3.88 and a reaction temperature of about 67.5°C. Reaction time and formic acid concentration are fixed at 240 minutes and 1.06 moles respectively.

Figure 4.3 presents the effect of varying reaction temperature against the concentration of formic acid. The effect of variation of reaction temperature is more significant as compared to the effect of the concentration of formic acid. This relationship, once again reveals the ability of the regeneration of formic acid hence variations in its amount are less effective. However, it can be observed that increasing formic acid concentration above 1 mole decreases epoxidation yield at all levels of temperature. Once again, it is observed that the effect of temperature is marginally negative at low concentrations of formic acid. At high concentrations of formic acid, the negative effect of temperature towards epoxidation yield is more pronounced. This shows that high temperature facilitates ring-opening reaction. Optimum conditions revealed here are 0.95 moles of formic acid/C=C moles and temperature of 75.51°C when hydrogen peroxide concentration and reaction time are fixed at 2.96 moles and 240 minutes respectively.

Figure 4.4 presents the effect of varying reaction temperature against reaction time. The reaction temperature, up to about 75°C has a positive effect and after that the effect becomes negative as the ring opening reaction commences. Likewise, at a suitable temperature, reaction time has a positive effect up to about 250 minutes and after that it becomes negative. The negative effect of temperature seems to be more detrimental to the epoxidation yield if compared to time. Optimum temperature and

reaction time can be assessed as 72.01°C and 295 minutes, respectively while hydrogen peroxide and formic acid are fixed at 2.96 and 1.00 moles respectively.

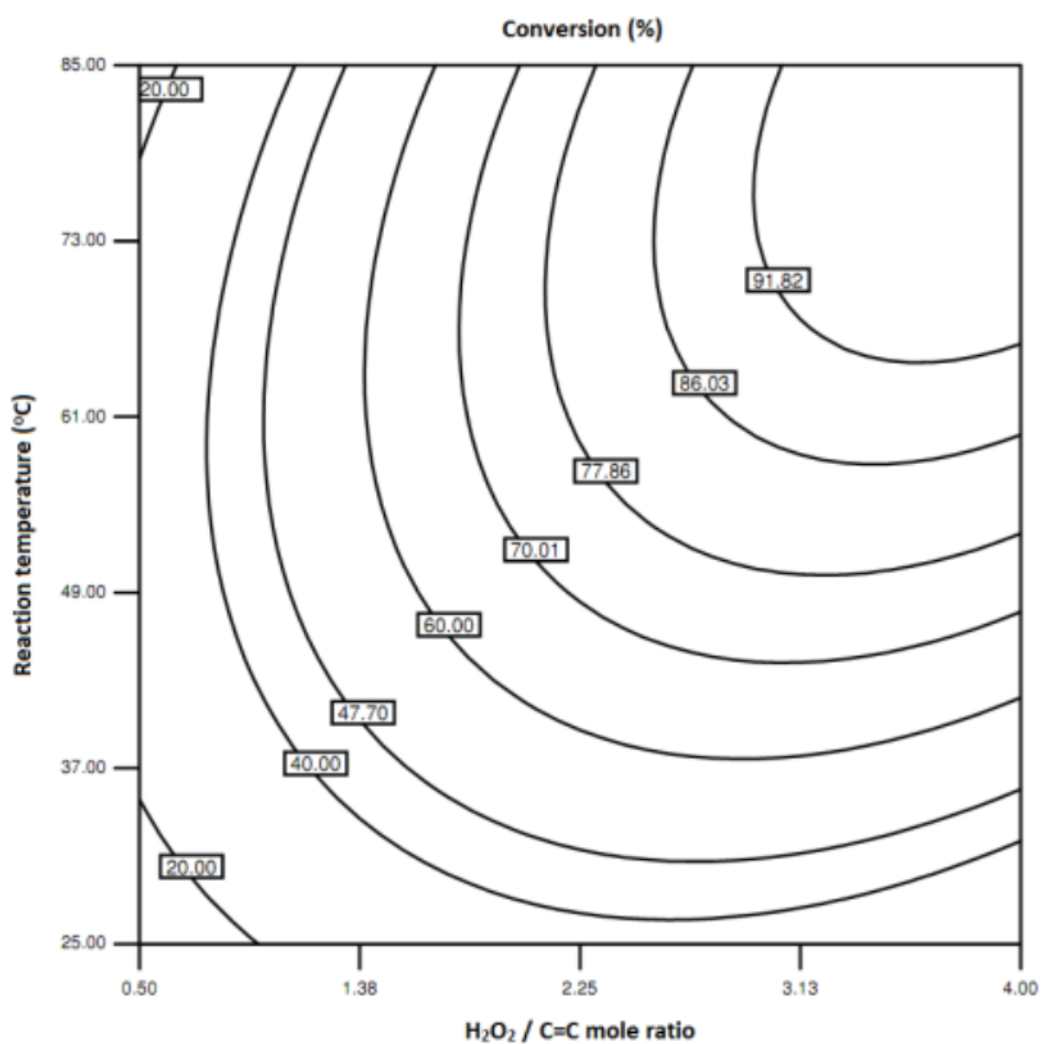


Figure 4.2: The effect of varying H<sub>2</sub>O<sub>2</sub>/C=C mole ratio and reaction temperature on epoxidation yield (%)

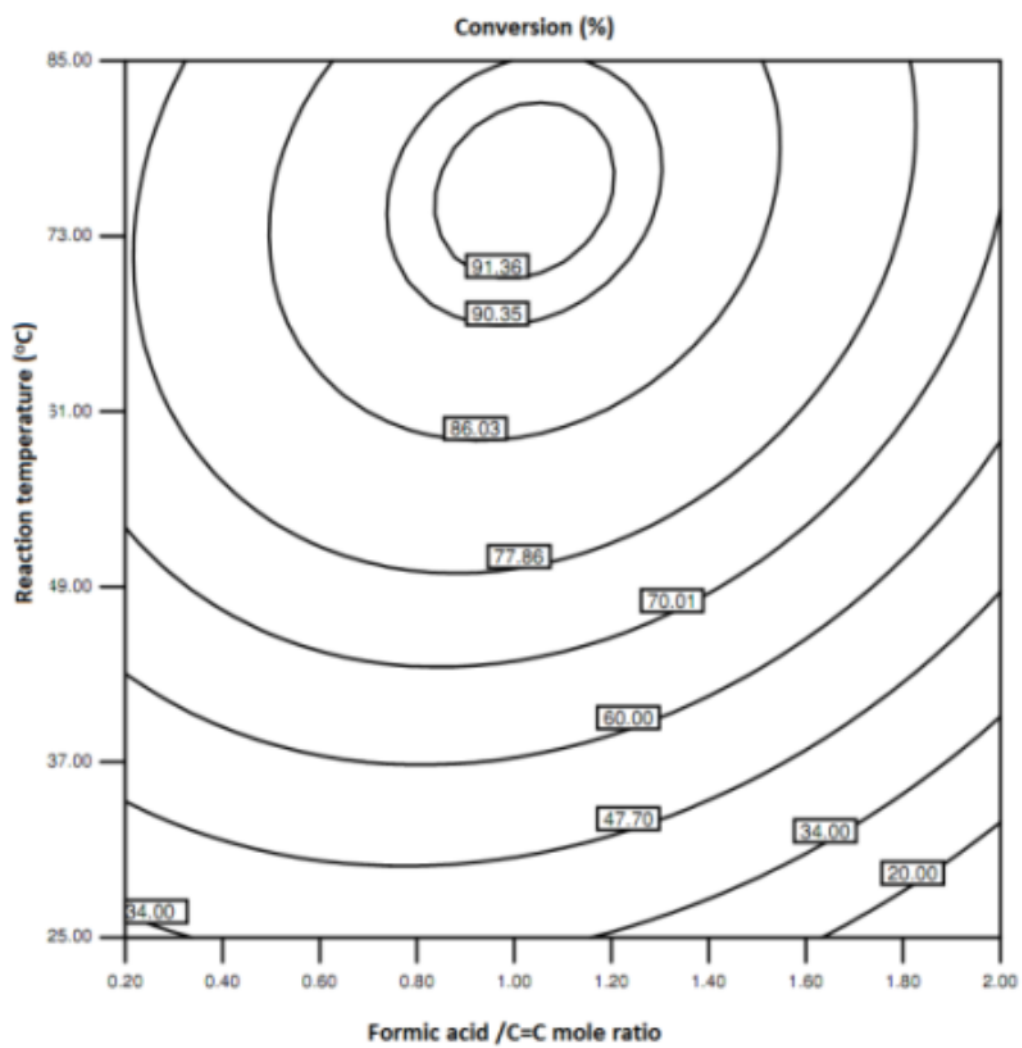


Figure 4.3: The effect of varying HCOOH/C=C mole ratio and reaction temperature on epoxidation yield (%)

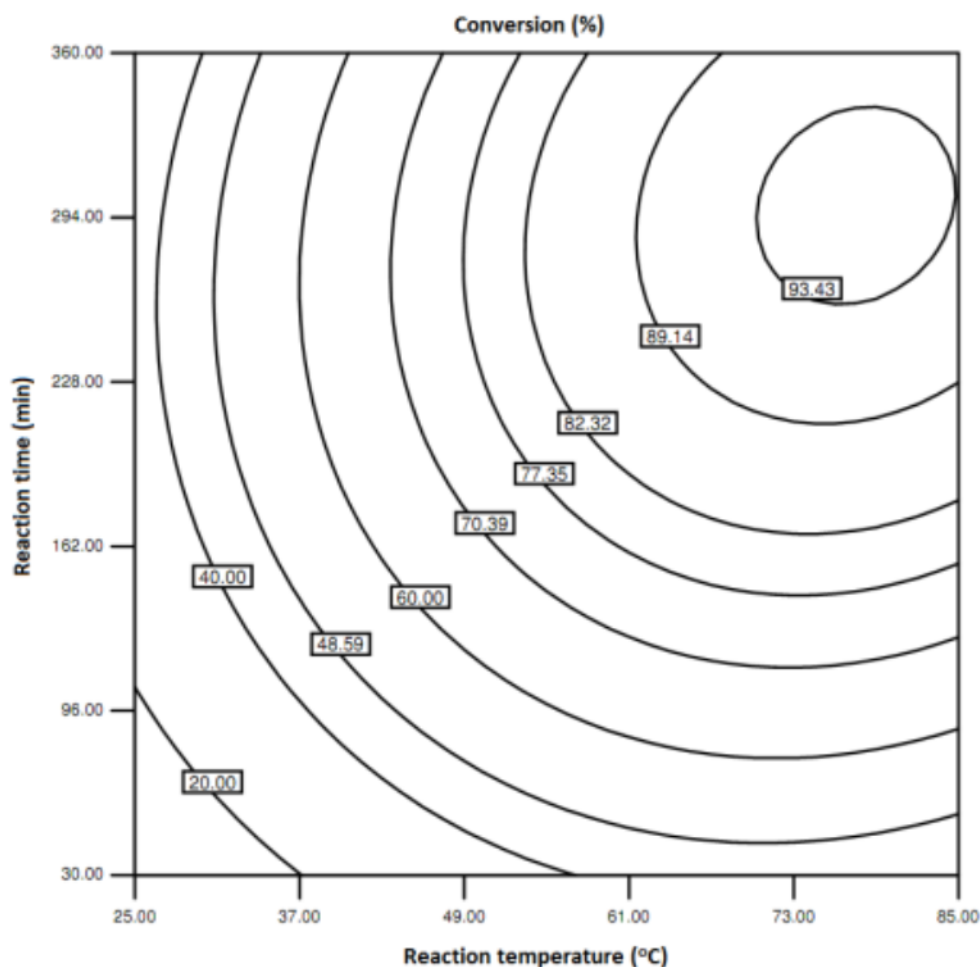


Figure 4.4: The effect of varying reaction temperature and time on epoxidation yield (%)

#### 4.2.1.1.3 Effect of reaction time

Reaction time also has a significant role in epoxidation reaction. As the ring opening reaction is also associated with ring generation reaction, prolonging reaction time promotes the former [54]. However, long reaction times at lower temperatures can lead to a high yield of oxirane with minimum ring opening reaction. Comparatively less significant quadratic term of reaction time suggests that the effect is almost linear with less curvature effect.

Figure 4.5 represents the effects of the amount of formic acid and reaction time. The effect of formic acid amount is positive up to a value of about 0.80 – 1.10

moles/C=C moles, after which the effect is negative. Reaction time has a relatively more significant and positive effect up to about 300 minutes before becoming non-effective. Optimum conditions can be assessed at 1.00 moles of formic acid and 307.50 minutes reaction time. Hydrogen peroxide and reaction temperature are fixed at 2.96 moles and 70°C respectively.

Figure 4.6 shows the effect of the varying the amount of hydrogen peroxide/C=C mole ratio and reaction time. Here the effect of varying the amount of hydrogen peroxide is relatively more significant than the effect of varying reaction time. An amount of about 3.81 moles hydrogen peroxide/C=C moles and 300 minutes for reaction time can be found optimum. The formic acid concentration and reaction temperature are fixed at 1 mole/C=C mole and 70°C respectively.

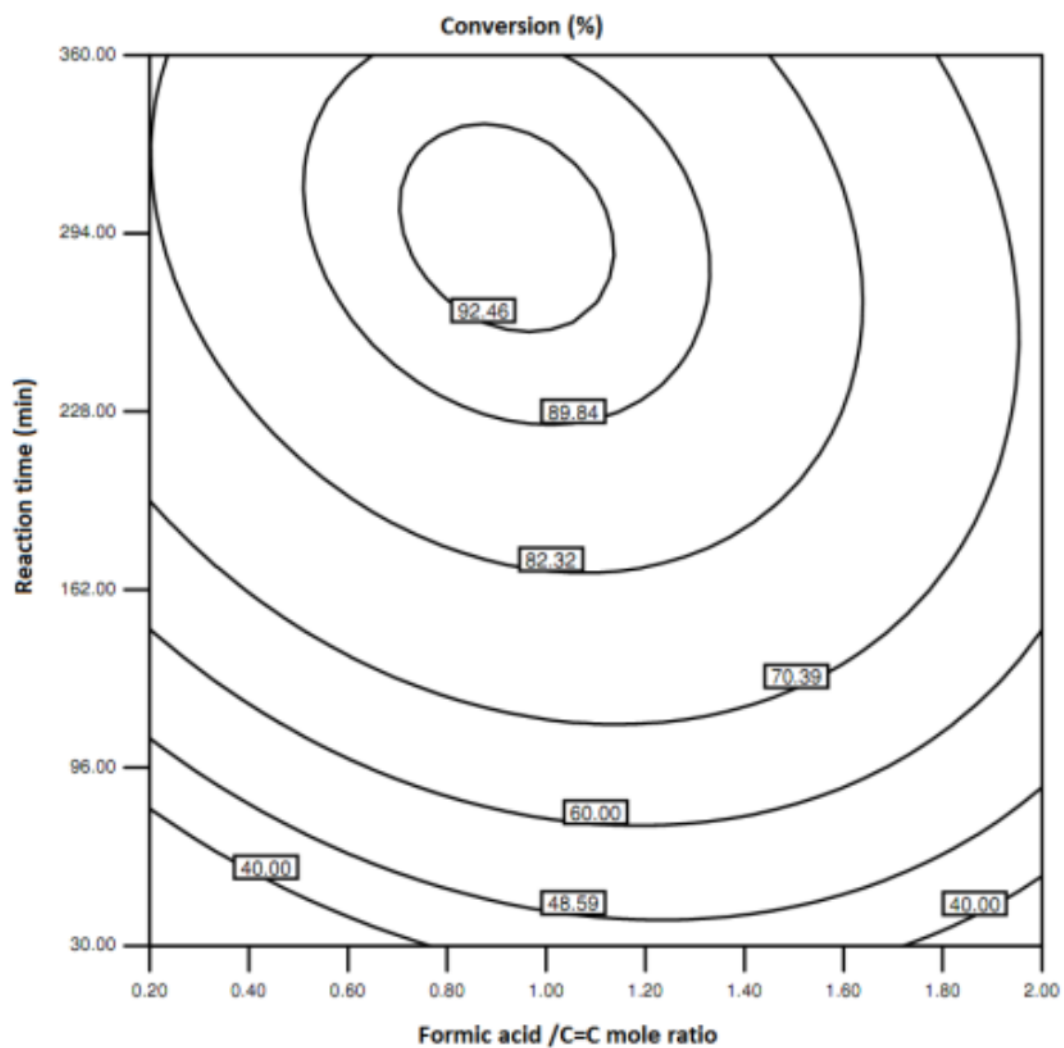


Figure 4.5: The effect of varying HCOOH/C=C mole ratio and reaction time on epoxidation yield (%)

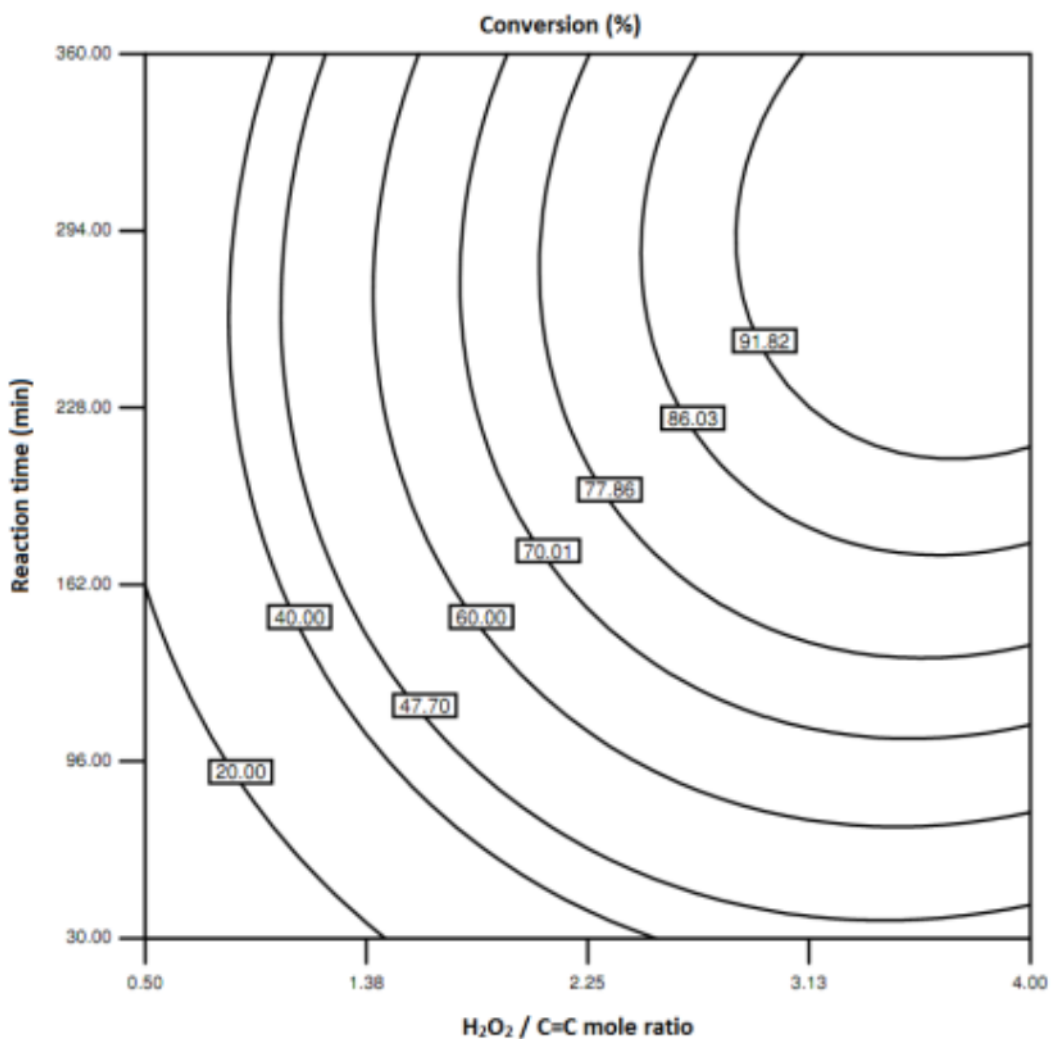


Figure 4.6: The effect of varying  $\text{H}_2\text{O}_2/\text{C}=\text{C}$  mole ratio and reaction time on epoxidation yield (%)

#### 4.2.1.1.4 Summary

Overall, it can be concluded that in order to produce high epoxidation yield, an optimum condition of high concentration of hydrogen peroxide (around 3 moles/ $\text{C}=\text{C}$  mole) and moderate concentration of formic acid (around 1 mole/ $\text{C}=\text{C}$  mole) is required. The method of conducting epoxidation reaction at low temperature with long reaction time to achieve high yield can be utilized, but this is not practical. The epoxidation reaction can be shortened to a mere few hours with higher temperature, as compared to reaction at  $20^\circ\text{C}$ - $40^\circ\text{C}$  for reaction time of 20-22 hours [54]. However,

there needs to be very good control in temperature as a slight increase above optimum temperature could cause a detrimental effect.

#### 4.2.1.1.5 Validation of RSM

##### 4.2.1.1.5.1 Statistics analyses

The results of the analysis of variance (ANOVA) in fitting the quadratic polynomial model are presented in Table 4.2. A high  $F_{model}$  value of 94.83 at a very low probability  $p < 0.0001$  is observed, implying that the model fit is significant with only less than 0.01% chance that  $F_{model}$  value of 94.83 could be attributed to noise. The coefficient of determination,  $R^2$  was calculated to be 0.9888, assuring the use of the model with significant reliability to predict results with good precision. The coefficient of variance, CV is a low 4.75%, indicating a high precision, low scatter and better repeatability in experimental results. A plot of actual values obtained from experiments against the values predicted by the model is presented. The data points are evenly distributed along the predicted line, showing excellent agreement between experimental results and model-predicted values (see Figure 4.7).



Table 4.2: ANOVA for the fitted quadratic polynomial model

Source of variations	Sum of Squares	Degrees of Freedom	Mean Square	<i>F</i> Value	<i>P</i> Value Probability > <i>F</i>
Model	9567.27	14	683.38	94.83	< 0.0001
Hydrogen peroxide/C=C mole ratio ( $X_1$ )	3265.03	1	3265.03	453.07	< 0.0001
Formic acid/C=C mole ratio ( $X_2$ )	110.12	1	110.12	15.28	0.0014
Reaction temperature ( $X_3$ )	2154.8	1	2154.8	299.01	< 0.0001
Reaction time ( $X_4$ )	1733.83	1	1733.83	240.6	< 0.0001
$X_1X_2$	10.84	1	10.84	1.5	0.2389
$X_1X_3$	321.4	1	321.4	44.6	< 0.0001
$X_1X_4$	30.72	1	30.72	4.26	0.0567
$X_2X_3$	692.79	1	692.79	96.14	< 0.0001
$X_2X_4$	579	1	579	80.34	< 0.0001
$X_3X_4$	637.42	1	637.42	88.45	< 0.0001
$X_1^2$	651.38	1	651.38	90.39	< 0.0001
$X_2^2$	108.1	15	7.21		
$X_3^2$	87.52	10	8.75	2.13	0.2095
$X_4^2$	20.58	5	4.12		
Residual	9675.36	29			
Lack of Fit	9567.27	14	683.38	94.83	< 0.0001
Pure Error	3265.03	1	3265.03	453.07	< 0.0001
<b>Total</b>	110.12	1	110.12	15.28	0.0014

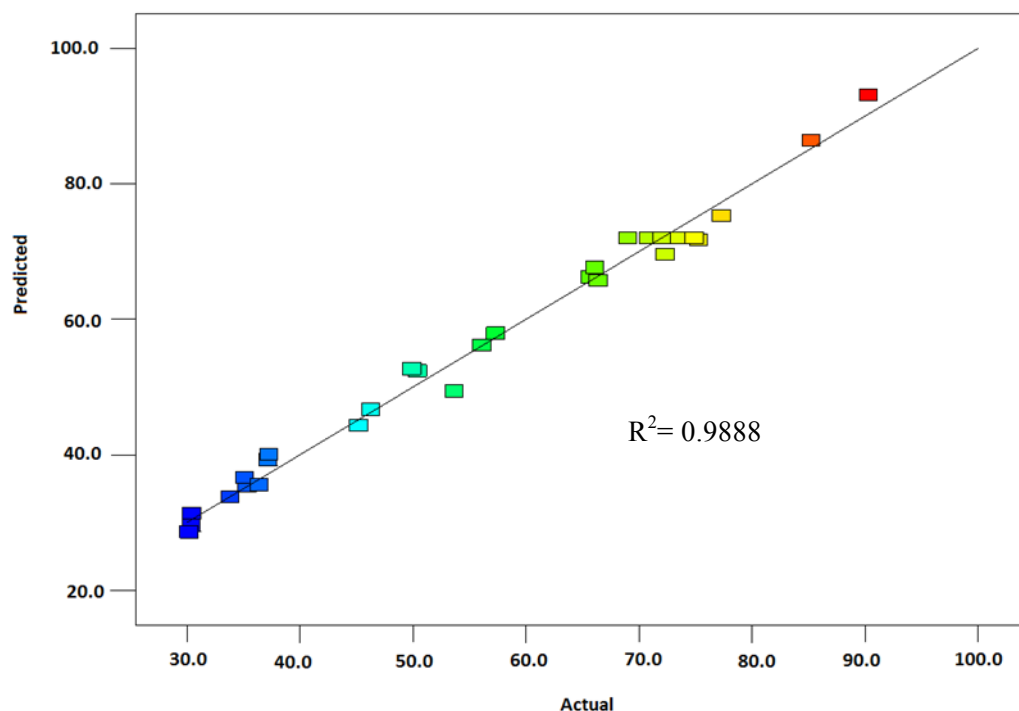


Figure 4.7: Comparison between predicted and actual epoxidation yield (%)

#### 4.2.1.1.5.2 Confirming experiment

The model predicted that a maximum epoxidation yield of 94.9% with a standard error of prediction of 1.68 can be obtained by using 3.12 mol of hydrogen peroxide/C=C mol, 0.96 mol of formic acid/C=C mol, at reaction temperature of 70.00°C for 277.50 minutes. Experimental yield by using optimized conditions was found to be 94.49%, which is agreeable to predicted yield. When compared to the results appeared in literature [54, 82], there is a marked difference in the amount of formic acid used. The results are summarized in Table 4.3. It may be concluded that a lower amount of formic acid requires longer reaction time to complete the reaction.

Table 4.3: Comparison of epoxidation yield (%) for three studies

Study	Mole ratio C=C/H <sub>2</sub> O <sub>2</sub> /H COOH	Temper ature (°C)	H <sub>2</sub> O <sub>2</sub> solution strength (%)	Time (mins)	Convers ion (%)
Campanella et. al, 2008 [54]	1/2/0.5	40	59	690	83.5
Petrović et. al, 2002 [82]	1/1.5/0.5	60	30	300	92-95
This study	1/3.12/0.96	70	30	278	94.49

#### 4.2.2 Attachment of PEG-ME

Hedman et. al [52] synthesized three ethoxylated nonionic surfactants using PEG-ME as the source of ethylene oxide (EO) with molecular weights 350, 550 and 750 with reported cloud points 15°C, 46°C and 63°C respectively. PEG-ME with molecular weight 750 was chosen for the synthesis of ethoxylated nonionic surfactant (this synthesized surfactant will be referred to as ENS-750 from here on) in this study due to two main reasons.

Firstly, it has the highest number of EO units and highest cloud point among the three reported surfactants. PEG-ME 750 corresponds to about 16 EO units while PEG-ME 350 and 550 correspond to about 7 and 11 EO units respectively. Higher cloud point shows better solubility of the nonionic surfactant in water. The nonionic surfactants are solubilized in water through hydrogen bonding – the bonding between oxygen from EO and hydrogen from water. With increasing EO units in the surfactant molecule, stronger bond between ENS and water is formed, hence enhances its solubility in water. This is due to the formation of more hydrogen bonds between the EO units in the surfactant and water.

Secondly, PEG-ME hydrophilic head would contribute to 70 wt% of the synthesized surfactant. Studies show that polyethoxylated surfactant with its polyethoxylate hydrophilic head contributing to 75 wt% of the surfactant shows

maximal foamability [83]. PEG-ME 350 and 550 would contribute to 52 wt% and 63 wt% respectively.

BF<sub>3</sub>-diethyl etherate complex, which is readily available commercially, was used as the source for BF<sub>3</sub> in this reaction. The complex is in the form of liquid, and it is commonly used as a source for BF<sub>3</sub> besides BF<sub>3</sub>-methanol complex. In this reaction, BF<sub>3</sub>-methanol complex is not used, as methanol would participate in the alkoxylation reaction and act as a competitor with PEG-ME for epoxides and hence decrease the yield of surfactant formed. The complex was utilized upon purchase in the reaction without further treatment and processing.

#### *4.2.2.1 Optimization study*

An optimization study was conducted to investigate the effects of three variables: reaction temperature, time and amount of catalyst used. The results obtained, in terms of product yield obtained were not very significant – the yield obtained by varying respective parameters fall in between 4-7%. The narrow range suggests that varying the parameters does not produce a significant impact. This is thought to be due to the high reactivity of the oxirane ring. During the epoxidation reaction the epoxides were introduced progressively into the system. Immediate ring opening reaction occurred – the reaction temperature rose above the set temperature during the addition of epoxides. By the time the last drop of epoxides was added into the reaction system, the reaction is almost complete. However, there were notable patterns that are worthy to be noted.

##### *4.2.2.1.1 Effect of reaction temperature*

The reaction temperature gave the most significant impact amongst the three variables. The experiments were conducted in the temperature range 40-70°C. A negative pattern is observed as the reaction temperature increases. As the reaction temperature increases, the yield obtained decreases and the gradient becomes more significant with higher reaction temperature. This is due to the release of BF<sub>3</sub> gas to

the atmosphere. An increase in the reaction temperature causes some of the  $\text{BF}_3$  to escape from the mixture and release to the surroundings, thus lowering the yield obtained.

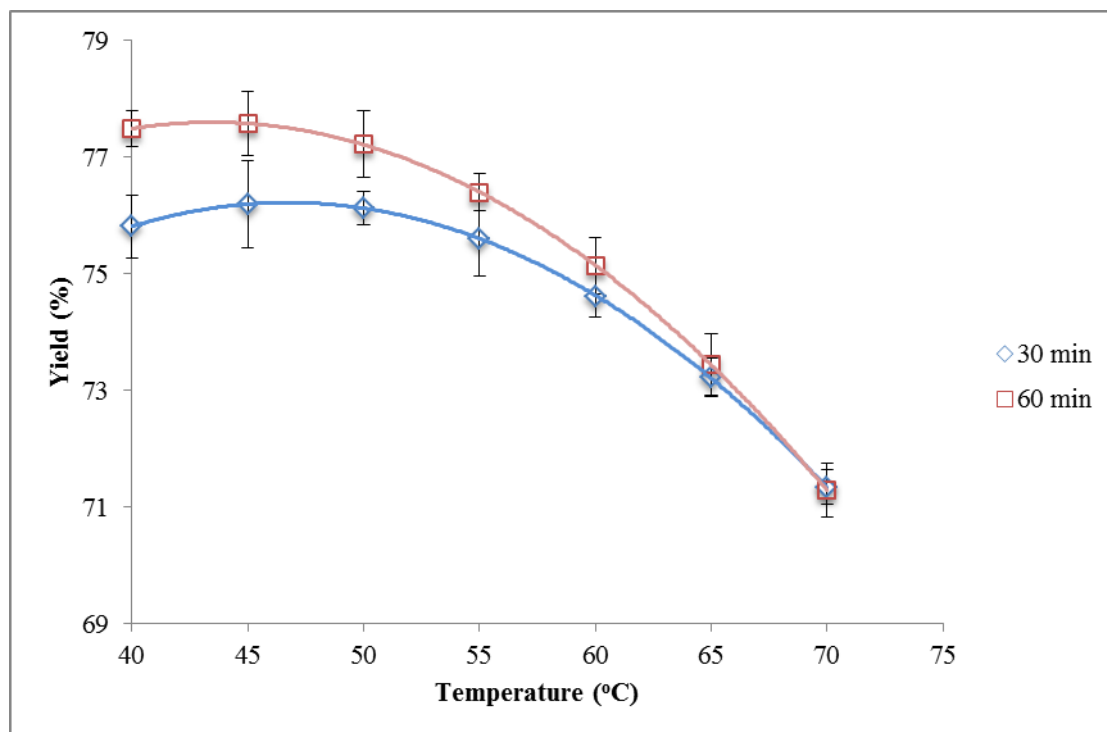


Figure 4.8: The effect of varying the reaction temperature on yield at reaction time = 30 mins and 60 mins. Catalyst amount was fixed at 1.25 wt% of PEG-ME 750.

#### 4.2.2.1.2 Effect of reaction time

Figure 4.9 shows the effect of reaction time at reaction temperatures 40°C and 60°C. Varying reaction time does not bring significant effect to the yield obtained, particularly so for reactions at 60°C. The yields obtained for reactions at 60°C from 0-120 minutes produced an almost linear line, indicating that there is little difference between a 0-minute and a 120-minute reaction time. There is a little increase observed (73.0-75.2%) until 60 minutes, after which the yield obtained plateaued as the reaction time is increased. A larger gap of increase is obtained with lower temperature. At 40°C, the yield increased from 73.1-78.1% from 0-90 minutes and remained at ~78% at 120 minutes. From this, it can be concluded that lower

temperature favors higher yield. Also, a longer time is needed for the reaction to be complete at lower temperature.

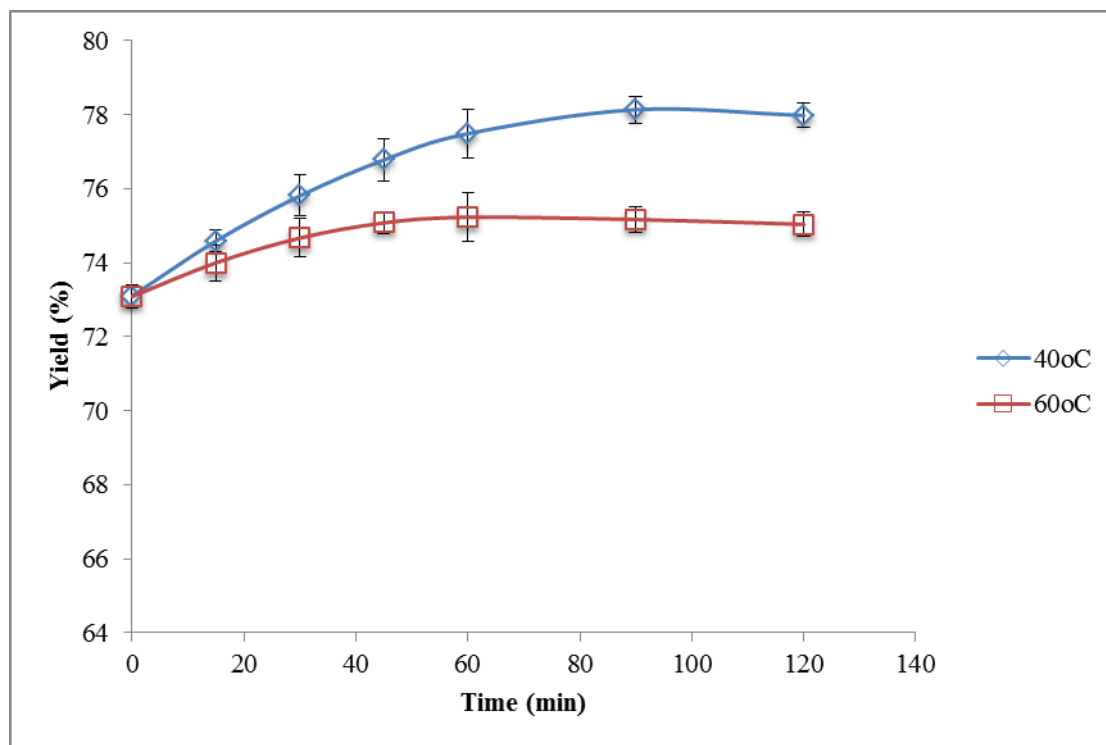


Figure 4.9: The effect of varying the reaction time on yield at reaction temperature = 40°C and 60°C. The catalyst amount was fixed at 1.25 wt% of PEG-ME 750.

#### 4.2.2.1.3 Effect of catalyst amount

Figure 4.10 shows the effect of catalyst amount on the yield of ENS-750 at reaction temperatures 40°C and 60°C. Once again, it is observed that a higher yield is obtained at a lower reaction temperature. As seen in Figure 4.10, both 40°C and 60°C exhibit a similar pattern. There is an optimum amount of  $\text{BF}_3$  needed for the reaction for both the temperatures. The optimum amount is found to be at 1.25 wt% for 40°C, and 1.50 wt% for 60°C. When the catalyst amount added exceeds the optimum amount, the reaction yield decreases. This is expected as side reactions are more significant when high amounts of  $\text{BF}_3$  is used in an organic reaction [66], hence a decrease in the reaction yield. Another possibility is that in reactions when high amounts of  $\text{BF}_3$  is used,  $\text{BF}_3$  may break the ether bond formed between the

hydrocarbon backbone and PEG-ME during when the reaction is going on and thus lowers the product yield [84].

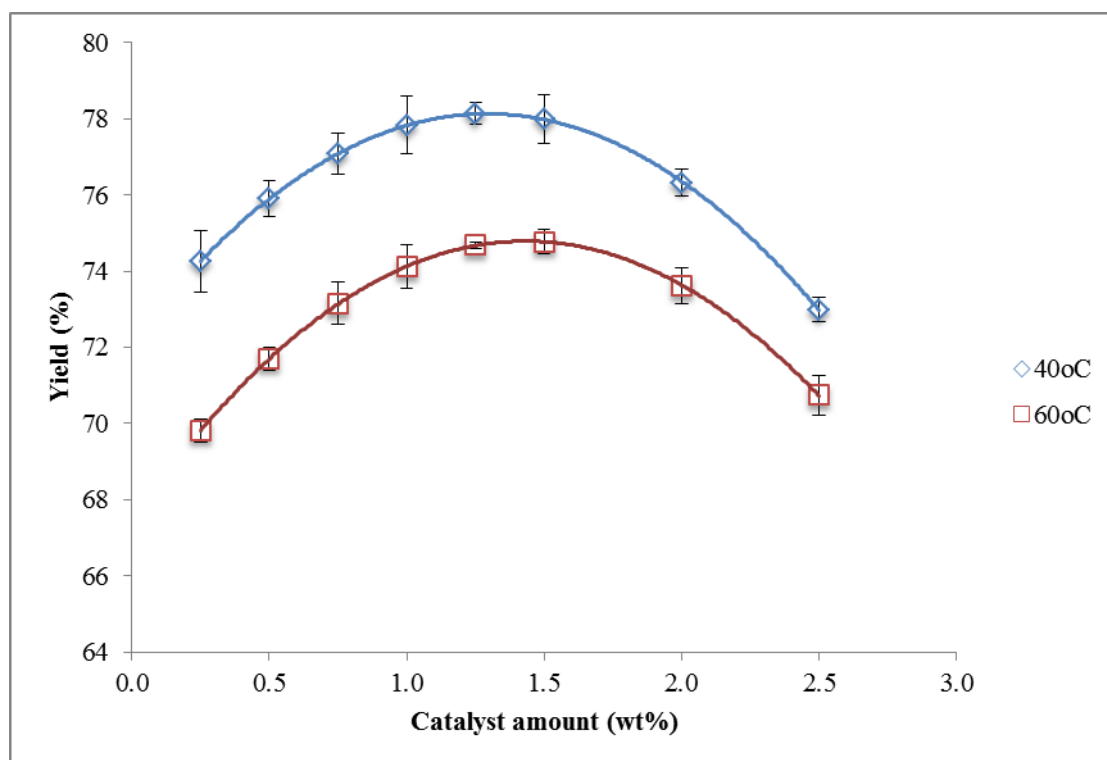


Figure 4.10: The effect of varying the catalyst amount on yield at reaction temperature = 40°C and 60°C. The reaction time was fixed at 90 minutes.

#### 4.2.2.1.4 Modification

As low temperature seems to produce favorable yield, a slight modification to the procedure adapted by Hedman et. al [52] was applied. Instead of introducing the epoxides at an elevated temperature, the epoxides were introduced into PEG-750 at room temperature. Temperature was raised to 60°C after all of the epoxides were added into PEG-750, and the reaction time was set at 90 minutes. The amount of catalyst used was fixed at 1.25 wt%. The final yield of ENS-750 obtained for this modified procedure was measured to be 86.66%, showing a significant increase when compared to reactions at elevated temperatures.

#### 4.2.2.2 Cloud point study

The cloud point for synthesized ENS-750 at 2.0 wt% concentration was measured to be 64°C, agreeable to literature [52]. The effect of surfactant concentration in a solution and the effect of salinity towards cloud point were studied.

##### 4.2.2.2.1 Effect of concentration of surfactant

Literatures have reported an increase of cloud point of nonionic surfactant with increasing surfactant concentrations [25, 52]. This is due to a change of shape in the micelles and increase in size of micelles that provides a more structured water-surfactant system [85, 86]. A cloud point study was performed on ENS-750 synthesized with varying concentrations ranging from 0.2 wt% to 2.0 wt% to determine the effect of this surfactant concentration range on cloud point value. The study was not carried out for concentration higher than 2.0 wt% because the usual surfactant concentration used for EOR applications is 0.5 – 1.0 wt%. The result obtained was that the cloud point value for ENS-750 maintained at 64°C from 0.2 wt% to 2.0 wt%. This shows that in this range the cloud point value for ENS-750 is not affected, indicating no significant change in size of micelles and no shape transition.

##### 4.2.2.2.2 Effect of salinity

The effect of salinity on the cloud point of ENS-750 at 2.0 wt% concentration was studied. The total dissolved solids content (TDS) of seawater in one of Malaysia's oilfields was determined to be approximately 35 000 ppm, with NaCl as the majority of the accounted electrolytes (see Table 3.1 in Section 3.2). Due to the high content of sodium chloride (NaCl) in seawater, the electrolyte chosen to study the effect of salinity was NaCl. Several literatures reported studied on the effect of different types of inorganic salts on the cloud points of nonionic surfactants [72, 73, 87]. From these literatures it is found that the general trend for the effect of NaCl on the cloud points



of nonionic surfactants is that NaCl depresses the cloud points of nonionic surfactants. ENS-750 synthesized follows the same trend. Figure 4.11 shows that the addition of NaCl decreases the cloud point of ENS-750. The change is linearly proportional to the concentration of NaCl in the solutions.

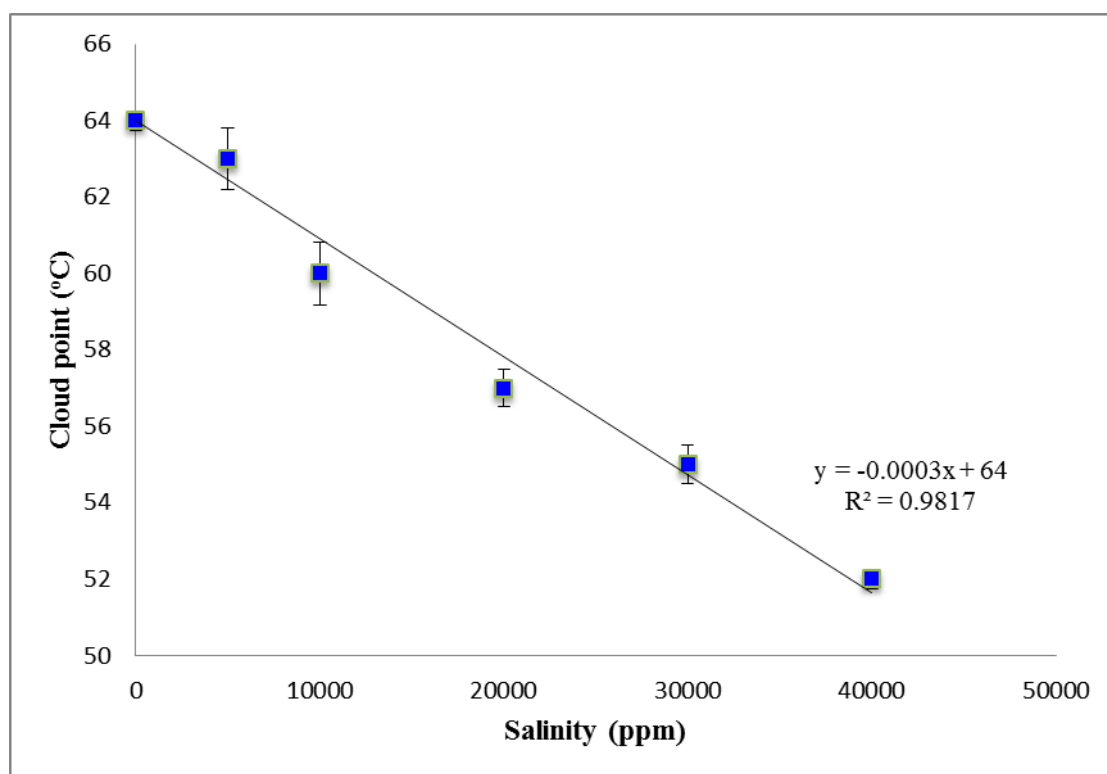


Figure 4.11: The effect of salinity on the cloud point of ENS-750

The depression of cloud point is due to the salting out effect of  $\text{Na}^+$  and  $\text{Cl}^-$  present in solution [88, 89]. Ions are either water structure-breaking or water structure-making. Water structure-breaking ions are ions with the effect of enhancing the solvent property of water, increasing the solubility of surfactants, resulting in increase in cloud points. The presence of water structure-breaking ions can hinder self-association of water molecules and hence will lead to an increasing extent of hydrogen bond formation between water molecules and EO units in nonionic surfactants. In contrast, the presence of water structure-making ions lowers the solvent property of water, encourages the self-association of water molecules and

hinders the formation of hydrogen bonds to an extent, thus leading to decreases in cloud points. Zaslavsky [88] reported the effects of various ions on the structure of water. Cations such as  $\text{Li}^+$ ,  $\text{Na}^+$ ,  $\text{K}^+$ ,  $\text{NH}_4^+$ ,  $\text{Ca}^{2+}$ ,  $\text{Mg}^{2+}$  and anions, such as  $\text{F}^-$ ,  $\text{SO}_4^{2-}$ ,  $\text{CO}_3^{2-}$ , and  $\text{PO}_4^{3-}$  are structure-making ions, while  $\text{Cl}^-$ ,  $\text{Br}^-$ ,  $\text{I}^-$  and  $\text{NO}_3^-$  are structure-breaking ions. According to Marcus [90],  $\text{Cl}^-$  is a structure-making ion while  $\text{Na}^+$  is a borderline case, and in general, effects of cations are relatively smaller in comparison with those of anions [72]. Hence, the cloud point of ENS-750 is depressed in the presence of NaCl.

The cloud point of ENS-750 was also measured in synthetic seawater. The measured cloud point value is  $54^\circ\text{C}$ . According to the plotted graph in Figure 4.11, at a concentration of 35000 ppm, the cloud point of ENS-750 should be  $53.5^\circ\text{C}$ , in agreement with the value measured experimentally.

As a conclusion for this section of the cloud point study, salinity would affect the application of nonionic surfactants as a chemical EOR agent when a high salinity injection medium is used (e.g. seawater). It would lower the cloud point of ENS-750, and hence the temperature range for ENS-750 to function as a foaming agent in the reservoir would be reduced. This problem is solved by the addition of cloud point boosters to increase the cloud point of ENS-750. With the addition of cloud point boosters, ENS-750 would be able to function as a foaming agent with a larger temperature range and applicable in high temperature reservoirs.

## **4.3 Characterization**

### **4.3.1 HOE**

Analysis using GC-MS shows that HOE oil contained high amount of unsaturation. Table 4.4 shows the composition of HOE. HOE contains 72.23% of methyl oleate and 15.36% of methyl linoleate, bringing to a total of 87.59% of unsaturated FAMES, with 1 mole of HOE containing 1.0295 mole of C=C double bonds. The calculated molecular weight of HOE based on GC-MS results is 295.994

gmol<sup>-1</sup>. FT-IR and <sup>1</sup>H NMR analyses were conducted for HOE and the detailed FT-IR results are reported in Table 4.5.

Table 4.4: Composition of HOE

FAMES Present	Composition (%)
Methyl Palmitate	1.73
Methyl Stearate	10.19
Methyl Eicosanoate	0.49
Methyl Oleate	72.07
Methyl Linoleate	15.36

Figure 4.12 shows the <sup>1</sup>H NMR spectrum of HOE and is explained with respect to methyl linoleate. Peak at 5.41 ppm (represented by G) is from the protons attached directly to the carbons having double bonds, while the peak at 2.01 ppm (represented by C) is from the protons attached to the carbons adjacent to the carbons having double bonds [91]. A small peak detected at 2.80 ppm (represented by E) shows the existence of methyl linoleate. This peak is from the protons attached to the carbon in between the two carbons having double bonds.

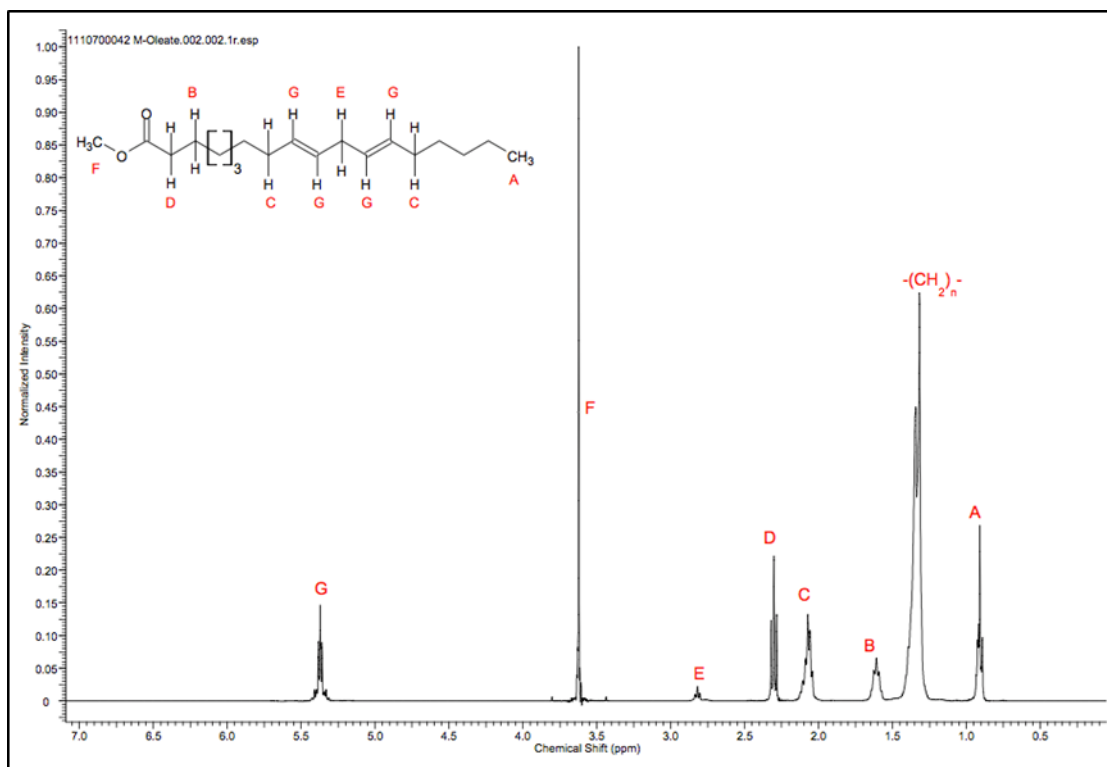


Figure 4.12:  $^1\text{H}$  NMR spectrum for HOE explained in respect to methyl linoleate

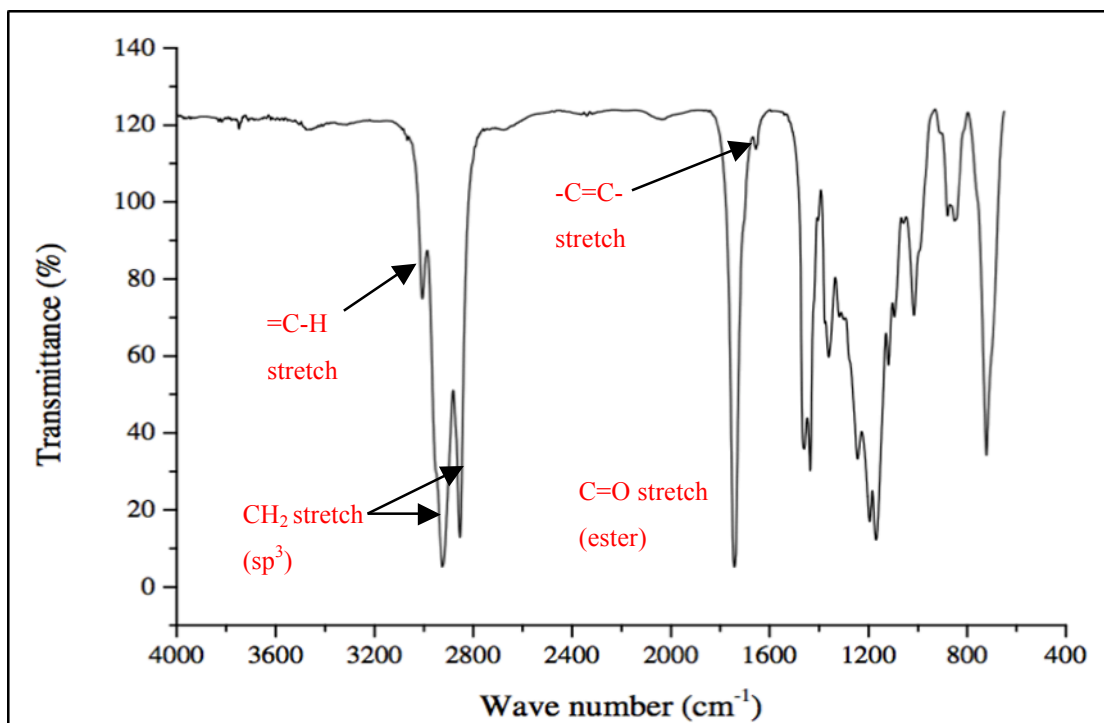


Figure 4.13: FT-IR spectrum for HOE

### 4.3.2 Epoxides

The disappearance of peaks at  $3006\text{ cm}^{-1}$  and  $1654\text{ cm}^{-1}$  from the FT-IR spectrum for epoxides indicates the complete utilization of unsaturation. This was further confirmed with GC-MS analysis, where no methyl linoleate and methyl oleate were detected. A new peak at  $828.53\text{ cm}^{-1}$  emerges in the epoxide's spectrum, indicating the presence of oxirane ring. The comparison between the FT-IR spectra of HOE and epoxides with their detailed peak assignments are as tabulated in Table 4.5.

Table 4.5: Comparison of FT-IR spectra of HOE and epoxides synthesized

Wave number ( $\text{cm}^{-1}$ )	Assignment		Functional group
	HOE	Epoxides of HOE	
3006	=C-H stretch	Not detected	Unsaturation
2920-2924, 2853-2854	$\text{CH}_2$ stretch ( $\text{sp}^3$ )	$\text{CH}_2$ stretch ( $\text{sp}^3$ )	Aliphatic
1739-1742	C=O (ester)	C=O (ester)	Methyl ester
1654	-C=C- stretch	Not detected	Unsaturation
1459	-C-H bend	-C-H bend	Aliphatic $\text{CH}_2$
1435-1436	-C-H bend	-C-H bend	Terminal $\text{CH}_3$
1361-1363	-C-H bend	-C-H bend	Terminal $\text{CH}_3$
1169-1170	C-O stretch (ester)	C-O stretch (ester)	Methyl ester
828	Not detected	C-O-C stretch	Oxirane ring
722-723	$\text{CH}_2$ rocking	$\text{CH}_2$ rocking	Aliphatic

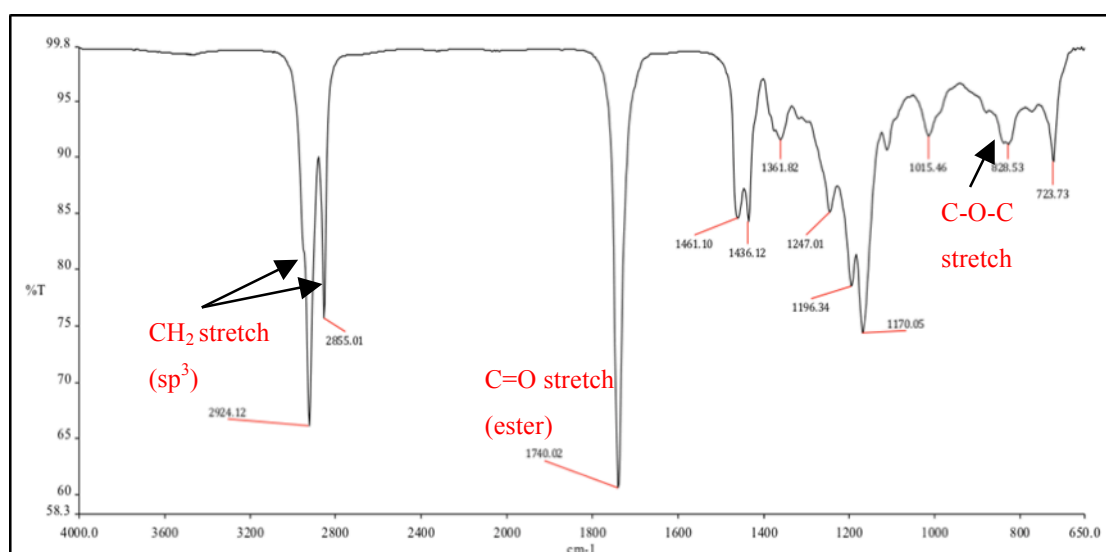


Figure 4.14: FT-IR spectrum of epoxide derived from HOE

$^1\text{H}$  NMR spectrum gives a clearer picture on the epoxides synthesized. Figure 4.15 shows the  $^1\text{H}$  NMR spectrum of epoxides and is explained with respect to diepoxy (epoxides derived from methyl linoleate) and monoepoxy (epoxides derived from methyl oleate). The peaks at 2.01 ppm, 2.80 ppm and 5.41 ppm indicating unsaturation in HOE have completely vanished and the emergence of peaks at 1.84 ppm (represented by A) and 2.44 ppm (represented by C) indicates the existence of epoxides. Peak A is from protons attached to the carbons that are adjacent to the carbons forming oxirane rings and peak C is from the protons attached to the carbons that form oxirane rings.  $^1\text{H}$  NMR analysis confirms [92] the presence of both diepoxy and monoepoxy. Weak peaks at 1.68 ppm (represented by B), 2.92 ppm (represented by D) and 3.06 ppm (represented by E) show the presence of diepoxy. HOE contains only 11% of methyl linoleate. Hence, the diepoxy formed gives only weak but nonetheless distinguishable peaks. A comparison of  $^1\text{H}$  NMR spectrum of HOE and epoxides synthesized is shown in Figure 4.16 and the peaks' details are tabulated in Table 4.6.

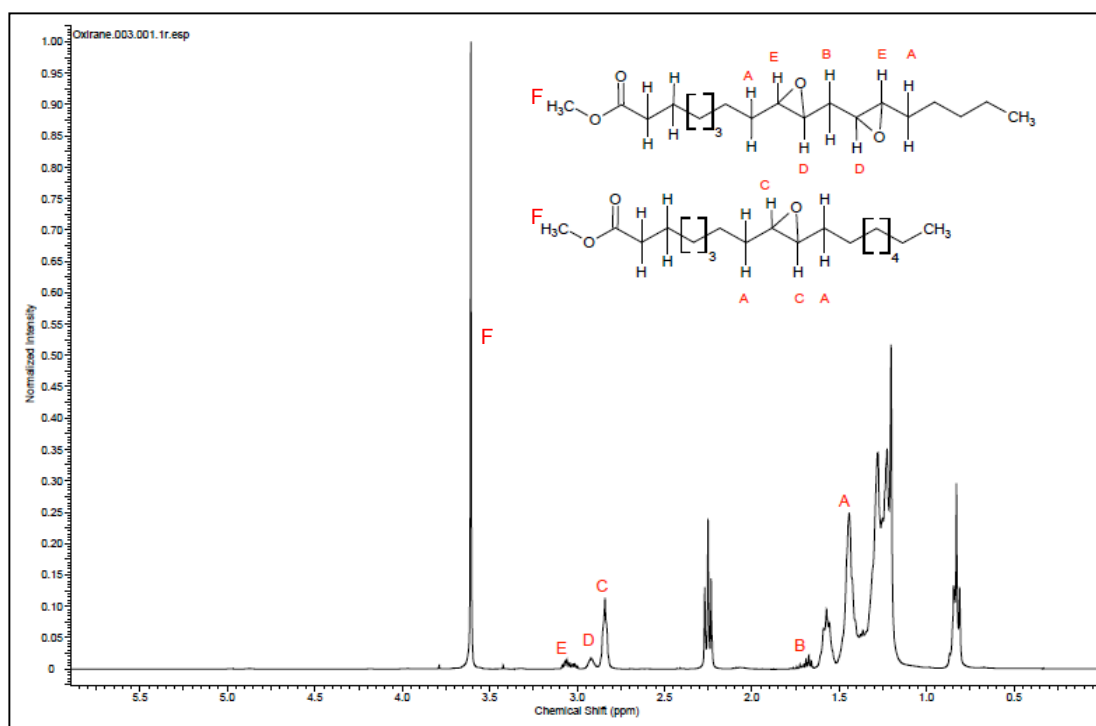


Figure 4.15:  $^1\text{H}$  NMR spectrum for epoxides synthesized explained in respect to: 1) diepoxy derived from methyl linoleate and 2) monoepoxy derived from methyl oleate

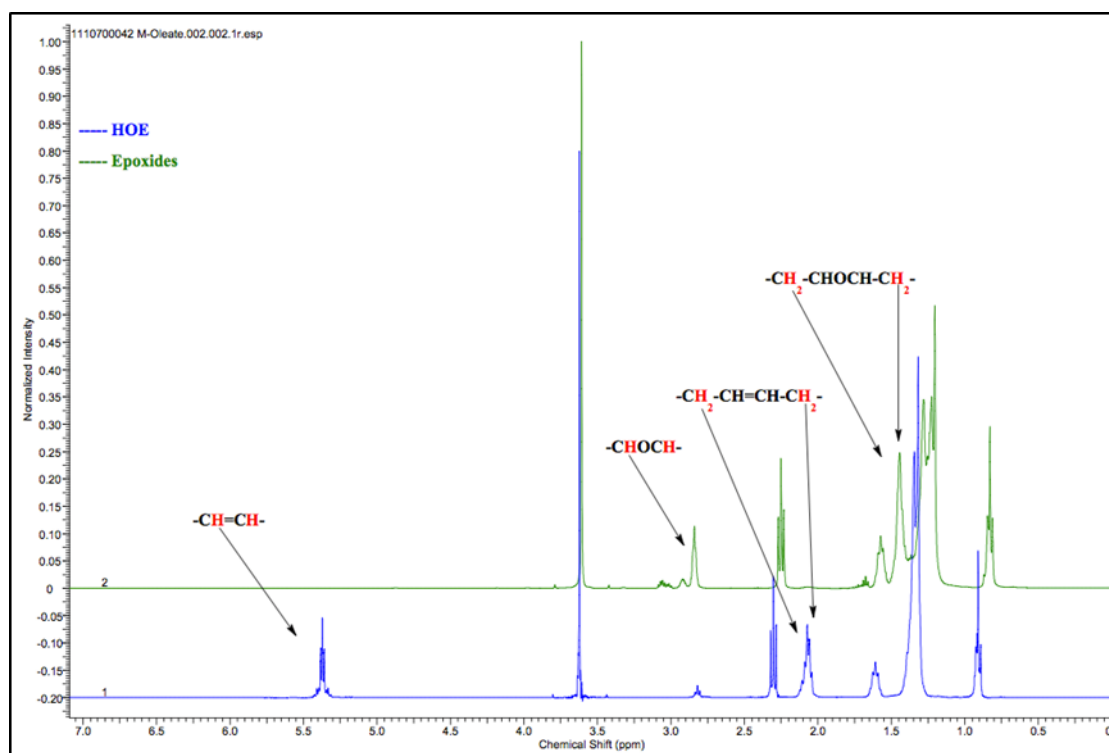


Figure 4.16: Comparison of  $^1\text{H}$  NMR spectra of HOE and epoxides

Table 4.6:  $^1\text{H}$  NMR peak table for HOE and epoxides synthesized from HOE

HOE	Epoxides of HOE
$^1\text{H}$ NMR (400 MHz, Acetone- $d_6$ ) $\delta$ 5.45-5.29 (m, 2H), 3.62 (s, 3H), 2.80 (t, 0H), 2.30 (t, $J = 7.4$ Hz, 2H), 2.15-1.99 (m, 4H), 1.61 (p, $J = 6.7$ Hz, 2H), 1.45-1.26 (m, 20H), 0.91 (t, 3H).	$^1\text{H}$ NMR (400 MHz, Chloroform- $d$ ) $\delta$ 3.61 (s, 3H), 3.06 (q, 0H), 2.96 – 2.89 (m, 0H), 2.89 – 2.79 (m, 1H), 2.25 (t, $J = 8.7, 6.3$ Hz, 2H), 1.68 (t, 0H), 1.57 (p, 2H), 1.51 – 1.39 (m, 6H), 1.34 – 1.18 (m, 17H), 0.89 – 0.79 (t, 3H).

A potential by-product of epoxidation – dihydroxy was not detected from both FT-IR and  $^1\text{H}$  NMR analyses. However, GC-MS analysis shows the presence of dihydroxy at 3.39% and oxirane at 96.61%, agreeable to the epoxidation yield value obtained through oxirane oxygen titration.



### 4.3.3 ENS-750

Attachment of PEG-ME onto FAMES from HOE could not be confirmed by FT-IR and  $^1\text{H}$  NMR analyses. This is because peaks from PEG-ME itself overshadow the peaks responsible for the C-OR that indicates the attachment of PEG-ME through oxirane ring opening. As PEG-ME contributes 70.59% of the molecular weight of the synthesized surfactant, peaks associated with PEG-ME – especially the repeated EO units – are very intense, making identifying of peaks for any successful attachment of PEG-ME difficult.

Table 4.7 shows the comparison of FT-IR peaks for epoxides and ENS-750. A very large and intense peak is observed at  $1098\text{ cm}^{-1}$ , indicating the presence of ether linkage that is contributed by PEG-ME 750 [93]. The peaks from PEG-ME mostly overshadow the peaks indicating hydrocarbon chain, particularly in the fingerprint region. Peaks indicating aliphatic hydrocarbon chain ( $1461$ ,  $1436$  and  $1361\text{ cm}^{-1}$ ) and methyl ester ( $1170\text{ cm}^{-1}$ ) could not be seen in the ENS-750's FT-IR spectrum. A peak emerging at  $3497\text{ cm}^{-1}$  indicates the existence of hydroxyl group, indirectly indicating the opening of oxirane ring and attachment of PEG-ME. Another noted difference is the disappearance of peak at  $827\text{ cm}^{-1}$ , showing the disappearance of oxirane rings.

The same is observed for  $^1\text{H}$  NMR spectra obtained for ENS-750. The peaks responsible for hydrocarbon backbone appear miniscule in comparison with peak at 3.57 ppm (refer to Figure 4.18), which is responsible for the repeating EO units of PEG-ME. This makes it difficult for the confirmation of PEG-ME attachment onto the hydrocarbon backbone. However, the peaks for oxirane ring at 1.84 and 2.44 ppm have disappeared, indicating the occurrence of oxirane ring opening reaction. A comparison of  $^1\text{H}$  NMR peaks obtained for epoxides and ENS-750 are tabulated in Table 4.8.

Figure 4.19 shows a comparison of  $^{13}\text{C}$  NMR spectrum for epoxides and ENS-750. The opening of oxirane ring and attachment of PEG-ME onto hydrocarbon backbone could be identified easily using this method. The emergence of peaks at 73 (peak H) and 84 ppm (peak G) indicate oxirane ring opening with PEG-ME. The hydroxyl group contributes the peak at 73 ppm and the peak at 84 ppm is due to the

ether linkage between the hydrocarbon backbone and PEG-ME. All peaks related to oxirane ring – peaks C, D and F [94] from Figure 4.19 – have disappeared. The molecular structure of the synthesized ENS-750 is presented in Figure 4.20.

Table 4.7: Comparison of FT-IR spectrum for epoxides and ENS-750

Wave number (cm <sup>-1</sup> )	Assignment		Functional group
	Epoxides from HOE	ENS-750	
3497	Not detected	Free -OH	Hydroxyl
2923-2924, 2855-2856	C-H stretch (sp <sup>3</sup> )	C-H stretch (sp <sup>3</sup> )	Aliphatic
1737-1740	C=O (ester)	C=O (ester)	Methyl ester
1461	-C-H bend	(Overshadowed)	Aliphatic CH <sub>2</sub>
1436	-C-H bend	(Overshadowed)	Terminal CH <sub>3</sub>
1361	CH <sub>3</sub> bend	(Overshadowed)	Terminal CH <sub>3</sub>
1349	Not detected	-C-H bend	Alkane
1248	Not detected	C-O-C stretch	Ether
1170	C=O stretch (ester)	(Overshadowed)	Methyl ester
1098	Not detected	C-O-C stretch	Ether
827	C-O-C stretch	Not detected	Oxirane ring
723	CH <sub>2</sub> rocking	CH <sub>2</sub> rocking	Aliphatic

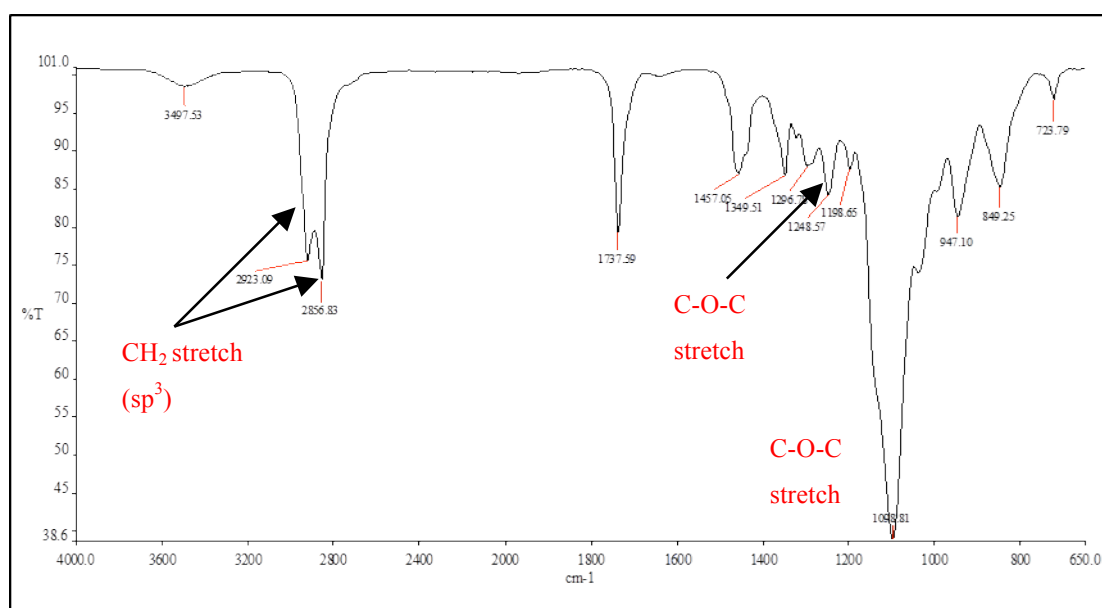


Figure 4.17: FT-IR spectrum of ENS-750

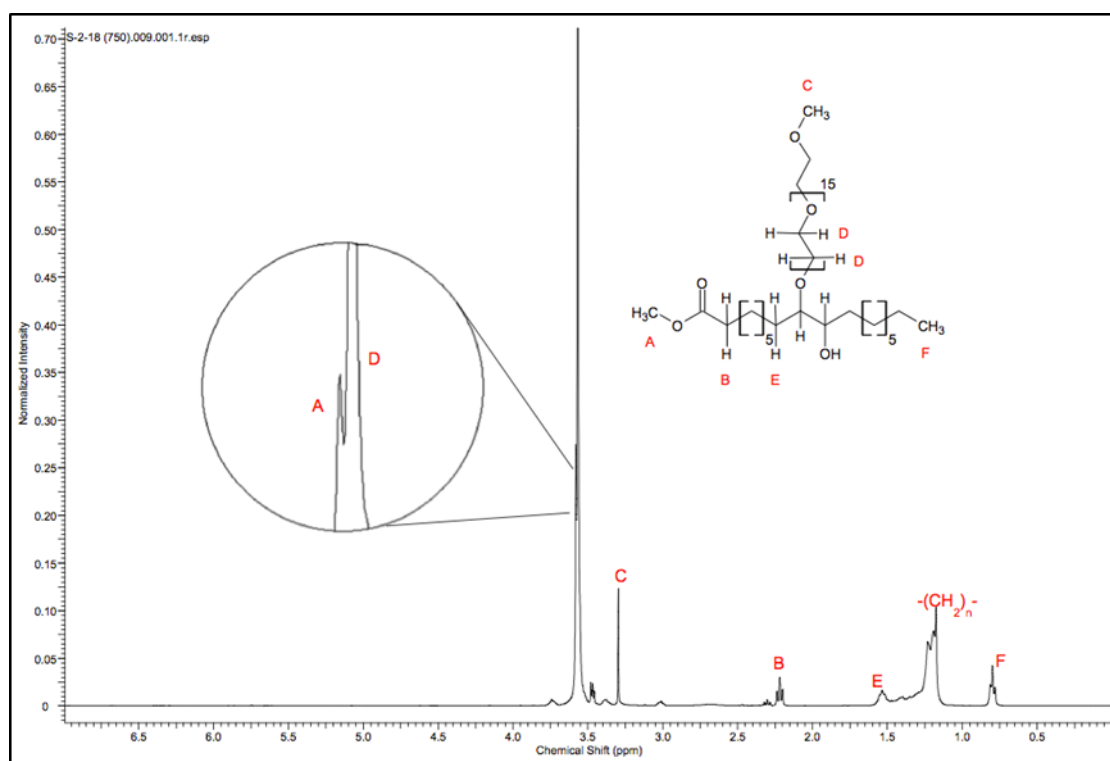


Figure 4.18: <sup>1</sup>H NMR spectrum of ENS-750. The peaks responsible for hydrocarbon backbone appear miniscule in comparison with peak D which is responsible for the repeating EO units of PEG-ME.

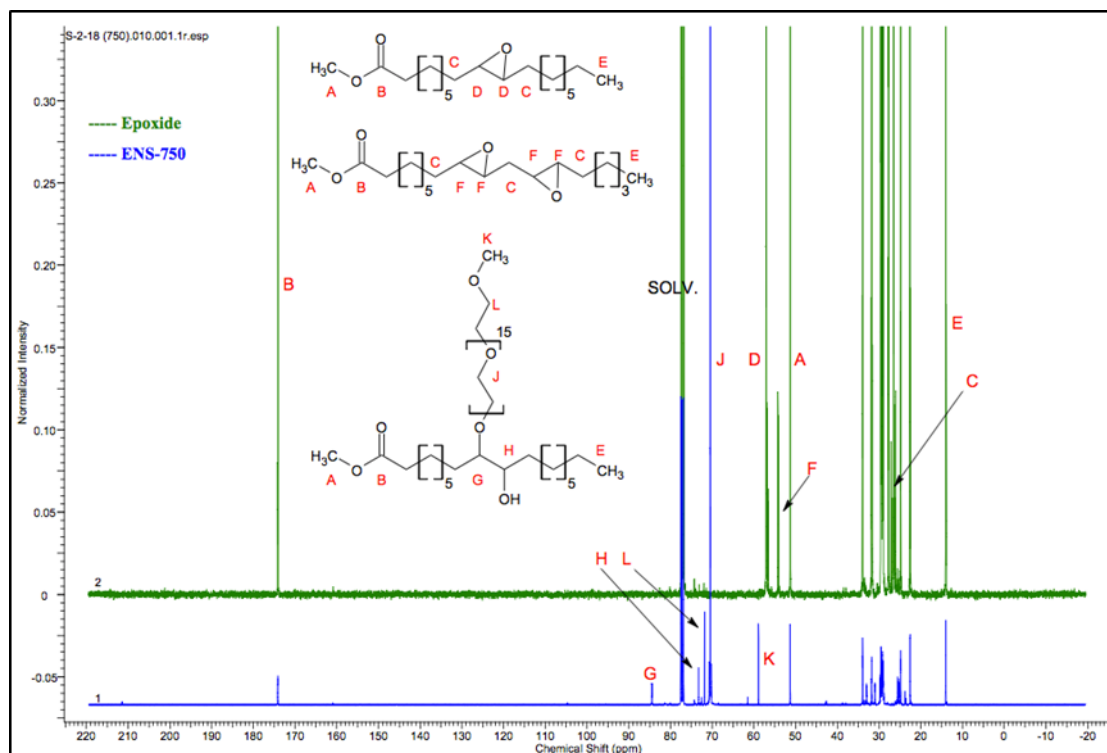


Figure 4.19: Comparison of  $^{13}\text{C}$  NMR spectra of epoxide and ENS-750 with (molecule from top to bottom): monoepoxy, diepoxy and ENS-750. Note the very strong peak for EO (peak J) from PEG-ME as compared to other peaks present in ENS-750 spectra.

Table 4.8:  $^1\text{H}$  NMR peak table for epoxides synthesized from HOE and ENS-750

Epoxides of HOE	ENS-750
$^1\text{H}$ NMR (400 MHz, Chloroform-d) $\delta$ 3.61 (s, 3H), 3.06 (q, 0H), 2.96 – 2.89 (m, 0H), 2.89 – 2.79 (m, 1H), 2.25 (t, $J$ = 8.7, 6.3 Hz, 2H), 1.68 (t, 0H), 1.57 (p, 2H), 1.51 – 1.39 (m, 6H), 1.34 – 1.18 (m, 17H), 0.89 – 0.79 (t, 3H).	$^1\text{H}$ NMR (400 MHz, Chloroform-d) $\delta$ 3.57 (d, $J$ = 5.4 Hz, 41H), 3.30 (s, 2H), 2.22 (t, $J$ = 7.5, 1.5 Hz, 2H), 1.57 – 1.48 (m, 2H), 1.45 – 1.37 (m, 2H), 1.33 – 1.15 (m, 20H), 0.80 (t, $J$ = 6.4 Hz, 3H).

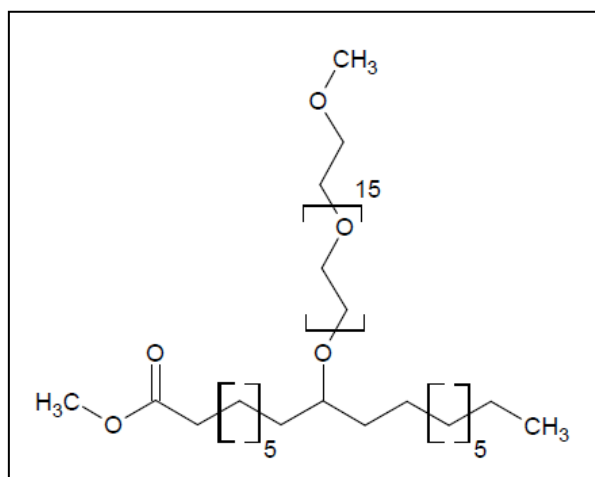


Figure 4.20: Molecular structure of ENS-750

#### 4.3.3.1 Critical Micelle Concentration

The CMC value of the synthesized ENS-750 was determined to be 0.30 mmol/L, close to the reported value in the literature [52] of 0.40 mmol/L. From the graph plotted (see Figure 4.21) on the conductivity of surfactant solution against the surfactant concentration, an abrupt change at 0.30 mmol/L was observed. Hence, the CMC value for ENS-750 was determined to be at 0.30 mmol/L.

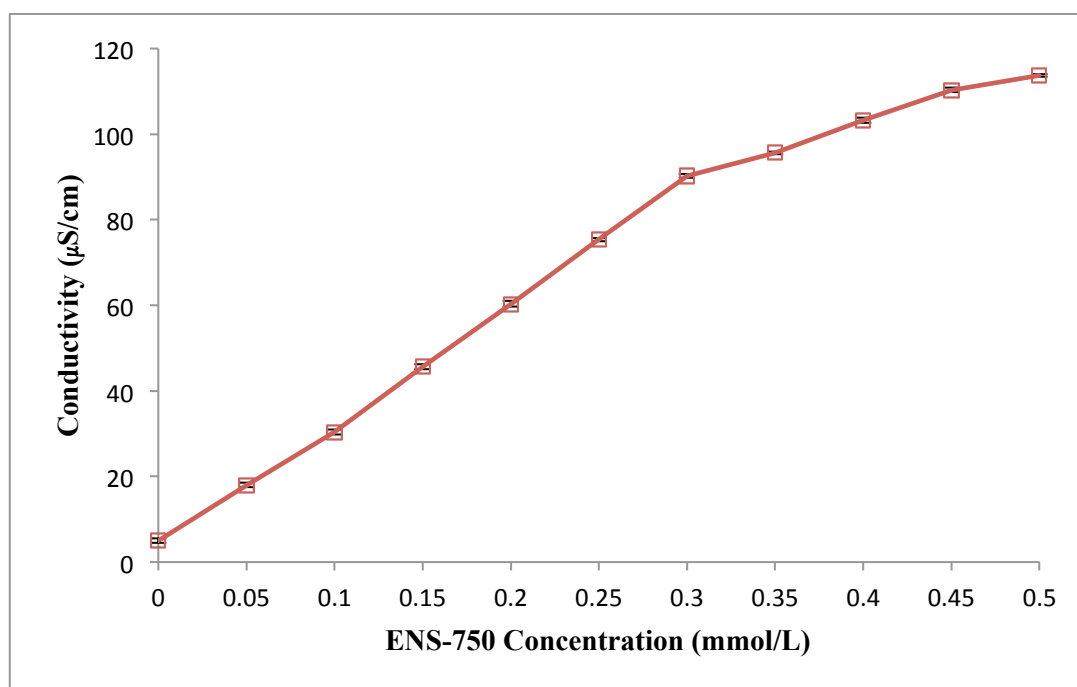


Figure 4.21: Conductivity measurements of ENS-750 surfactant solutions.

## 4.4 Formulation

### 4.4.1 Addition of ionic surfactants as cloud point boosters (CPB)

Five ionic surfactants were used to elevate the cloud point of synthesized ENS-750. The five surfactants were alpha-olefin C12-16 sulfonate (AOS), sodium dodecyl benzene sulfonate (DBS), sodium dodecyl sulfate (SDS), methyl ester C16-18 sulfonate (MES) and cetyltrimethyl ammonium bromide (CTABr). Of the 5 surfactants, only CTABr is a cationic surfactant with the remaining 4, anionics. The anionic surfactants were of sulfonate and sulfate groups. Only one of the anionic surfactants is sulfate, with the rest, sulfonates. Sulfonates are generally more favorable than sulfates for higher temperature applications due to the fact that sulfates tend to be unstable and hydrolyze at high temperature [95]. Of the 3 sulfonates, AOS possesses aliphatic hydrophobic tail, DBS contains an aromatic ring with an attached aliphatic hydrocarbon chain as its hydrophobic tail and MES is an anionic surfactant derived from FAMES produced from palm oil. Mixed ionic-nonionic surfactant solutions were prepared in such a way that the final concentration of solutions remains at 2.0 wt%, which means that the ratio between nonionic and ionic was varied. The effect of the ionic surfactants on the cloud point of ENS-750 was studied with and without the presence of electrolyte (NaCl).

#### 4.4.1.1 Without electrolyte

Figures 4.22 – 4.26 show the effect of ionic surfactants with and without the presence of NaCl. From the figures, it is shown that in general, the presence of ionic surfactants increased the cloud point of ENS-750. The charged ionic surfactant molecules can either be adsorbed on nonionic surfactant micelles or can form mixed micelles with nonionic surfactant molecules. The increase in the cloud point is due to the increased electrostatic repulsion between nonionic micelles caused by the ionic surfactants and, thus, making it more difficult for the micelles to aggregate together [96, 97]. The difficulty to aggregate together leads to an increase in the cloud point. The extent of repulsion between the micelles depends on the mixing ratio of ionic-

nonionic surfactant. The more ionic surfactant is added, the stronger the repulsion between micelles and hence the higher the cloud point of ionic-nonionic surfactant solution. This relationship has been observed to be linear [87, 97]. It is observed from the graphs that in the absence of NaCl, the presence of ionic surfactants result in profound increase to the cloud point of ENS-750. With a mere 0.1 wt% of ionic surfactant (5% of the mixed ionic-nonionic surfactant composition), the cloud point of ENS-750 was generally increased by approximately 20°C from its original cloud point. No significant difference in terms of performance among the 5 ionic surfactants was observed.

#### 4.4.1.2 With electrolyte

As with the previous section on the effect of salinity on cloud point of ENS 750, the electrolyte used in studying the effect of salinity on elevated cloud point was NaCl. The effect of the 5 ionic surfactants on the increase of the cloud point of ENS-750 in the presence of NaCl was studied. The degree of cloud point suppression is generally proportional in relation to the concentration of NaCl. However, the gradient of plotted lines in Figures 4.22 – 4.26 generally lessens with increasing salinity (see Table 4.9), proving that the ionic surfactants become less effective in elevating the cloud point of ENS-750 with increasing salinity. In the presence of NaCl, the original charge distribution of the mixed ionic/nonionic micelle is swamped and the corresponding repulsion is screened [98]. This makes the micelles' aggregation easier and hence lowers the elevated cloud point.

Table 4.9: The gradient of plotted lines for Figures 4.22 – 4.26

NaCl concentration (ppm)	AOS	DBS	SDS	MES	CTABr
5000	0.1	0.0518	0.12	0.08	0.1
10000	0.02	0.0282	0.0927	0.06	0.06
20000	0.0373	0.0042	0.0491	0.018	0.0364
30000	0.0336	-	0.0325	0.0228	0.0222
40000	0.0101	-	0.023	0.0099	0.0098

The five ionic surfactants used for the study seemed to be effective in elevating the cloud point of ENS-750 at salinity conditions up to 40 000 ppm except for DBS. At 20 000 ppm salinity, DBS seemed to be ineffective in elevating the cloud point of ENS-750. Even a large mixing ratio of 40/60 (DBS/ENS-750) was unable to elevate the cloud point of ENS-750 above 95°C. It could only elevate the cloud point of ENS-750 to 73°C. Another point to note is that at salinity above 20 000 ppm, DBS could not solubilize in brine solutions, hence no further cloud point tests involving DBS were conducted. The relative strength of ionic surfactants in elevating the cloud point of ENS-750 is in the order:



The efficiency of ionic surfactants in elevating cloud point is governed by the solubility of surfactant in brine solutions, which in turn, seemed to be governed by the structure of the surfactants' hydrocarbon tail. Of the 5 ionic surfactants, DBS possess an aromatic ring, giving its hydrocarbon tail bulkiness. MES contains a 'branch' in the form of methyl ester with the sulfonate group,  $-\text{SO}_3^-$  situated at the  $\alpha$ -carbon position and not at the terminal of the hydrocarbon chain giving it a methyl ester branch. AOS, CTABr and SDS have aliphatic hydrocarbon tail with C12-C16, C16 and C12 carbon chains respectively.

The structure of the surfactants' hydrocarbon tail was found to affect the solubility of ionic surfactants in brine solutions. Bulkiness in surfactants' hydrocarbon tail – in branching as well as pendant attachment (aromatic ring) – decreases its solubility in brine and hence its poor performance in elevating the cloud point of nonionic surfactants. The bulkier the hydrocarbon chain, the more difficult it is for the ionic surfactant to solubilize in brine solutions. This pattern has also been observed by Skauge and Palmgren [99]. The preferred hydrocarbon tail structure is the aliphatic, saturated hydrocarbon tail.



The length of the aliphatic hydrocarbon tail also affects the efficiency of ionic surfactants to elevate cloud point. Longer carbon chain length shows better efficiency in elevating cloud point. Sharma and Bahadur [73] and Na et. al [74] both observed a similar pattern in their respective studies. Surfactants with longer hydrocarbon tail are found to be better CPBs.

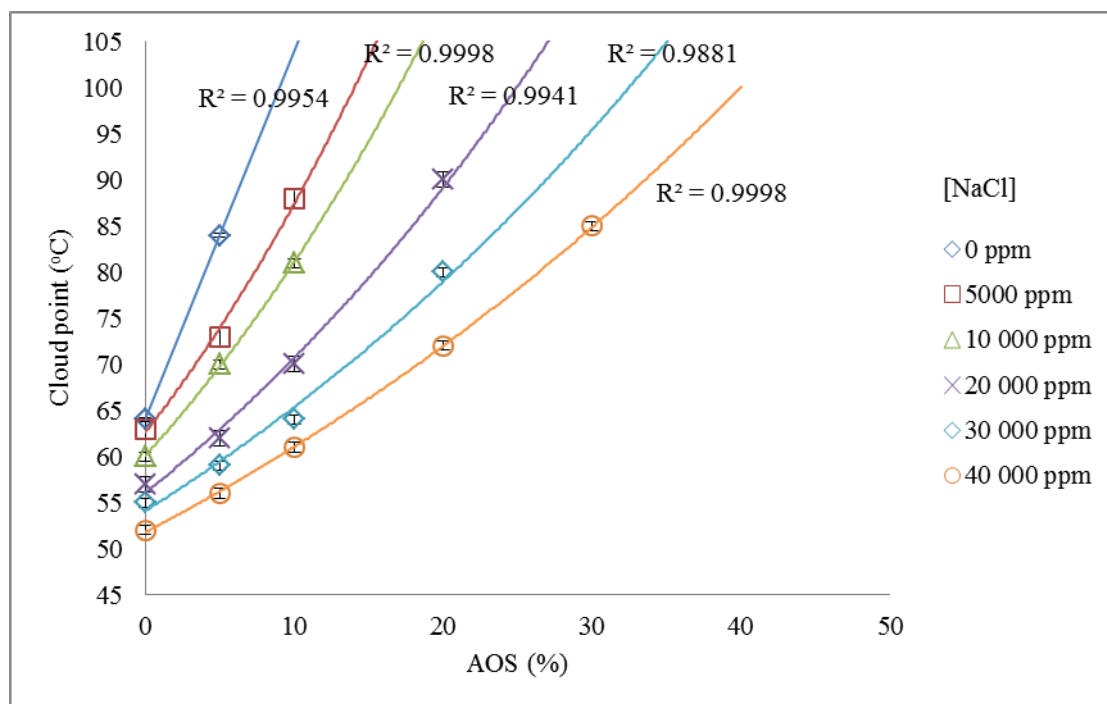


Figure 4.22: Cloud point of AOS/ENS-750 mixtures in the presence of NaCl

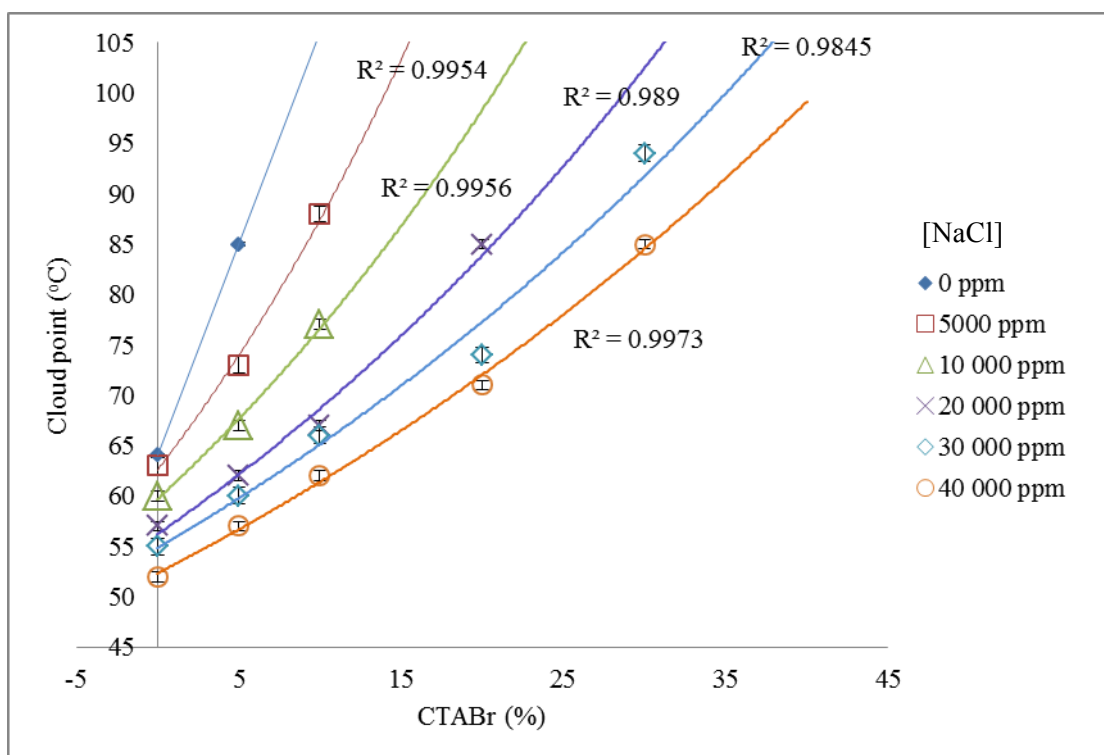


Figure 4.23: Cloud point of CTABr/ENS-750 mixtures in the presence of NaCl

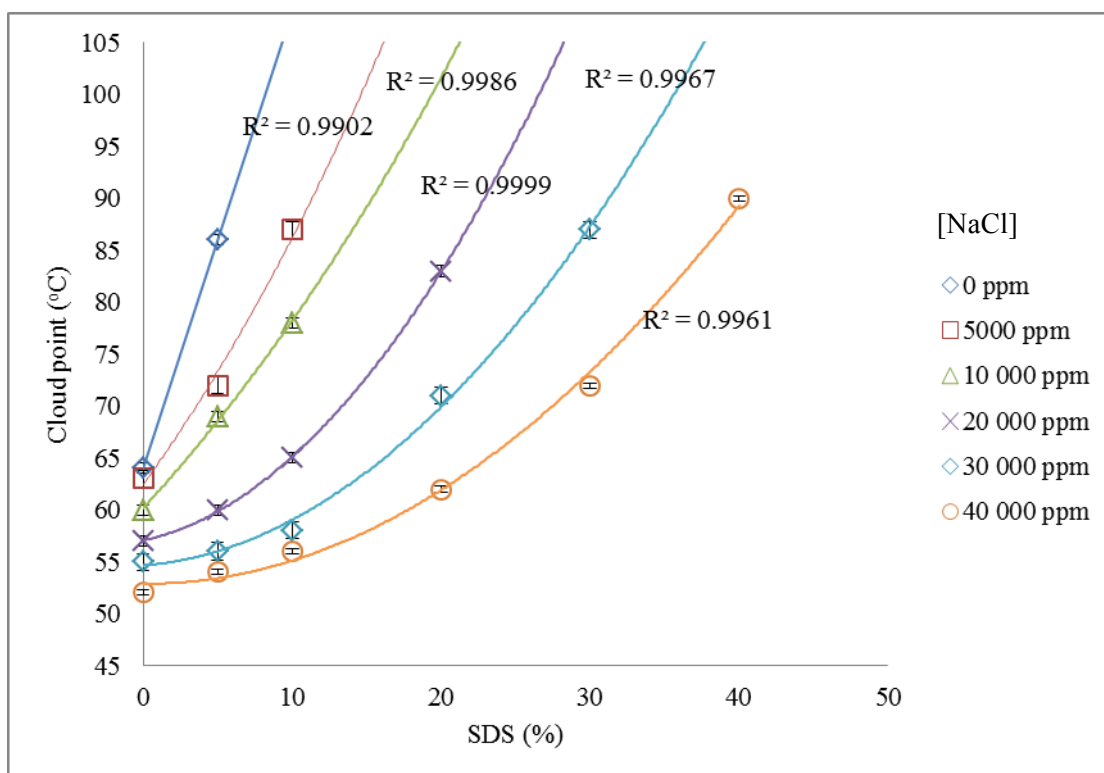


Figure 4.24: Cloud point of SDS/ENS-750 mixtures in the presence of NaCl

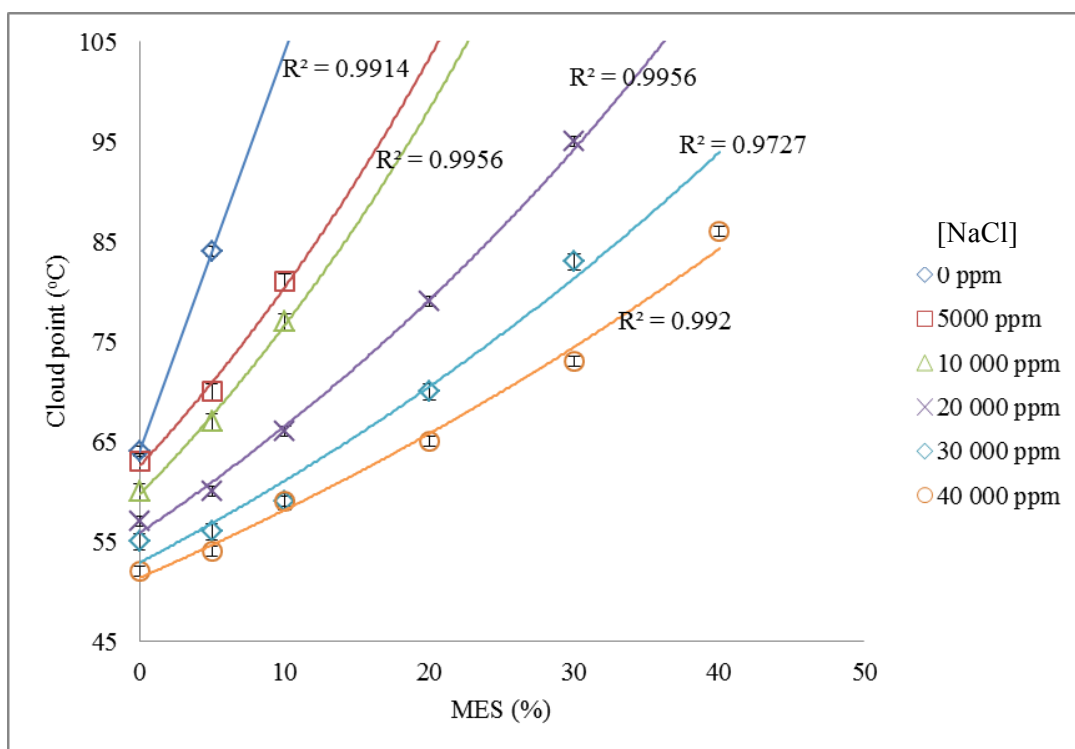


Figure 4.25: Cloud point of MES/ENS-750 mixtures in the presence of NaCl

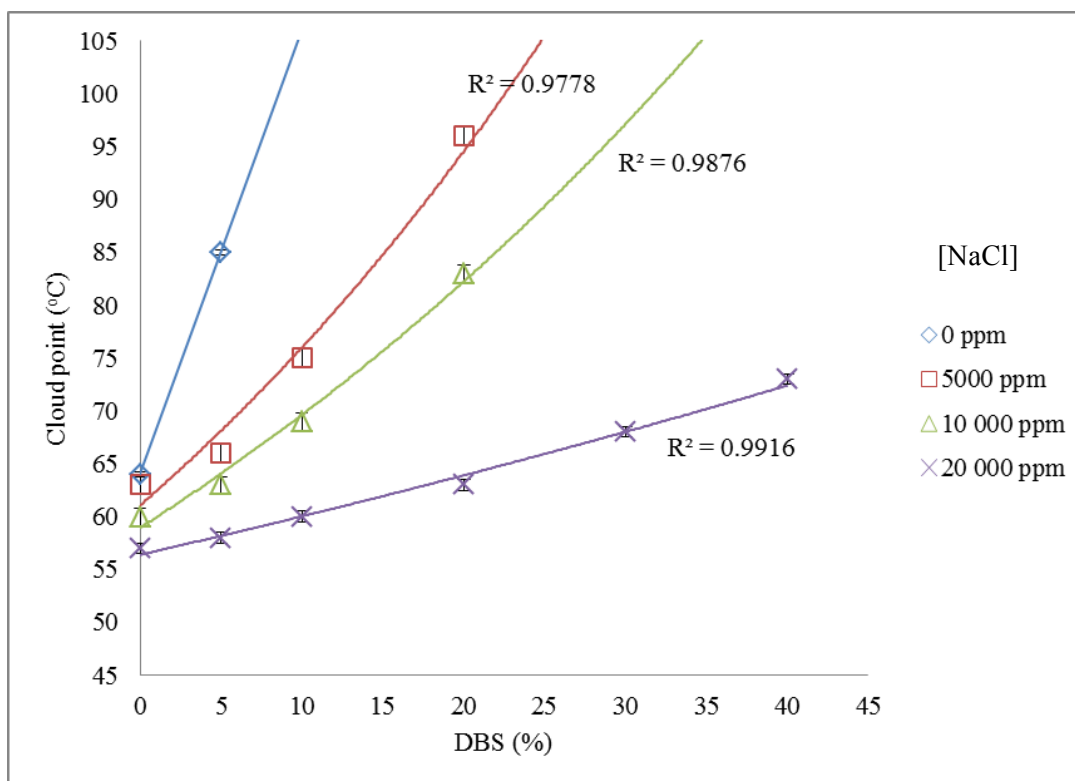


Figure 4.26: Cloud point of DBS/ENS-750 mixtures in the presence of NaCl

Of the five ionic surfactants used in the study of CPBs, three were chosen to be used in the final step of surfactant blend formulation: AOS, SDS and MES. DBS was not included due to its low tolerance toward salinity. Although CTABr appears to be more effective in elevating the cloud point of ENS-750 than SDS and MES in saline condition, it was not included in the final formulation. This is due to the cationic nature of CTABr. Cationic surfactants are generally not applied in sandstone reservoirs due to the high adsorption of surfactants onto reservoir rocks and thus high surfactant loss. The use of CTABr as a CPB for ENS-750 can be considered for limestone reservoirs.

#### **4.4.2 Addition of foam booster**

Three foam boosters available commercially were used to boost the foam formation of ENS-750/anionic surfactant mixtures. These foam boosters are betaines. The three foam boosters used were lauryl hydroxysultaine (LHS), BETADET SHR (SHR) and BETADET HR-60K (HR). Both SHR and HR are foam boosters comprised of cocamidopropyl dimethylhydroxysultaine and cocamidopropyl betaine respectively. Sultaines are betaines with its carboxylate ( $\text{COO}^-$ ) group substituted with a sulfonate ( $\text{SO}_3^-$ ) group. SHR and HR are derived from plant oil with C12 carbon chain fatty acids whereas LHS is derived from alkyl C12.

Many surfactant formulations in synthetic seawater with various combinations of ENS-750, CPBs and foam boosters were screened to determine the recipe for a formulation that could withstand high temperature and high salinity. The formulations that could tolerate harsh conditions were tested for their foam stability.

##### *4.4.2.1 Screening test*

A total of 144 formulations with various combinations of ENS-750, CPBs and foam boosters were screened for their thermal stability and tolerance toward seawater. Formulations were prepared at 2.0 wt% concentration in seawater and were placed in an oven at 100°C. Three observations were done over a period of 15 days. The first

observation was done after 2 hours (Day 1), the second after 24 hours (Day 2) and the third on the 15<sup>th</sup> day (Day 15). Formulations that remain clear at Day 2 indicate that they are thermally stable. Formulations that remain clear at Day 15 indicate that the formulations are both thermally stable as well as tolerant towards high salinity condition (seawater).

The screening test results are tabulated in Table 4.10. Of the 144 formulations, 17 formulations remained clear after the first 2 hours at 100°C. From the 17 formulations, 13 formulations remained clear solutions after 24 hours in the oven at 100°C, with the other 4 giving a cloudy appearance. After 15 days however, only 7 formulations remained clear. All of the 7 formulations with clear solutions contained LHS as foam booster.

Precipitates at the bottom of test tubes were observed in formulations containing SHR, indicating incompatibility of formulations using seawater at high temperature. A separate layer on the top of solution was observed for formulations containing HR. The separate layer formed indicates that HR is unstable at high temperature and thus underwent hydrolysis to produce carboxylic acid and amine [100]. From the results obtained, it is clear that LHS is the only foam booster tolerant towards harsh conditions of high salinity and high temperature.

The formulation recipe with ENS-750, anionic surfactant and LSH was set at the ratio of 4:3:3 respectively for further testing.

Table 4.10: Results obtained for screening test

Formulation	Ratio	Day 1	Day 2	Day 15
ENS-750:AOS:LHS	5:3:2	C	C	C
	5:2:3	C	C	C
	4:3:3	C	C	C
ENS-750:AOS:SHR	5:2:3	C	C	P
	4:3:3	C	C	P
ENS-750:AOS:HR	4:3:3	C	C	H
ENS-750:SDS:LHS	5:3:2	C	C	C
	5:2:3	C	C	C
	4:3:3	C	C	C
ENS-750:SDS:SHR	5:2:3	C	C	P
	4:3:3	C	C	P
ENS-750:SDS:HR	4:3:3	C	C	H
ENS-750:MES:LHS	5:3:2	C	CL	-
	5:2:3	C	CL	-
	4:3:3	C	C	C
ENS-750:MES:SHR	5:2:3	C	CL	-
	4:3:3	C	CL	-

\*Note: C = clear, CL = cloudy, P = precipitate, H = hydrolyzed. Observation on Day 1 was done after 2 hours in oven and Day 2 at the 25<sup>th</sup> hour.

#### 4.4.2.2 Foam stability

Foam stability tests are divided into two categories: dynamic and static test. In a dynamic foam stability test, foam is generated by flowing gas at a constant rate through a gas-dispersion tube (or any other device with porous orifice) into the test solution. Foam volume generated under the constant flow of gas is then measured.

In general, the static foam stability test involves a static introduction of air into the test solution. There are many variations to the static foam stability test. In a Ross-Miles test, foam is generated by allowing a test solution with specified volume to fall at a specified height into a vessel containing the same test solution [28]. Some tests involve manual shaking of a sealed container containing a test solution. Some others employ the use of blender to introduce air into the test solution [16, 101].

The reproducibility of the results for foam stability tests is low because the foam generation and collapse are not usually uniform [28]. However, these two methods are usually used for foam stability tests.

In this study, the gas used for the foam stability test was CO<sub>2</sub> because the produced gas in Malaysian oilfields has high content of CO<sub>2</sub>. As such, the dynamic foam stability test method was employed, as it is easier to introduce CO<sub>2</sub> gas into the system with a dynamic foam stability test setup. The foam stability tests conducted involved the foam stability without the presence of oil (diesel) as well as with the presence of oil (diesel).

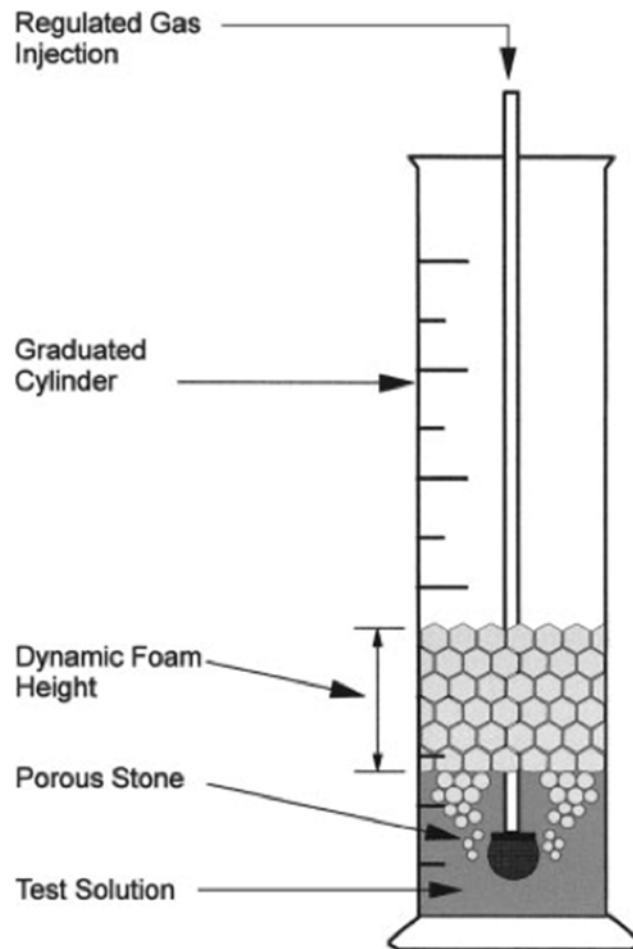


Figure 4.27: A graphical illustration of a dynamic foam stability test [28]

The objective of this study is to determine which of the 3 previously selected formulations from the screening test could generate the most stable foam against oil. The results are presented in the form of relative foam height against time. The relative foam height is  $h/h_i$  where  $h$  is the foam height at present time and  $h_i$  is the initial foam height. The stability of foam generated is determined by the time it takes for a foam system to reach its half-life. The half-life of foam  $t_{half}$ , is the time taken for foam height to decrease to half of its initial height. Hence, the longer the time taken for a foam system to collapse to half of its initial height, the more stable the foam system is.

#### 4.4.2.2.1 Without diesel

After the generation of foam, the foam was observed to collapse with a significantly fast rate. The results are presented in Figure 4.28. The half-life of foams generated was reached within five minutes of the experiment. The collapse is due to the liquid drainage from the foam films, causing film thinning and ultimately, rupture. In the absence of diesel, the formulation ENS-750:AOS:LHS is shown to be the most stable among the three formulations. Its foam has the longest half-life among the three formulations. The foam stability of ENS-750:SDS:LHS and ENS-750:MES:LHS are almost identical. The half-life values of these two formulations are almost the same, slightly below the 2.5-minute mark. However, the foam generated by ENS-750:SDS:LHS collapse drastically after the half-life mark.



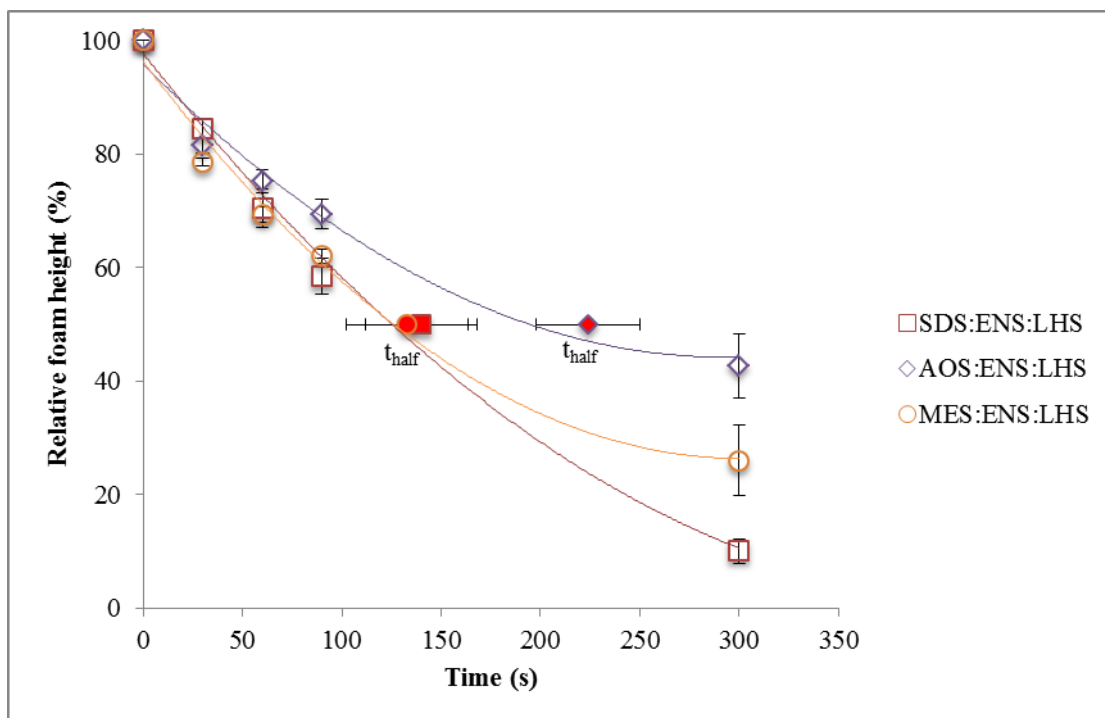


Figure 4.28: Foam relative height for 1.0 wt% surfactant formulations in the absence of diesel

#### 4.4.2.2.2 With diesel

Oil is known to destabilize foam [70]. Hence, experiments were conducted to test the foam stability performance of the formulations in the presence of oil. Diesel was chosen as the model oil for the experiment rather than the actual crude oil as the actual crude oil exists in the form of wax at room temperature. Its waxy nature prevents the bubbling of the surfactant solutions at the room temperature.

Since oil destabilizes foam, the performance of the formulations in the presence of diesel was expected to be indifferent, if not worse than the tests conducted in the absence of diesel. This was observed to be true for the ENS-750:AOS:LHS and ENS-750:MES:LHS formulations. However, the ENS-750:SDS:LHS formulation was observed to perform even better in the presence of diesel. The foam stability of ENS-750:AOS:LHS decreased in the presence of diesel while the foam stability of ENS-750:MES:LHS in the presence of diesel did not differ much from the foam stability in the absence of diesel. Figures 4.29 – 4.32 show the relative foam height of the three

formulations against time in the presence of diesel. From Figure 4.28, it is clear that the ENS-750:SDS:LHS formulation produced the most stable foam among the three formulations, exceeding the performance of ENS-750:AOS:LHS. The half-life was recorded to be above 5 minutes. This was not expected as ENS-750:SDS:LHS seemed to perform poorly in the absence of diesel.

The difference observed in the foam stability of the three formulations in the presence of diesel is thought to be caused by the amount of foam booster added. Basheva et. al [70] observed that the amount of betaine used as a foam booster affects the foam stability of surfactant solution in the presence of oil. The more betaine is used, the better it is the stability of the generated foam against oil. The three different anionic surfactants added undoubtedly had affected the amount of betaine that is needed to stabilize foam in oil. Hence, a less amount of betaine is needed to stabilize the foam generated by ENS-750:SDS:LHS as compared to the other two formulations.

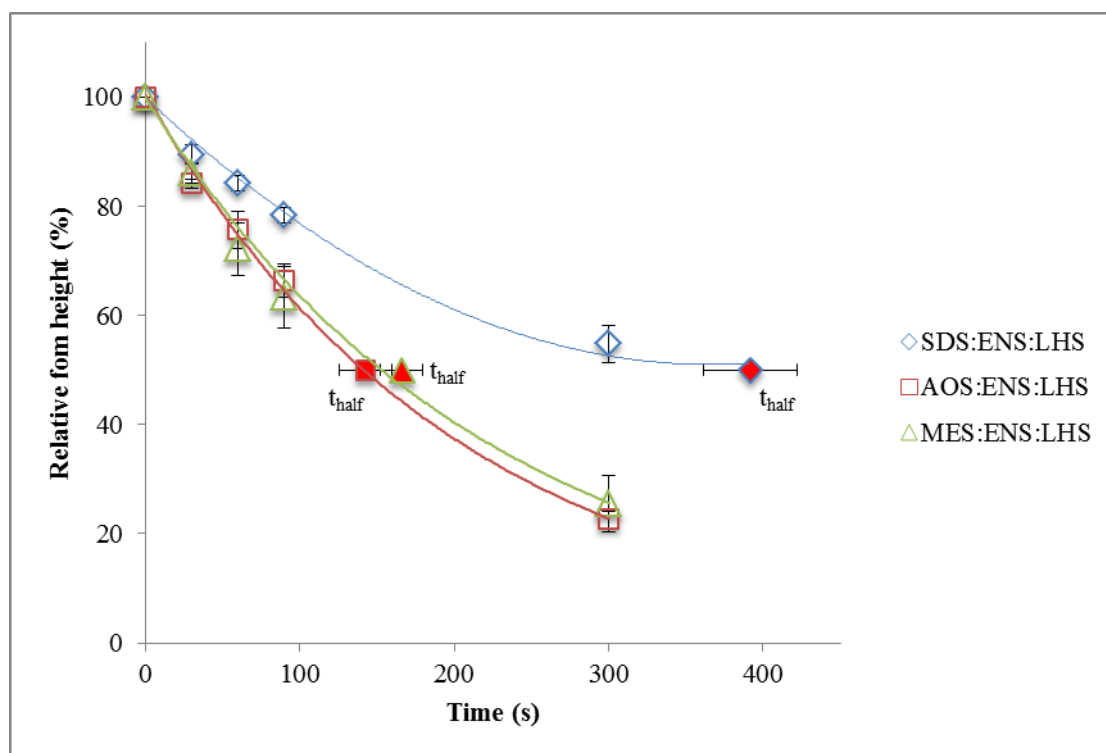


Figure 4.29: Foam relative height for 1.0 wt% surfactant formulations in the presence of diesel

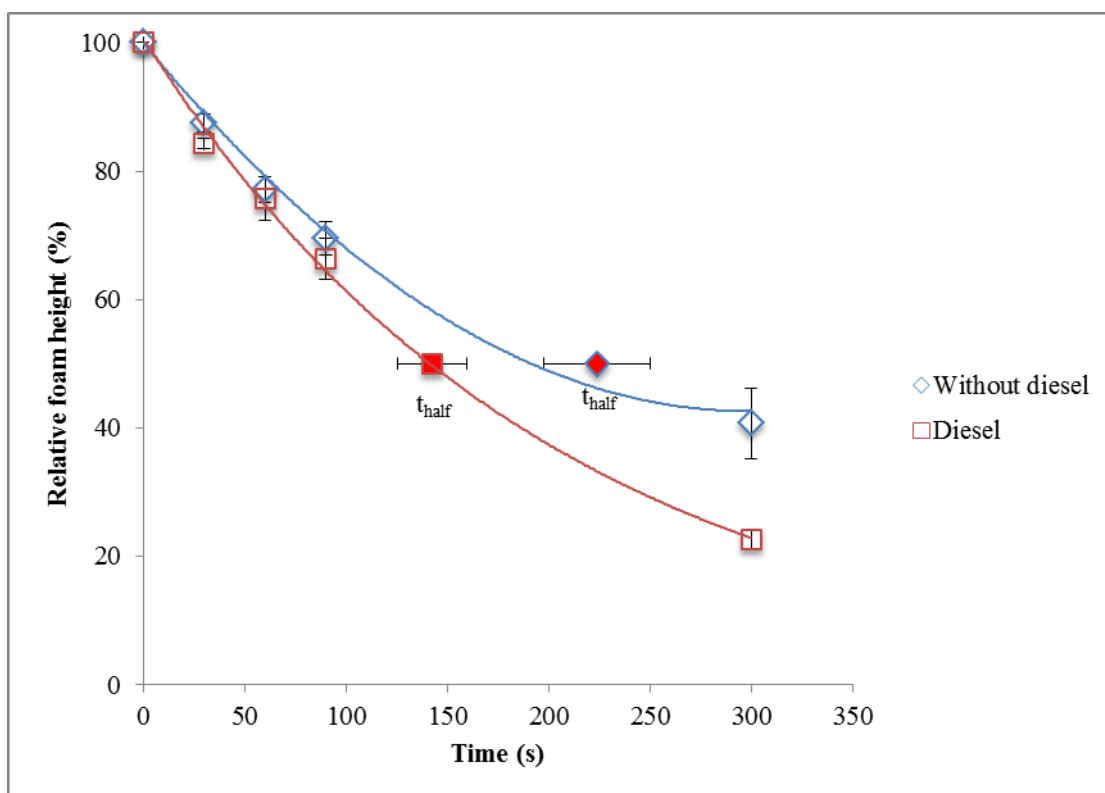


Figure 4.30: Comparison of foam relative height of 1.0 wt% of AOS:ENS:LHS formulation with and without the presence of diesel

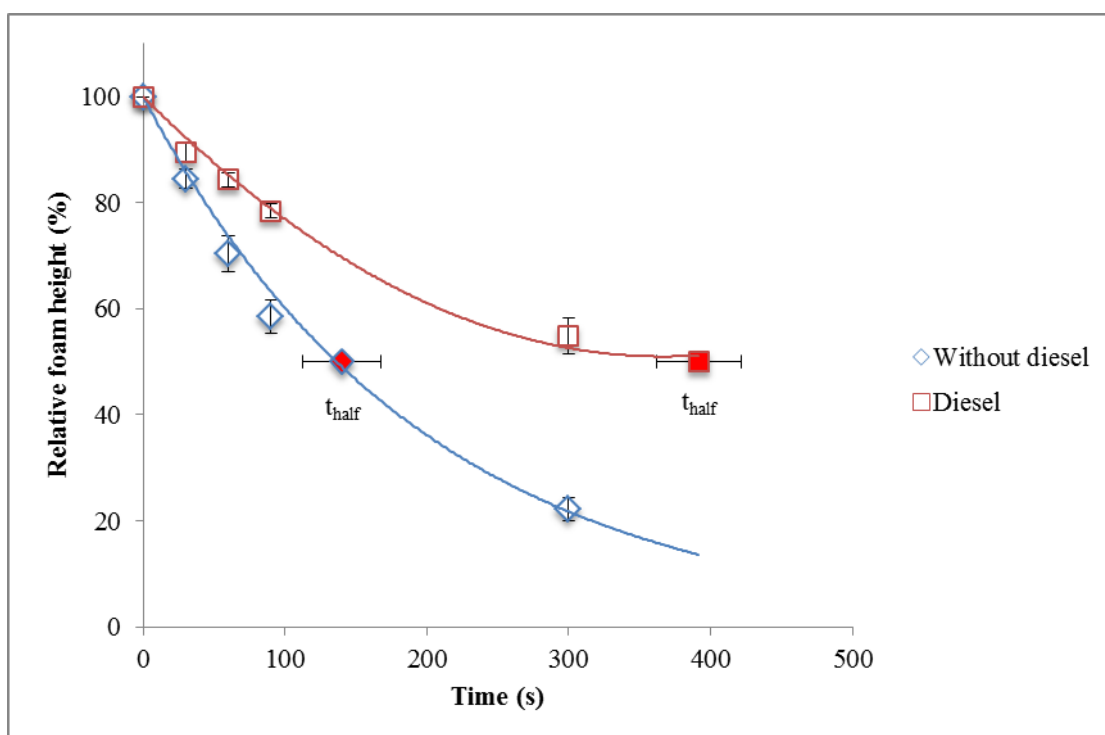


Figure 4.31: Comparison of foam relative height of 1.0 wt% of SDS:ENS:LHS formulation with and without the presence of diesel

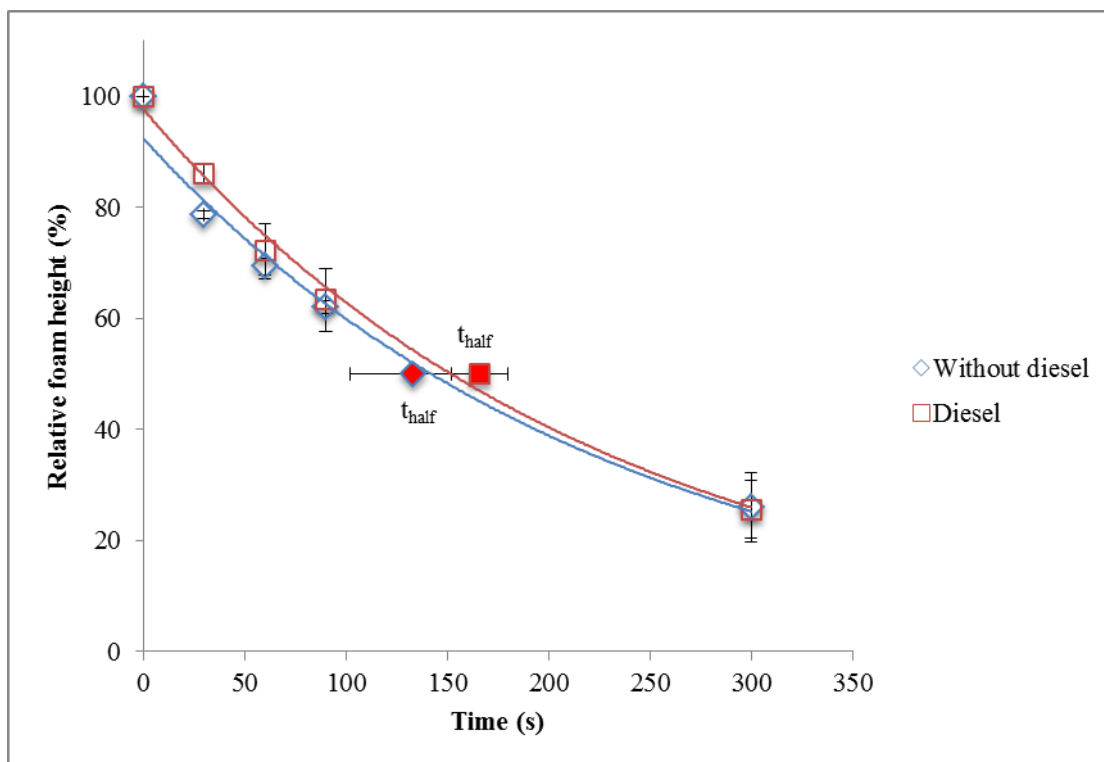


Figure 4.32: Comparison of foam relative height of 1.0 wt% of MES:ENS:LHS formulation with and without the presence of diesel

## CHAPTER 5

### CONCLUSION

As a conclusion, the objectives of this study were met with the following remarks:

1. A nonionic surfactant was successfully synthesized using a natural oil (safflower oil) derived fatty acid methyl ester through epoxidation and alkoxylation. Optimisation studies were done for both the reactions and high product yields were obtained for both reactions: 94.49% for epoxidation and 86.6% for alkoxylation.
2. The yields for both epoxidation and alkoxylation reactions were successfully characterized in detail using GC-MS, NMR and FT-IR.
3. In the study of the cloud point behavior for the synthesized surfactant (ENS-750), the cloud point of ENS-750 was found to decrease with increasing salinity. In the presence of cloud point boosters, it is found that the structure of the cloud point boosters affects the cloud point behavior of ENS-750. Cloud point boosters with straight, long hydrocarbon tail elevate the cloud point of ENS-750 more effectively.
4. A new surfactant blend was successfully formulated using the synthesized ENS-750 with SDS as cloud point booster and a commercially available surfactant as foam booster. The formulation was found to be stable at 100°C and at 35000 ppm salinity for 15 days. Moreover, the formulation produced foams that are stable in the presence of oil with an increase of 116.22% of its original half-life.

## 5.1 Recommended future work/direction

This study focused on the synthesis and the early developments of a natural oil-derived surfactant for EOR applications in Malaysia. The early developments included solving possible issues related to the conditions usually encountered in a Malaysian oilfield reservoir. A further and thorough study should be conducted to better understand the chemical properties of the surfactant synthesized and the formulation produced. For the synthesized surfactant, properties such as the phase diagram and the hydrophilic-lipophilic balance (HLB) should be conducted to better characterize the surfactant produced. Also, for the alkoxylation reaction, a kinetic study should be included and the optimization study for the alkoxylation reaction can be further improved to include the amount of PEG-ME added as a parameter to further understand the reaction mechanism of the alkoxylation reaction to produce the surfactant.

For the development of the formulation for EOR applications, future studies should include core flood tests under more realistic conditions to evaluate its performance as an EOR surfactant suitable for FAWAG. Also, adsorption studies for the new formulation on the reservoir rocks should be carried out for a better understanding of the interaction between the surfactant formulation and the reservoir rock.

## 5.2 Journal Publications and Conferences

- **Susan Lee**, Isa M. Tan, Muhammad Mushtaq, “Study of the Cloud Point Behavior of High Oleate Ester-Derived Nonionic Surfactant”, ICFAS 2012, Kuala Lumpur, Malaysia.
- Muhammd Mushtaq, I.B. Tan, C. Devi, S. Majidaie, M. Nadeem, **Susan Lee**, “Epoxidation of Fatty Acid Methyl Esters derived from Jatropha oil”, National Postgraduate Conference, 2011.

- Muhammad Mushtaq, Isa M. Tan, Muhammad Nadeem, **Susan Lee**, Saeed Majidaie, Rehan Hashmet, Rizwan Azam, “The Determination of Point of Zero Charge (PZC) and Static Adsorption of an Anionic Surfactant On Malaysian Sandstone”, ICIPEG 2012 Kuala Lumpur, Malaysia.
- Saeed Majidaie, Muhammad Mushtaq, Isa M. Tan, Birol Demiral, **Susan Lee**, “Non-petrochemical based surfactants for EOR applications”, Poster presented at SPE EOR Conference at Oil and Gas West Asia held in Muscat, Oman, 16–18 April 2012.
- M. Mushtaq, Isa M. Tan, M. Nadeem, C. Devi, **Susan Lee**, M.Sagir and Umer Rashid, “Epoxidation of methyl esters derived from Jatropha oil: An optimization study”, accepted for publication in Grasas y Aceites (International Journal of Oils and Fats), DOI: 10.3989/gya.084612.
- M. Mushtaq, Isa M. Tan, M. Nadeem, C. Devi, Susan Y. C. Lee, M. Sagir, “A convenient route for the alkoxylation of biodiesel and its influence on cold flow properties”, accepted for publication in International Journal of Green Energy, Volume 11, 2014.





## REFERENCES

1. Hamdan, M. K., Darman, N., Hussain, D. & Ibrahim, Z. (2005) Enhanced Oil Recovery in Malaysia: Making it a Reality in *2005 Asia Pacific Oil and Gas Conference and Exhibition* Jakarta, Indonesia.
2. PETRONAS (2010) Annual Report 2010.
3. Aarra, M. G., Skauge, A. & Martinsen, H. A. (2002) FAWAG: A Breakthrough for EOR in the North Sea in *SPE Annual Technical Conference and Exhibition*, Society of Petroleum Engineers, San Antonio, Texas, USA.
4. Ivanhoe, L. F. (1997) Get Ready for Another Oil Shock! in *The Futurist*
5. Holmberg, K., Jo'nsson, B., Kronberg, B. & Lindman, B. r. (2002) *Surfactants and Polymers in Aqueous Solution*, John Wiley & Sons, Ltd., England.
6. Alvarado, V. & Manrique, E. (2010) Enhanced Oil Recovery: An Update Review, *Energies*. **3**, 1529-1575.
7. Moritis, G. (2008) Worldwide EOR Survey, *Oil and Gas Journal*. **106**, 41-42, 44-59.
8. Hirasaki, G. J., Miller, C., A. & Puerto, M. (2008) Recent Advances in Surfactant EOR in *International Petroleum Technology Conference*, Society of Petroleum Engineers, Kuala Lumpur, Malaysia.
9. Poolen, H. K. V. & Associates (1980) *Fundamentals of enhanced oil recovery*, PennWell Books.
10. Tehrani, D. H., Danesh, A., Sohrabi, M. & Henderson, G. Enhanced Oil Recovery by Water Alternating Gas (WAG) Injection in Department of Petroleum Engineering, Heriot-Watt University, Edinburgh, UK.
11. Christensen, J. R., Stenby, E. H. & Skauge, A. (1998) Review of WAG Field Experience in *International Petroleum Conference and Exhibition of Mexico*, Society of Petroleum Engineers, Villahermosa, Mexico.
12. Skauge, A., Aarra, M. G., Surguchev, L., Martinsen, H. A. & Rasmussen, L. (2002) Foam-Assisted WAG: Experience from the Snorre Field in *SPE/DOE Improved Oil Recovery Symposium*, Society of Petroleum Engineers, Tulsa, Oklahoma, USA.

13. Blaker, T., Celius, H. K., Lie, T., Martinsen, H. A., Rasmussen, L. & Vassenden, F. (1999) Foam for Gas Mobility Control in the Snorre Field: The FAWAG Project in *SPE Annual Technical Conference and Exhibition*, Society of Petroleum Engineers, Houston, Texas, USA.
14. Surguchev, L. M. & Hanssen, J. E. (1996) Foam Application in North Sea Reservoirs, I: design and Technical Support of Field Trials in *SPE/DOE Tenth Symposium on Improved Oil Recovery*, Society of Petroleum Engineers, Tulsa, Oklahoma, USA.
15. Svorstal, I., Vassenden, F. & Mannhardt, K. (1996) Laboratory Studies for Design of a Foam Pilot in the Snorre Field in *SPE/DOE Tenth Symposium on Improved Oil Recovery*, Society of Petroleum Engineers, Tulsa, Oklahoma, USA.
16. Andrianov, A., Farajzadeh, R., Nick, M. M., Talanana, M. & Zitha, P. L. J. (2011) Immiscible Foam for Enhancing Oil Recovery: Bulk and Porous Media Experiments in *SPE Enhanced Oil Recovery Conference*, Society of Petroleum Engineers, Kuala Lumpur, Malaysia.
17. Mustafa, S., Dilara, B., Nargis, K., Naeem, A. & Shahida, P. (2002) Surface Properties of the Mixed Oxides of Iron and Silica, *Colloids and Surfaces A: Physicochemical and Engineering Aspects*. **205**, 273-282.
18. Salager, J.-L. (2002) *Surfactants: Types and Uses*, Universidad de Los Andes, Venezuela.
19. Myers, D. (2006) *Surfactant Science and Technology*, 3 edn, John Wiley & Sons.
20. Narayanan, R., Anderez, J. M., Anton, R. E., Bose, A. & Bracho, C. (2008) *Interfacial Processes and Molecular Aggregation of Surfactants*, Springer-Verlag Berlin, Heidelberg.
21. Barnes, J. R., Dirkzwager, H., Smit, J. R., Smit, J. P., On, A., Navarrete, R. C., Ellison, B. H. & Buijse, M. A. (2010) Application of Internal Olefin Sulfonates and Other Surfactants to EOR. Part 1: Structure - Performance Relationships for Selection at Different Reservoir Conditions in *SPE Improved Oil Recovery Symposium*, Society of Petroleum Engineers, Tulsa, Oklahoma, USA.
22. Adkins, S., Liyanage, P. J., Pinnawala Arachchilage, G. W. P., Mudiyanse, T., Weerasooriya, U. & Pope, G. A. (2010) A New Process for Manufacturing and Stabilizing High-Performance EOR Surfactants at Low Cost for High-Temperature, High-Salinity Oil Reservoirs in *SPE Improved Oil Recovery Symposium* Society of Petroleum Engineers, Tulsa, Oklahoma, USA.
23. Domsch, A. (1995) Biodegradability of Amphoteric Surfactants in *Biodegradability of Surfactants* (Karsa, D. R. & Porter, M. R., eds), Blackie Academic and Professional, Glasgow, United Kingdom.

24. Hayes, M. E., Bourrel, M., El-Emary, M. M., Schechter, R. S. & Wade, W. H. (1979) Interfacial Tension and Behaviour of Nonionic Surfactants, *SPE Journal*. **19**, 349-356.
25. Alauddin, M., Parvin, T. & Begum, T. (2009) Effect of Organic Additives on the Cloud Point of Triton X-100 Micelles, *Journal of Applied Sciences*. **9**, 2301-2306.
26. Hey, M. J., Ilett, S. M. & Davidson, G. (1995) Effect of temperature on poly(ethylene oxide) chains in aqueous solution. A viscometric, <sup>1</sup>H NMR and Raman spectroscopic study, *Journal of the Chemical Society, Faraday Transactions*. **91**, 3897-3900.
27. Winsor, P. A. (1968) Binary and Multicomponent Solutions of Amphiphilic Compounds. Solubilization and the Formation, Structure, and Theoretical Significance of Liquid Crystalline Solutions., *Chemical Reviews*. **68**, 1-40.
28. Schramm, L. L. (2005) *Emulsions, Foams, and Suspensions: Fundamentals and Applications*, Wiley-VCH, Weinheim, Germany.
29. Taylor, J. E. (1976) The structure of singularities in soap-bubble-like and soap-film-like minimal surfaces, *The Annals of Mathematics*. **103**, 489-539.
30. Pugh, R. J. (2005) Experimental techniques for studying the structure of foams and froths, *Advances in Colloid and Interface Science*. **114–115**, 239-251.
31. Uren, L. C. & Fahmy, E. H. (1927) Factors Influencing the Recovery of Petroleum from Unconsolidated Sands by Waterflooding, *Petroleum Transactions, AIME*. **77**, 318-335.
32. Lyons, W. C. (2010) *Working Guide to Reservoir Engineering*, Elsevier Inc.
33. Lawson, J. B. & Reisberg, J. (1980) Alternate Slugs of Gas and Dilute Surfactant for Mobility Control during Chemical Flooding in *First Joint SPE/DOE Symposium on Enhanced Oil Recovery*, Society of Petroleum Engineers, Tulsa, Oklahoma, USA.
34. Patzek, T. W. (1996) Field Applications of Steam Foam for Mobility Improvement and Profile Control, *SPE Reservoir Engineering*. **11**, 79-86.
35. Wang, D., Cheng, J., Yang, Z., Li, Q., Wu, W. & Yu, H. (2001) Successful Field Test of the First Ultra-low Interfacial Tension Foam Flood in *SPE Asia Pacific Improved Oil Recovery Conference*, Society of Petroleum Engineers, Kuala Lumpur, Malaysia.
36. Li, R. F., Yan, W., Liu, S., Hirasaki, G. J. & Miller, C., A. (2008) Foam Mobility Control for Surfactant EOR in *SPE/DOE Improved Oil Recovery Symposium*, Society of Petroleum Engineers, Tulsa, Oklahoma, USA.
37. Shupe, R. D. (1981) Chemical Stability of Polyacrylamide Polymers, *Journal of Petroleum Technology*. **33**, 1513-1529.

38. Li, R. F., Hirasaki, G. J., Miller, C., A. & Masalmeh, S. K. (2011) Wettability Alteration and Foam Mobility Control in a Layered 2-D Heterogeneous System in *SPE International Symposium on Oilfield Chemistry*, Society of Petroleum Engineers, Woodlands, Texas, USA.
39. Tunio, S. Q., Chandio, T. A. & Memon, M. K. (2012) Comparative Study of FAWAG and SWAG as an Effective EOR Technique for a Malaysian Field, *Research Journal of Applied Sciences, Engineering and Technology*. **4**, 645-648.
40. Guo, H., Faber, R., Buijse, M. & Zitha, P. L. J. (2011) A Novel Alkaline-Surfactant-Foam EOR process in *SPE Enhanced Oil Recovery Conference*, Society of Petroleum Engineers, Kuala Lumpur, Malaysia.
41. Lau, H. C. (2011) Alkaline Steam Foam: Concepts and Experimental Results in *SPE Enhanced Oil Recovery Conference*, Society of Petroleum Engineers, Kuala Lumpur, Malaysia.
42. Kuehne, D. L., Frazier, R. H., Cantor, J. & Horn Jr., W. (1992) Evaluation of Surfactants for CO<sub>2</sub> Mobility Control in Dolomite Reservoirs in *SPE/DOE Eighth Symposium on Enhanced Oil Recovery*, Society of Petroleum Engineers, Tulsa, Oklahoma, USA.
43. de Guzman, D. (2004) Surfactants Squeezed on High Feedstock Costs, Rising Demand, *Chemical Market Reporter*. **266**, 1-3.
44. McCoy, M. (2006) Surfactant Firms End a Tough Year, *Chemical and Engineering News*. **84**, 21-22.
45. Giardi, C., Lapinte, V., Charnay, C. & Robin, J. J. (2009) Nonionic polyoxazoline surfactants based on renewable source: Synthesis, surface and bulk properties, *Reactive and Functional Polymers*. **69**, 643-649.
46. Patel, M. (2004) Surfactants Based on Renewable Raw Materials: Carbon Dioxide Reduction Potential and Policies and Measures for the European Union, *Industrial Ecology*. **7**, 47-62.
47. Baumann, H., Bühler, M., Fochem, H., Hirsinger, F., Zobebelein, H. & Falbe, J. (1988) Natural Fats and Oils—Renewable Raw Materials for the Chemical Industry, *Angewandte Chemie International Edition in English*. **27**, 41-62.
48. Biermann, U., Friedt, W., Lang, S., Luhs, W., Machmuller, G., Metzger, J., Klass, M. R., Schafer, H. J. & Schneider, M. P. (2000) New syntheses with oils and fats as renewable raw materials for the chemical industry, *Angewandte Chemie International Edition*. **39**, 2206-2224.
49. Moser, B. R. & Erhan, S. Z. (2008) Branched chain derivatives of alkyl oleates: Tribological, rheological, oxidation, and low temperature properties, *Fuel*. **87**, 2253-2257.

50. Smith, P. C., Ngothai, Y., Nguyen, Q. D. & O'Neill, B. K. (2009) Alkoxylation of biodiesel and its impact on low-temperature properties, *Fuel*. **88**, 605-612.
51. Smith, P. C., Ngothai, Y., Nguyen, Q. D. & O'Neill, B. K. (2010) The addition of alkoxy side-chains to biodiesel and the impact on flow properties, *Fuel*. **89**, 3517-3522.
52. Hedman, B., Piispanen, P., Alami, E. & Norin, T. (2003) Synthesis and Characterization of Surfactants via Epoxidation of Tall Oil Fatty Acid, *Journal of Surfactants and Detergents*. **6**, 47-53.
53. Levitt, D. B., Jackson, A. C., Helnson, C., Britton, L. N., Malik, T., Dwarakanath, V. & Pope, G. A. (April, 2009) Identification and Evaluation of High-Performance EOR Surfactants, *SPE Reservoir Evaluation & Engineering*, 243-253.
54. Campanella, A., Fontanini, C. & Baltanás, M. A. (2008) High yield epoxidation of fatty acid methyl esters with performic acid generated in situ, *Chemical Engineering Journal*. **144**, 466-475.
55. Gan, L. H., Goh, S. H. & Ooi, K. S. (1992) Kinetic Studies of Epoxidation and Oxirane Cleavage of Palm Olein Methyl Esters, *Journal of the American Oil Chemists' Society*. **69**, 347-351.
56. Mungroo, R., Pradhan, N. C., Goud, V. V. & Dalai, A. K. (2008) Epoxidation of Canola Oil with Hydrogen Peroxide Catalyzed by Acidic Ion Exchange Resin, *Journal of the American Oil Chemists' Society*. **85**, 887-896.
57. Goud, V. V., Pradhan, N. C. & Patwardhan, A. V. (2006) Epoxidation of Karanja (*Pongamia glabra*) Oil by H<sub>2</sub>O<sub>2</sub>, *Journal of the American Oil Chemists' Society*. **83**, 635-640.
58. Findley, T. W., Swern, D. & Scanlan, J. T. (1945) Epoxidation of Unsaturated Fatty Materials with Peracetic Acid in Glacial Acetic Acid Solution, *Journal of the American Chemical Society*. **67**, 412-414.
59. Piazza, G., Foglia, T. & Nuñez, A. (2001) Optimizing reaction parameters for the enzymatic synthesis of epoxidized oleic acid with oat seed peroxygenase, *Journal of the American Oil Chemists' Society*. **78**, 589-592.
60. Piazza, G. J., Nuñez, A. & Foglia, T. A. (2003) Epoxidation of fatty acids, fatty methyl esters, and alkenes by immobilized oat seed peroxygenase, *Journal of Molecular Catalysis B: Enzymatic*. **21**, 143-151.
61. Du, G., Tekin, A., Hammond, E. G. & Woo, L. K. (2004) Catalytic Epoxidation of Methyl Linoleate, *Journal of the American Oil Chemists' Society*. **81**, 477-480.
62. Suarez, P. A. Z., Pereira, M. S. C., Doll, K. M., Sharma, B. K. & Erhan, S. Z. (2009) Epoxidation of Methyl Oleate Using Heterogeneous Catalyst, *Industrial & Engineering Chemical Research*. **48**, 3268-3270.

63. Khlebnikova, T. B., Pai, Z. P., Fedoseeva, L. A. & Mattsat, Y. V. (2009) Catalytic oxidation of fatty acids. II. Epoxidation and oxidative cleavage of unsaturated fatty acid esters containing additional functional groups, *Reaction Kinetics and Catalysis Letters*. **98**, 9-17.
64. Goud, V. V., Patwardhan, A. V., Dinda, S. & Pradhan, N. C. (2007) Kinetics of epoxidation of jatropha oil with peroxyacetic and peroxyformic acid catalysed by acidic ion exchange resin, *Chemical Engineering Science*. **62**, 4065-4076.
65. Goud, V. V., Dinda, S., Patwardhan, A. V. & Pradhan, N. C. (2010) Epoxidation of Jatropha (*Jatropha curcas*) oil by peroxyacids, *Asia-Pacific Journal of Chemical Engineering*. **5**, 346-354.
66. Morrison, W. B. & Smith, L. M. (1964) Preparation of fatty acid methyl esters and dimethylacetals from lipids with boron fluoride-methanol, *Journal of Lipid Research*. **5**, 600-608.
67. Garrett, P. R. (1993) *The Mode of Action of Antifoams*, Marcel Dekker, New York, USA.
68. Aveyard, R., Binks, B. P., Fletcher, P. D. I., Peck, T. G. & Rutherford, C. E. (1994) Aspects of aqueous foam stability in the presence of hydrocarbon oils and solid particles, *Advances in Colloid and Interface Science*. **48**, 93-120.
69. von Phul, S. A. & Stern, L. Antifoam. What is it? How does it work? Why do they say to limit its use? in, D-Foam, Inc., Texas, USA.
70. Basheva, E. S., Ganchev, D., Denkov, N. D., Kasuga, K., Satoh, N. & Tsujii, K. (1999) Role of Betaine as Foam Booster in the Presence of Silicone Oil Drops, *Langmuir*. **16**, 1000-1013.
71. Marszall, L. (1990) Effect of aromatic hydrotropic agents on the cloud point of mixed ionic-nonionic surfactant solutions, *Langmuir*. **6**, 347-350.
72. Li, J.-L., Bai, D.-S. & Chen, B.-H. (2009) Effects of additives on the cloud points of selected nonionic linear ethoxylated alcohol surfactants, *Colloids and Surfaces A: Physicochemical and Engineering Aspects*. **346**, 237-243.
73. Sharma, R. & Bahadur, P. (2002) Effect of Different Additives on the Cloud Point of a Polyethylene Oxide-Polypropylene Oxide-Polyethylene Oxide Block Copolymer in Aqueous Solution, *Journal of Surfactants and Detergents*. **5**, 263-268.
74. Na, G. C., Yuan, B. O., Stevens Jr., H. J., Weekley, B. S. & Rajagopalan, N. (1999) Cloud Point of Nonionic Surfactants: Modulation with Pharmaceutical Excipients, *Pharmaceutical Research*. **16**, 562-568.
75. Wilson, R., Smith, R., Wilson, P., Shepherd, M. J. & Riemersma, R. A. (1997) Quantitative gas chromatography-mass spectrometry isomer-specific measurement of hydroxy fatty acids in biological samples and food as a marker of lipid peroxidation, *Analytical Biochemistry*. **248**, 76-85.

76. Gallegos, R. D. (1993) Titrations of non-ionic surfactants with sodium tetraphenylborate using the orion surfactant electrode, *Analyst*. **118**, 1137-1141.
77. Titrimetric/potentiometric determination of non-ionic surfactants based on oleyoxyethylene adducts using the NIO electrode in pp. 1-8, Metrohm,
78. Moser, B. R. & Erhan, S. Z. (2007) Preparation and evaluation of a series of  $\alpha$ -hydroxy ethers from 9,10-epoxystearates, *European Journal of Lipid Science and Technology*. **109**, 206-213.
79. Moser, B. R., Sharma, B. K., Doll, K. M. & Erhan, S. Z. (2007) Diesters from Oleic Acid: Synthesis, Low Temperature Properties, and Oxidation Stability, *Journal of the American Oil Chemists' Society*. **84**, 675-680.
80. Goswami, D., Basu, J. K. & De, S. (2012) Optimal hydrolysis of mustard oil to erucic acid: A biocatalytic approach, *Chem Eng J*. **181-182**, 7-7.
81. Lin, B., Yang, L., Dai, H. & Yi, A. (2007) Kinetic Studies on Oxirane Cleavage of Epoxidized Soybean Oil by Methanol and Characterization of Polyols, *Journal of the American Oil Chemists' Society*. **85**, 113-117.
82. Petrović, Z. S., Zlatanić, A., Lava, C. C. & Sinadinović-Fišer, S. (2002) Epoxidation of soybean oil in toluene with peroxyacetic and peroxyformic acids - kinetics and side reactions, *European Journal of Lipid Science and Technology*. **104**, 293-299.
83. Piispanen, P. S., Persson, M., Claesson, P. & Norin, T. r. (2004) Surface Properties of Surfactants Derived from Natural Products. PART 2: Structure/Property Relationships - Foaming, Dispersion, and Wetting, *Journal of Surfactants and Detergents*. **7**, 161-167.
84. Lukac, M., Smolarikova, E., Lacko, I. & Devinsky, F. (2005) The methoxybenzyl ethers as useful protecting groups for hydroxy compounds: Methods of deprotection, *Acta Facult Pharm Univ Comenianae*. **52**, 31-45.
85. Koshy, L., Saiyad, A. H. & Rakshit, A. K. (1996) The effects of various foreign substances on the cloud point of Triton X 100 and Triton X 114, *Colloid & Polymer Science*. **274**, 582-587.
86. Mandal, A. B., Ray, S., Biswas, A. M. & Moulik, S. P. (1980) Physicochemical studies on the characterization of Triton X 100 micelles in an aqueous environment and in the presence of additives, *The Journal of Physical Chemistry*. **84**, 856-859.
87. Marszall, L. (1987) The Effect of Electrolytes on the Cloud Point of Ionic-Nonionic Surfactant Solutions, *Colloids and Surfaces*. **25**, 279-285.
88. Zaslavsky, B. Y. (1995) *Aqueous Two-Phase Partitioning – Physical Chemistry and Bioanalytical Applications*, Wiley-VCH Verlag GmbH & Co. KGaA, New York.

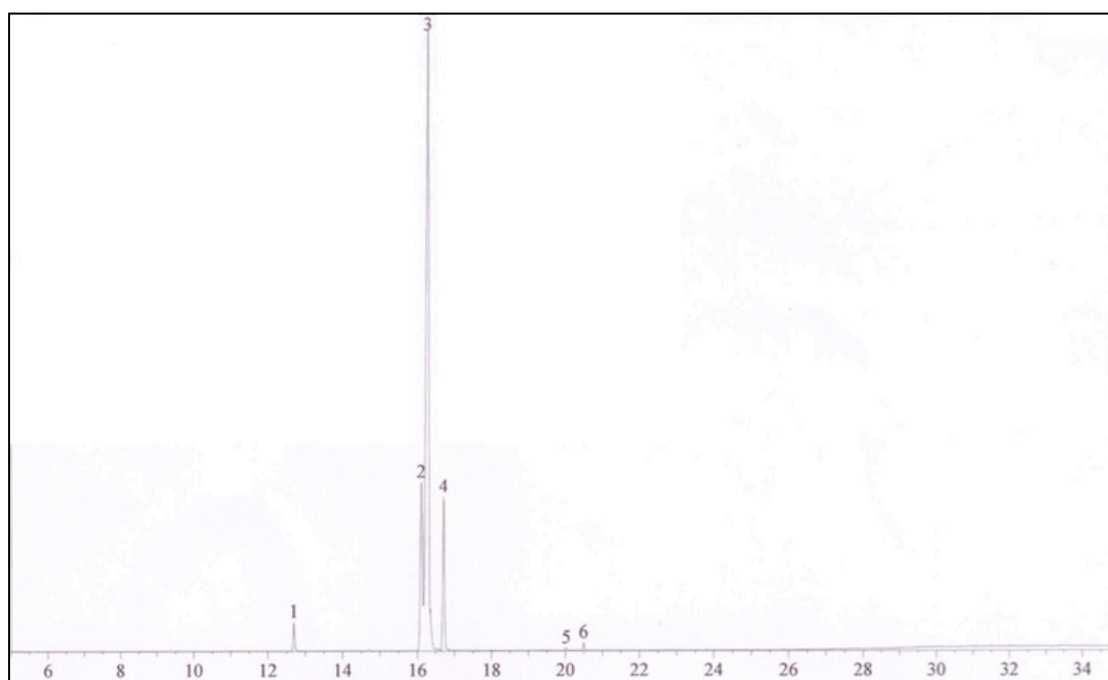
89. Marcus, Y. (2009) Effect of Ions on the Structure of Water: Structure Making and Breaking, *Chemical Reviews*. **109**, 1346-1370.
90. Marcus, Y. (2010) Effect of ions on the structure of water, *Pure and Applied Chemistry*. **82**, 1889-1899.
91. Miyake, Y., Yokomizo, K. & Matsuzaki, N. (1998) Determination of Unsaturated Fatty Acid Composition by High-Resolution Nuclear Magnetic Resonance Spectroscopy, *Journal of the American Oil Chemists' Society*. **75**, 1091-1094.
92. Aerts, H. & Jacobs, P. (2004) Epoxide yield determination of oils and fatty acid methyl esters using <sup>1</sup>H NMR, *Journal of the American Oil Chemists' Society*. **81**, 841-846.
93. <https://sites.google.com/site/isumate453lab3group8/data/polyethylene-glycol-peg>, last visited on 3 December, 2012.
94. Gunstone, F. D. (2007) <sup>13</sup>C-NMR SPECTROSCOPY OF FATTY ACIDS AND DERIVATIVES: Epoxides and Acyclic Ethers in lipidlibrary.aocs.org.
95. Talley, L. D. (1988) Hydrolytic stability of alkylethoxy sulfate, *SPE Reservoir Engineering*. **3**, 235-242.
96. Gu, T., Qin, S. & Ma, C. (1989) The effect of electrolytes on the cloud point of mixed solutions of ionic and nonionic surfactants, *Journal of colloid and interface science*. **127**, 586-588.
97. Valaulikar, B. S. & Manohar, C. (1985) The mechanism of clouding in triton X-100: The effect of additives, *Journal of colloid and interface science*. **108**, 403-406.
98. Lad, K., Bahadur, A. & Bahadur, P. (1997) Clouding Behaviour of an Ethylene Oxide-Propylene Oxide Block Copolymer, *Tenside Surfactants Detergents*. **34**, 37-42.
99. Skauge, A. & Palmgren, O. (1989) Phase Behavior and Solution Properties of Ethoxylated Anionic Surfactants in *SPE International Symposium on Oilfield Chemistry*, Society of Petroleum Engineers, Houston, TX, US.
100. Walker, H. G. & Owens, H. S. (1952) The Hydrolysis Rate of Betaine Amide and Ester Chlorides, *Journal of the American Chemical Society*. **74**, 2547-2549.
101. Vikingstad, A. K., Skauge, A., Høiland, H. & Aarra, M. (2005) Foam-oil interactions analyzed by static foam tests, *Colloids and Surfaces A: Physicochemical and Engineering Aspects*. **260**, 189-198.



APPENDIX A

ADDITIONAL ANALYTICAL SPECTRA





Appendix 0.1: GC-MS spectrum of HOE used.

Peaks 1: Methyl Palmitate. 2: Methyl Linoleate. 3: Methyl Oleate. 4: Methyl Stearate.  
5: Methyl Eicosanoate.



## APPENDIX B

### PUBLISHED PAPERS AND CONFERENCES



# Study of the Cloud Point Behavior of High Oleate Ester-Derived Nonionic Surfactant

Isa M Tan, Susan Y C Lee and M Mushtaq

*Universiti Teknologi PETRONAS  
Bandar Seri Iskandar,  
Tronoh, 31750, Perak.*

**Abstract.** The cloud point behavior of high oleate ester-derived nonionic surfactant has been studied. The effect of various polyethoxylate chain lengths (polyethylene glycol with ethylene oxide monomer 7, 11 and 16 units) as the surfactant's hydrophilic head and the effect of sodium chloride and ionic surfactants on the cloud points of nonionic surfactants synthesized were investigated. When the chain length of polyethoxylate increased, the cloud point of the synthesized nonionic surfactant also increased. Sodium chloride was found to depress the cloud point values of the formed nonionic surfactants with a linear decrease in relation to the concentration of sodium chloride used. Ionic surfactants lifted the cloud points of synthesized nonionic surfactant but in the presence of sodium chloride, the cloud point of mixed ionic-nonionic solution was suppressed.

**Keywords:** nonionic surfactant; cloud point; ionic-nonionic; turbidity; salinity.

## INTRODUCTION

Clouding is a characteristic behavior of nonionic surfactants, particularly those with polyethoxylate as the hydrophilic head. Clouding occurs when surfactants separate out of a homogenous surfactant solution and forms two phases, thus causing turbidity. The temperature at which this phenomenon happens is called the cloud point. The phase separation is reversible. When the surfactant solution system is cooled to a temperature below the cloud point, the surfactant system would once again form a homogenous solution.

Cloud point of a nonionic surfactant is an important factor to be considered, as the performance of nonionic surfactants is dependent on the cloud point. For example, nonionic surfactant solutions above the cloud point would not be favorable for foaming applications as surfactant solutions above the cloud point would lose its function as a foaming agent and vice versa. Hence, it is of considerable importance to acquire knowledge of the clouding behavior of a nonionic surfactant so that the cloud point can be tailored to desired levels to meet the requirements of different applications.

The cloud point of a nonionic surfactant is determined basically by its molecular structure [1-3]. Solubility of a nonionic surfactant in an aqueous system is through the formation of O-H bonds between

surfactant and water [4]. Therefore, the structure of a nonionic surfactant plays a major role in its cloud point behavior. Besides this, the cloud point of a nonionic surfactant is strongly affected by the presence of various additives. The effect of additives such as inorganic electrolytes [5-8], organic additives [9-11] and ionic surfactants [12] on the cloud point temperatures of nonionic surfactants have been studied.

In the literature, we found no thorough study done on the cloud point behavior of natural oil-derived polyethoxylated nonionic surfactants with two branches of hydrophobic chains. Only one study by Hedman et al. [13] discussed about the clouding behavior in relation to surfactant concentration and in comparison with their linear counterpart.

High oleate ester (HOE) oil-derived polyethoxylated nonionic surfactants with various polyethoxylate chain lengths were used in this study. The effects of polyethoxylate chain length, salinity (sodium chloride as electrolyte) and ionic surfactant on the cloud points of the synthesized nonionic surfactants were studied.

## MATERIALS

Nonionic surfactants with varying polyethoxylate chain lengths (7, 11 and 16 ethylene oxide units - ENS-350, -550 and -750 respectively) were

## Epoxidation of methyl esters derived from *Jatropha* oil: An optimization study

By M. Mushtaq<sup>1,\*</sup>, Isa M. Tan<sup>1</sup>, M. Nadeem<sup>2</sup>, C. Devi<sup>1</sup>, S.Y. C. Lee<sup>1</sup>, M. Sagir<sup>1</sup> and U. Rashid<sup>3,\*</sup>

<sup>1</sup> Chemical Engineering Department, Universiti Teknologi PETRONAS,  
Bandar Seri Iskandar 31750, Tronoh, Perak, Malaysia

<sup>2</sup> Subsurface Technology, PETRONAS Research Sdn. Bhd (PRSB), Kajang 43000, Selangor, Malaysia

<sup>3</sup> Institute of Advanced Technology, Universiti Putra Malaysia, Serdang 43400, Selangor, Malaysia

\* Corresponding authors: mmushtaq3@gmail.com; umer.rashid@yahoo.com

### RESUMEN

#### Epoxidación de ésteres metílicos derivados del aceite de *Jatropha*: Optimización del estudio

Se ha evaluado la optimización de la reacción de epoxidación de ésteres metílicos obtenidos a partir de aceite de *Jatropha*. Se ha empleado para el diseño experimental una metodología de superficie de respuesta (RSM), basada en un diseño compuesto central giratorio (CCRD). Cuatro variables de la reacción fueron evaluadas: relación molar peróxido de hidrógeno/C=C, relación molar ácido fórmico/C=C, temperatura de reacción y tiempo de reacción. Las condiciones óptimas de epoxidación calculadas por el modelo cuadrático fueron 3.12 moles de peróxido de hidrógeno/C=C moles, 0.96 moles de ácido fórmico/C=C moles, una temperatura de reacción de 70.0 °C y un tiempo de reacción de 277 minutos. Una reacción optimizada mediante los parámetros propuestos del proceso proporciona un rendimiento de  $92.89 \pm 1.29\%$  en peso con un tiempo de reacción relativamente mejorado. La concentración de peróxido de hidrógeno y la temperatura de la reacción fueron las variables más significativas, además la temperatura de la reacción y la concentración de peróxido de hidrógeno mostraron fuertes interacciones. Los ésteres metílicos epoxidados se analizaron mediante FT-IR, <sup>1</sup>H RMN y RMN de <sup>13</sup>C. Este estudio indica que se requiere una proporción molar relativamente mayor de ácido fórmico que la propuesta en la literatura.

**PALABRAS CLAVE:** Aceite epoxidado de *Jatropha* – Caracterización – Metodología de superficie – Optimización – Respuesta.

### SUMMARY

#### Epoxidation of methyl esters derived from *Jatropha* oil: An optimization study

The optimization of the epoxidation reaction of methyl esters obtained from *Jatropha* oil was appraised. Response surface methodology (RSM) based on a central composite rotatable design (CCRD) was employed for the experimental design. Four reaction variables namely hydrogen peroxide/C=C mole ratio, formic acid/C=C mole ratio, reaction temperature and reaction time were evaluated. The optimum epoxidation conditions calculated by the quadratic model were 3.12 moles of hydrogen peroxide/C=C moles, 0.96 moles of formic acid/C=C moles, a reaction temperature of 70.0 °C and a reaction time of 277 minutes. A reaction optimized by the proposed process parameters provided a yield of  $92.89 \pm 1.29$  wt.% with relatively improved reaction time. Hydrogen peroxide concentration and reaction

temperature were found to be the most significant variables while reaction temperature and hydrogen peroxide showed strong interactions. The epoxidized methyl esters were analyzed using FT-IR, <sup>1</sup>H NMR and <sup>13</sup>C NMR techniques. This study suggested relatively higher molar ratio of formic acid required than was proposed in the literature.

**KEY-WORDS:** Characterization – Epoxidised *Jatropha* oil – Optimization – Response surface methodology.

### 1. INTRODUCTION

The epoxidation reaction in natural oils and alkyl esters has gained prominence in recent years due to its multifarious usage in many industrial synthetic processes. As natural products are being used extensively in recent years due to the depletion of petroleum reserves and environmental concerns (Ibrahim *et al.*, 2011, Anwar *et al.*, 2006), the epoxidation reaction is gaining more importance as a reaction route in natural oils, fatty acid methyl esters and related oleo chemical conversions (Seniha Güner *et al.*, 2006). Products such as polymers, resins, biodiesel, cutting oils, high-tech surfactants, lubricating oils and nano composites benefit from the epoxidation reaction (Kleinová *et al.*, 2008, Dahlke *et al.*, 1995, Doll and Erhan, 2006).

Traditionally, an organic acid such as acetic or formic acid is used with hydrogen peroxide to generate per oxyacid as the oxygen carrier for the epoxidation of oils and fatty acid alkyl esters (Du *et al.*, 2004). These per oxyacids can be employed as a separate reagent or can be synthesized in-situ, but the most common method is the in-situ generation of peroxy acid. Nevertheless, many heterogeneous catalysts and enzymes have been suggested and employed to augment the effects of organic acids and hydrogen peroxide to enhance the yield. It was also found that peroxy formic acid was more efficient than peroxy acetic acid (Du *et al.*, 2004, Mungroo *et al.*, 2008).

A schematic representation of the epoxidation reaction is presented in Figure 1. In the course of the epoxidation reaction, an epoxidized product can undergo a ring opening reaction which is highly undesirable. This ring opening reaction has



## A CONVENIENT ROUTE FOR THE ALKOXYLATION OF BIODIESEL AND ITS INFLUENCE ON COLD FLOW PROPERTIES

M. Mushtaq<sup>1</sup>, Isa M. Tan<sup>1</sup>, M. Nadeem<sup>2</sup>, Cecilia Devi<sup>1</sup>,  
Susan Y. C. Lee<sup>2</sup>, and M. Sagir<sup>1</sup>

<sup>1</sup>Chemical Engineering Department, Universiti Teknologi PETRONAS, Bandar Seri Iskandar, Perak, Malaysia

<sup>2</sup>Subsurface Technology, PETRONAS Research Sdn. Bhd., Kajang, Selangor, Malaysia

*The attachment of alkoxy side chains to biodiesel and the associated effects on its cold flow properties are reported. High oleic methyl ester biodiesel was epoxidized using peroxy formic acid and subsequently alkoxyated using nine different alcohols employing BF<sub>3</sub>-etherate complex as catalyst. A low molar excess for alcohols was used at moderately low reaction temperatures (40–50°C). A high conversion for attachment of alkoxy group ranging 84%–93% was achieved with excellent selectivity. Cloud points, pour points, and kinematic viscosities were measured to evaluate the cold flow properties of modified biodiesel. The lowest cloud point –11°C and pour point –14°C were obtained with n-decoxy biodiesel. Elevated kinematic viscosities were observed for all alkoxyated products. The lowest kinematic viscosity (6.26 mm<sup>2</sup>·s<sup>–1</sup>) was observed for methoxy biodiesel. Gas chromatography mass spectrometry (GC-MS), proton nuclear magnetic resonance (<sup>1</sup>H NMR), <sup>13</sup>C NMR, and Fourier transform infrared (FT-IR) were used for structural elucidation. The reported alkoxylation route has high conversion rate and is convenient to implement.*

**Keywords:** Biodiesel; Alkoxylation; BF<sub>3</sub>; Cloud point; Pour point; Kinematic viscosity

## INTRODUCTION

The production of biodiesel from natural oils has been extensively studied in recent years as a possible substitute of diesel derived from fossil fuel (Meher, Vidya Sagar, and Naik 2006; Carlsson 2009; Özcanlı, Keskin, and Aydın 2011; Adebawale, Adewuyi, and Ajulo 2012). Biodiesel in its “pure” form is seldom tested due to high viscosity and oxidative instability. It is generally mixed with conventional diesel fuel in varying proportions for internal combustion engines (Reddy et al. 2011). The degree of unsaturation in the fatty acid chains is the cause for low melting points and is also responsible for a low oxidative stability to the product. The biodiesel derived from relatively saturated (either natural or hydrogenated) oils has good oxidative stability. However, it has a high melting point and possesses undesirable cold flow properties such as cloud point (CP), pour point (PP),

Address correspondence to M. Mushtaq, Chemical Engineering Department, Universiti Teknologi PETRONAS, Bandar Seri Iskandar, Tronoh, Perak 31750, Malaysia. E-mail: mmushtaq3@gmail.com